Lighting Strategies for the Flowering Stage of Indoor Cannabis Production

by

Victoria A. Rodriguez Morrison

A Thesis

presented to

The University of Guelph

In partial fulfilment of requirements
for the degree of

Master of Science

in

Environmental Sciences

Guelph, Ontario, Canada

ABSTRACT

LIGHTING STRATEGIES FOR THE FLOWERING STAGE OF INDOOR CANNABIS PRODUCTION

Victoria A. Rodriguez Morrison
University of Guelph, 2021

Advisor:
Dr. Youbin Zheng

Given the paucity of scientific research regarding lighting in cannabis production, this thesis investigated the effects of light intensity (LI) and ultraviolet (UV) radiation on indoor cannabis production during the flowering stage. When plants grew under LI ranging from 120 to 1800 $\mu mol \cdot m^{-2} \cdot s^{-1}$ provided by light emitting diodes (LEDs), inflorescence yield increased linearly as LI increased up to 1800 $\mu mol \cdot m^{-2} \cdot s^{-1}$. When plants were grown under 400 $\mu mol \cdot m^{-2} \cdot s^{-1}$ supplemented with UV (peak wavelength of 287 nm) levels from 0.01 to 0.8 $\mu mol \cdot m^{-2} \cdot s^{-1}$, for 3.5 $h \cdot d^{-1}$, there were no changes in total Δ^9-tetrahydrocannabinol or total cannabidiol concentrations. The severity of UV-induced cannabis morphology and physiology symptoms worsened as UV exposure level increased. The light response models developed in this thesis can be used to determine the optimum LI for a production environment, but caution should be used when exposing cannabis to UV radiation.

ACKNOWLEDGEMENTS

I would like to thank my advisor, Dr. Youbin Zheng for the wisdom you have shared with me throughout my graduate studies. I will carry the academic, professional, and personal life lessons you have taught me through all my next chapters in life. I am so grateful to have had an advisor that values a holistic education, allowing me to gain practical experience in the industry, expand my knowledge of plant science, and learn from your experience.

I would sincerely like to thank David Llewellyn for the endless technical support, writing feedback, and encouragement. Your passion for research, attention to specificity, and compassionate guidance have made a lasting impression on me. I will always be deeply grateful for the amount of time and effort you have put into teaching me to be a better researcher, and that you somehow always knew when words of encouragement would be helpful. I would also like to thank my advisory committee, Dr. Nigel Gale and Dr. Gale Bozzo, for providing guidance throughout my studies.

I would like to thank the Natural Sciences and Engineering Research Council for funding this research, and Green Relief Inc., for providing the research facility, cannabis plants, experimental materials, and logistical support for the experiments. Thank you to the Green Relief Inc. staff: Derek Bravo, Tim Moffat, Dane Cronin and Madeline Baker for the technical support during my trials. I also thank Angus Footman and Erica Emery for supporting the experiment through a change of management.

Thank you to the Dr. Zheng lab, for providing feedback for presentations, answering academic questions, providing graduate advice and helping with long harvests. Thank you Qinglu Ying, Brandon Yep, Melissa Moher, Devdutt Kamath, James Nesbitt, Yun Kong, Chase Jones-Baumgardt and Lewys Bevan. Lab trivia nights will be missed!

And finally, thank you to my supportive friends and loved ones, who have all contributed to getting me here and keeping me grounded along the way. Thank you to my mom, dad and brother for providing me with a lifetime full of love and encouragement, which helped make all of my accomplishments possible.

TABLE OF CONTENTS

LIST OF TABLES

LIST OF FIGURES

LIST OF SYMBOLS, ABBREVIATIONS OR NOMENCLATURE

APPFD: average PPFD at the plant apex integrated over time

A_{sat}: light-saturated NCER

BSWF: biological spectral weighting function

CB: culture basin

CBD: cannabidiol

CBG: cannabigerol

CBGA: cannabigerolic acid

CBN: cannabinol

CCI: chlorophyll content index

COP1: constitutively photomorphogenic 1

DLI: daily light integral

DW: dry weight

F_v/F_m: variable to maximum chlorophyll fluorescence

FW: fresh weight

g: gram

HPS: high pressure sodium

HY5: elongated hypocotyl 5

LAI: leaf area index

LED: light emitting diode

LI: light intensity

LNCER: NCER at LPPFD

LPPFD: localized PPFD at the measured leaf

LRC: light response curve

LSP: light saturation point

m: metre

mg: milligram

NCER: net CO_2 exchange rate

PAR: photosynthetically active radiation

PFD: photon flux density

PPFD: photosynthetic photon flux

QY: maximum quantum yield

RH: relative humidity

ROS: reactive oxygen species

SD: standard deviation of the mean

SE: standard error of the mean

SLW: specific leaf weight

TCBD: total equivalent cannabidiol

TCBG: total equivalent cannabigerol

TLI: total light integral

TΔ^9-THC: total equivalent Δ^9-tetrahydrocannabinol

UDL: under detection limit

UV: ultraviolet

UVA: ultraviolet-A

UVB: ultraviolet-B

UV_{BE}: biologically effective ultraviolet

UVC: ultraviolet-C

UVR8: UV resistant phytoreceptor-8

Δ^9-THC: Δ^9-tetrahydrocannabinol

Δ^9-THCA: Δ^9-tetrahydrocannabinolic acid

CHAPTER ONE

INTRODUCTION

1.1 INTRODUCTION TO CANNABIS

Cannabis (*Cannabis sativa L.*) is an annual herbaceous species in the Cannabaceae family, which also includes hops (*Humulus spp.*) (Russo, 2019). Cannabis is primarily a dioecious species (i.e., male and female reproductive organs usually develop on separate plants), but hermaphrodism can occur under stressful conditions (Clarke and Merlin, 2016; Larsson and Lagerås, 2015; Punja and Holmes, 2020). Sexual dimorphism occurs late in cannabis plant development, where female plants are differentiated from male plants at the onset of flowering (Cristiana Moliterni et al., 2004; ElSohly et al., 2017). The growth cycle of cultivated cannabis typically consists of three stages: propagation, vegetative growth, and flowering. Cannabis is typically a short-day plant; where the vegetative stage is maintained under long days (e.g., 16-h to 18-h days), and the flowering stage is initiated under short days when a critical uninterrupted dark period per day is met, with commercial producers typically using a 12-h light and 12-h dark regime (Potter, 2014). There is the exception of some cultivars that flower depending on plant age rather than the number of hours of uninterrupted dark exposure, which are labelled as day-neutral or auto-flowering, but they are not yet extensively used commercially (Clarke and Merlin, 2016).

Unseeded female cannabis flowers are typically cultivated due to their higher cannabinoid concentration than seeded flowers, vegetative tissues or male flowers (Potter et al., 2018). Each enlarging female inflorescence consists of bracts that are covered in multicellular, secretory glandular trichomes that accumulate a sticky resin containing a mixture of secondary metabolites (Farag and Kayser, 2015; Small, 2017). These secondary metabolites include aromatic terpenes and a class of terpenophenolic compounds called phytocannabinoids (ElSohly et al., 2017). In humans, phytocannabinoids bind to endocannabinoid system receptors, specifically the cannabinoid receptor 1 and cannabinoid receptor 2 (Pertwee, 1997). These receptors allow cannabinoids to induce psychoactive and therapeutic effects in humans (Gonçalves et al., 2019). The term phytocannabinoid is used to characterize cannabinoids that originate from plants, as

opposed to endocannabinoids which originate from the mammalian brain (Maroon and Bost, 2018). Given the botanical focus of this thesis, phytocannabinoids will be referred to as cannabinoids hereafter. The dominant cannabinoids in mature cannabis inflorescence tissues are Δ^9-tetrahydrocannabidiolic acid (Δ^9-THCA), cannabidiolic acid (CBDA), and cannabigerolic acid (CBGA), which are converted to the more medicinally relevant compounds, Δ^9-tetrahydrocannabidiol (Δ^9-THC), cannabidiol (CBD) and cannabigerol (CBG), through decarboxylation (Eichler et al., 2012; Zou and Kumar, 2018). Medicinally relevant cannabinoids can be psychoactive (e.g., Δ^9-THC), or non-psychoactive [e.g., CBD, CBG, cannabichromene (CBC)] (ElSohly et al., 2017; Flores-Sanchez and Verpoorte, 2008). Cannabinoid receptor 1 was discovered in 1988, followed by cannabinoid receptor 2 in 1993 (Pertwee, 2006). Δ^9-THC exerts its analgesic and psychoactive effects through interacting with cannabinoid receptors, especially cannabinoid receptor 1 (Gonçalves et al., 2019). The cannabinoids in cannabis inflorescences are therefore valuable to the medicinal market.

There has been some controversy over differentiating between the subspecies of cannabis; *Cannabis sativa* sp. *sativa* and *Cannabis sativa* sp. *indica* (McPartland, 2018), both genetically and morphologically. McPartland (2018) argues that the interbreeding and hybridization between subspecies renders the distinction between them irrelevant. Conversely, it is more relevant for producers and consumers to distinguish cannabis by chemotypes as per their cannabinoid content, ratio of Δ^9-THC to CBD in the inflorescence (i.e., chemotypes) or anticipated product end-use. Chemotype I has a Δ^9-THC to CBD ratio >1, chemotype II has and intermediate Δ^9-THC to CBD ratio ≈1, whereas chemotype III contains has a Δ^9-THC to CBD ratio <1 (Small and Beckstead, 1973). Cannabis product end-uses are usually categorized by either fiber-type or drug-type. Fiber-type cannabis is cultivated for the edible seeds and oil, and/or for the bast-fibers used to make textiles (Behr et al., 2016; Clarke and Merlin, 2016), whereas drug-type cannabis is often cultivated for the unfertilized female flowers containing psychoactive Δ^9-THC, which can induce relaxation and euphoria (Clarke and Merlin, 2016). In recent years, research has elucidated the therapeutic benefits of CBD, and all three chemotypes are now cultivated for the medicinal and recreational use of cannabinoids in the unfertilized female flower (Lewis et al., 2018). Thus, all three chemotypes could be considered “drug-types”.

1.2 HISTORY OF CANNABIS

1.2.1 MEDICINAL USES THROUGH HISTORY

Humans have a long history with cannabis, with cultivation dating back millennia (Clarke and Merlin, 2016). Pollen fossils indicate that cannabis may have originated in the northeastern Tibetan Plateau 19.6 million years ago, and also may have dispersed to Europe over a million years ago (McPartland, 2018). The earliest record of cannabis use dates back to the 28th century BC, in the *Shennong Ben Cao Jing*, one of the oldest books of Chinese medicine compiling oral traditions (Russo, 2007). There is reference to the medicinal use of cannabis throughout history, including in Ancient Egypt, Greece, and the Roman Empire (Russo, 2007).

1.2.2 PROHIBITION

Cannabis was used as a medicinal drug in the United States pharmacopeia before it was prohibited in the early 20th century (Valdez and Kaplan, 2019). In 1923, cannabis drug use and possession became illegal in Canada under the Opium and Narcotic Drug Act (Graham, 2004), but it was not commonly used. There were only 25 convictions for cannabis possession in Canada between 1930 and 1946, but after a cultural shift often attributed to the hippie movement, there were 12,000 convictions in 1972 alone (Kenny and Nolin, 2003). The cannabis market quickly dominated the illicit drug market in North America and worldwide, in terms of number of consumers and amount of production [United Nations Office on Drugs and Crime (UNODC), 2009; 2019]. However, the lack of reliable data and scientific research on the production and use of cannabis complicates the accurate estimation of its prevalence (UNODC, 2009). In 2007, the majority of the world's cannabis seizures occurred in Mexico (37%) followed by the United States (26%) (UNODC, 2009). Due to the legal restrictions on cannabis in Canada and much of the world, there has been very limited scientific research on both cannabis cultivation and medicinal cannabis use throughout the 20th century (Graham, 2004; Magagnini et al., 2018).

1.2.3 LEGALIZATION AND USAGE

In 2002, Canada became the first country to introduce government-regulated access to cannabis for a list of medicinal purposes with the Marijuana Medical Access Regulations (Government of Canada, 2016; Graham, 2004). Subsequently in 2013, the Government of Canada implemented the Marijuana for Medical Purposes and Regulations, which provided the commercial industry rules and regulations for production and distribution of dried cannabis inflorescences (Government of Canada, 2016). Following that, the Government of Canada permitted licensed producers to sell cannabis oil and allowed authorized users to possess other forms of cannabis in 2015 (Government of Canada, 2016). The Marijuana for Medical Purposes and Regulations was updated and renamed in 2016 to the Access to Cannabis for Medical Purposes Regulations, which allowed authorized cannabis users to possess 4 cannabis plants in order to produce their own medicine (Government of Canada, 2016). As of October 17 2018, the production and sale of recreational cannabis became legal in Canada under the Cannabis Act (Government of Canada, 2019a). The objectives of this legislation were to reduce cannabis use in youth (under the age of 18), prevent organized crime from profiting from the sale and distribution of cannabis, and to protect public health and safety by allowing Canadian adults to access regulated, legal cannabis (Government of Canada, 2019b). Several other countries have decriminalized medicinal and recreational cannabis use including Uruguay, Georgia, Jamaica, the Netherlands, Israel and even some US states (Cannigma, 2019; Leggett, 2006; UNODC, 2019).

The legal cannabis market faces the economic challenge of competing with illicit trade (UNODC, 2019). When governments decide on the tax rates for cannabis products, one consideration is keep the cost low enough to displace the illegal cannabis market and prevent organized crime from profiting (UNODC, 2019). In 2019 about 40% of cannabis consumers obtained cannabis from an illegal supplier (Rotermann, 2020). Despite revenue lost to criminals involved with the illicit trade of cannabis, the legal cannabis industry benefits the economies of countries where it has become legal by creating jobs. The legal cannabis industry provided 211,000 Americans with jobs in 2019 (Barcott and Whitney, 2019).

The legalization of cannabis across North America has been accompanied with a resurgence of interest in its medicinal properties. Recent research on cannabinoids has elucidated their analgesic, anti-inflammatory, appetite stimulating and anti-emetic properties have the potential to treat a number of ailments including pain, nausea, depression and alleviation of symptoms of HIV/AIDS, Parkinson's and Huntington's disease, and cancer, to name a few (Guindon and Hohmann, 2009; Pacher et al., 2006; Slatkin, 2007; Viveros et al., 2005). In the Americas, cannabis use has increased from 42 million people (i.e., 7% of the population aged 15-65) in 2007 to 57 million people (i.e., 8.4% of the population aged 15-65) in 2017 (UNODC, 2019). In Canada alone, it was reported in 2015 that 14.7% of the Canadian population aged 15 and older used cannabis at least once in the past year (Government of Canada, 2015). As cannabis usage continues to increase with worldwide legalization, cannabis cultivation methods must improve to keep up with the increasing demand.

1.3 CANNABIS CULTIVATION

1.3.1 CURRENT PRACTICES

Cannabis is produced in the majority of countries around the world, unlike other plant-based drug production that are often only produced in a select number of countries (UNODC, 2019). Cannabis is cultivated either in outdoor fields or in controlled environments, such as indoors or in greenhouses (Chandra et al., 2017; Leggett, 2006; Potter, 2014). According to qualitative data reported by Member States to the UNODC (2019), both outdoor and controlled-environment cannabis cultivation increased globally from 2013 to 2017, although controlled-environment cultivation appears to have a larger increase than outdoor. The increase in controlled-environment cannabis cultivation is closely associated with an increase in Δ^9-THC content on the market (UNODC, 2019). The advantage of indoor cultivation (vs. greenhouse or outdoor) is that it affords *complete* control over the lighting environment including the manipulation of light intensity (LI), spectrum or "quality", as well as photoperiod. Cannabis growers alter the photoperiod to control the growing cycle, specifically to maintain the vegetative stage or trigger flowering (Leggett, 2006; UNODC, 2019). Controlled-environment cultivation allows growers to yield more crops per year than outdoor production in northern climates (ElSohly et al., 2017; Leggett, 2006). Controlled-environment cannabis cultivation allows for sinsemilla production,

which originates from the Spanish term “sin semilla,” meaning without seeds. In other words, controlled environments protect against pollination from male plants, except in the event of stress-induced hermaphrodism (Punja and Holmes, 2020). In sinsemilla cannabis production, female plants are mainly propagated asexually using uniform vegetative cuttings (Chandra et al., 2017; Clarke and Merlin, 2016), often grown in soilless production systems (Farag and Kayser, 2015; Leggett, 2006). Sinsemilla production results in consistent, unfertilized inflorescences with higher Δ^9-THC concentrations as compared to fertilized inflorescences (Chandra et al., 2017; Clarke and Merlin, 2016; Leggett, 2006; UNODC, 2019), presumably due to carbon costs of seed rather than glandular trichome production. Clarke and Merlin (2016) indicate that sinsemilla growers typically look for six economically desirable traits in their plants: 1) high dry biomass yields, 2) high proportion of inflorescences compared to stems and leaves, 3) many large glandular trichomes, 4) high total cannabinoid content in inflorescences, 5) reproducible profile of cannabinoids, and 6) desirable aromatic terpenes. These traits are not only genetically selected for, but they may also be impacted by the plant’s growing environment and horticultural management strategies. Of the environmental parameters in a plant’s growing environment, light may be the most influential.

1.4 LIGHT INTENSITY IN CANNABIS PRODUCTION

The plasticity of morphological and physiological traits in plants is determined by an equilibrium between endogenous growth processes and exogenous environmental influences (Barthélémy and Caraglio, 2007; Jansen et al., 2017). LI and spectrum modulate photosynthetic activity and photomorphogenic signals, which initiate processes such as cell division and elongation, directional growth and branching, all of which contribute to plant vegetative growth and development (Huché-Thélier et al., 2016). In indoor cannabis production, LI is a controlled environmental input that has a major impact on plant photosynthesis, growth and yield. Understanding the morphological, physiological and yield-related impacts of LI on cannabis plants through the flowering stage will assist cannabis growers in determining optimal LI for their production. In temperate environments, e.g., regions such as Ontario, the low natural LI and shorter photoperiods (i.e., more than 12-hr nights) than those required in the winter months is not optimal for cannabis production. As a result, either supplemental lighting in greenhouses or sole-

source lighting in indoor production is required winter production. The energy costs related to lighting (and heat and ventilation associated) in indoor cannabis production make up about 60% of the total energy consumed by cannabis growers, meaning that lighting is one of the most expensive environmental inputs (Mills, 2012). Since light is a valuable resource for cannabis production, the selected LI for production should be chosen to maximize yield in proportion to energy use. However, there is a lack of scientifically-validated information in the literature on cannabis' response to LI in indoor production.

It is well-known that a plant's photosynthesis, growth and yield (e.g., total aboveground biomass) respond proportionally to photosynthetically active radiation (PAR) at lower light levels, followed by a logarithmic phase (gradual decreasing gains in productivity) up to maxima LI (light saturation point; LSP) whereby further increases of PAR do not result in additional photosynthesis and biomass production and other plant growth indices (Lobo et al. 2013). For example, the meta-analysis by Poorter et al. (2019) demonstrates that total dry biomass saturates in both woody and herbaceous species as function of LI, with high plasticity. Photosynthesis is often measured as a Net CO_2 Exchange Rate (NCER), and is often referred to in the literature as CO_2 assimilation or "A" (Zheng et al., 2006; Bernacchi et al., 2003; Ainsworth and Rogers, 2007). The NCER at the LSP is called the light-saturated NCER, which often referred to as "A_{sat}" in the literature (Bernacchi et al., 2003; Ainsworth and Rogers, 2007). The LI resulting in the highest NCER, growth or biomass in proportion to the light energy input is optimal for production. In this light response curve (LRC), the "optimal" LI is at the end of the linear increase, before the LSP. The availability of PAR is often a limiting factor (i.e., in the linear portion of the LRC) for yield in indoor production. Growing crops with insufficient light (i.e., below "optimal," as defined here) limits the yield potential, which in turn wastes the other production inputs including labour, water, nutrients and electricity. Choosing a LI for production that is above optimal results in diminished yield returns in proportion to the energy input, thereby increasing costs without yield gain. The optimum LI may also depend on other factors in the production environment (including the production goals of the grower), since lighting is only one of the input costs for production. Overall, LRCs are a useful tool to identify saturating LIs, but there are no yield LRCs for cannabis growers to use for optimizing their light intensity.

1.4.1 EFFECTS OF LIGHT INTENSITY ON CANNABIS PHOTOSYNTHESIS, GROWTH AND YIELD

Plants in nature are restricted to their permanent locations – i.e., they are sessile and must acclimate to their surrounding light environment to maintain photosynthesis, growth and yield. Leaves contain light-activated proteins called photoreceptors that perceive LI, light quality and light duration and subsequently signal changes to gene expression (Casal, 2013; Thoma et al., 2020). High-light grown plants typically have higher total vegetative dry mass and more branching than low-light grown plants (Poorter et al., 2019). The lighting environment in which an individual leaf is acclimated also has a substantial impact on its morphology (e.g., high-light grown leaves often have thicker leaves with smaller leaf area) and physiology (e.g., high-light grown leaves often have higher LSPs compared to low-light grown leaves) (Murchie et al., 2002; Walker et al., 1989). Consequently, the varying LI within a canopy (i.e., upper canopy leaves compared to lower canopy leaves) results in leaves with varying morphology and physiology (Bauerle et al., 2020; Campbell et al., 1992; Namdar et al., 2018). Although plant LRCs all follow a similar asymptotic trend, specific LRC equations are dependent on several factors, such as plant species, leaf age and the growing environment in which the plant was acclimated (e.g., temperature, CO_2 concentration, vapour pressure deficit, and the lighting environment).

Chandra et al. (2008) is a frequently cited study in relation to canopy-level lighting strategies for optimal cannabis growth (Jaeger, 2019), yield (Coco for Cannabis, n.d.; Mammoth Lighting, n.d.) and productivity (Downer, 2018; Royal Queen Seeds, 2019). Chandra et al. (2008) found that A_{sat} in a Mexican variety of cannabis was 24.6 $\mu mol \cdot m^{-2} \cdot s^{-1}$ at the estimated LSP of 1500 $\mu mol \cdot m^{-2} \cdot s^{-1}$ based on LRCs for single-leaf in the upper canopy; however, the LI that the leaves were acclimated to and the leaves' ages are unknown. Photosynthetic responses do not directly predict yield response, especially when important context (e.g., leaf age and light history) is unreported (Sadras and Richards, 2014).

Although an outcome of photosynthesis in a leaf is CO_2 assimilation, there are many factors within a canopy to consider before correlating leaf-level photosynthesis with aboveground biomass yield. Leaves in the upper canopy are exposed to higher LI than the lower canopy, so their NCER, A_{sat} and LSPs are typically higher by comparison (Bauerle et al., 2020; Murchie et

al., 2002; Pettersen et al., 2010). Even within the same plant, leaves with higher vertical leaf positions are younger and have higher A_{sat} (i.e., higher CO_2 assimilation capacity) (Bauerle et al., 2020; Murchie et al., 2002), higher nitrogen and carbon (% dry weight) and higher chlorophyll content per area ($\mu g \cdot cm^{-2}$) compared to lower leaf positions (Gara et al., 2018). Additionally, respiration must be factored in to comprehend the net CO_2 assimilation in a whole plant. Leaf respiration tends to be more pronounced in leaves that undergo high rates of photosynthesis compared to lower rates of photosynthesis, therefore, similar to the variability of photosynthesis throughout a canopy, respiration varies with vertical leaf position (i.e., a leaf at the top of the plant having the highest A_{sat} is associated with the highest light-dependent and -independent respiration) (Weerasinghe et al., 2014). Additionally, the canopy does not absorb all available light; some light is reflected and the transmittance through the canopy depends on the leaf area index [LAI; $m^2_{(leaf)}/m^2_{(ground)}$] and the leaf angle relative to incoming light (Posada et al., 2012). Since light absorption varies drastically throughout the canopy, leaf photosynthetic responses vary throughout the canopy as well.

Increased LAI can increase the amount of CO_2 assimilation within a plant, but depending on the level of LAI increase, there could be too much shade within the canopy and the cost of increased leaf area no longer outweighs the benefit (Peng, 2000). The aforementioned complexity of varying morphology and physiology means that several parameters must be considered to accurately understand whole-canopy photosynthesis, and single-leaf gas exchange measurements from only the upper canopy leaves are not indicative of whole-canopy photosynthesis. Due to the many factors to consider when relating leaf-level photosynthesis to whole-canopy yield responses to light, the impact of LI on cannabis yield must be related to the actual yield (i.e., cannabis inflorescence weight) to accurately model the relationship. In other terms, a yield LRC for cannabis will be useful for cannabis growers to understand the relationship between canopy-level LI and yield.

Some studies have established that cannabis yields are greater at higher LIs relative to low LIs. For example, Potter and Duncombe (2012) grew cannabis plants under high pressure sodium (HPS) lamps with varying canopy-level PPFDs during the flowering stage and found that increasing PPFD from 400 to 900 $\mu mol \cdot m^{-2} \cdot s^{-1}$ increased yield an average of 1.3 times higher,

across seven cultivars, with no LI treatment effects on floral cannabinoid concentrations. Vanhove et al. (2011) found that cannabis yields were 1.3 to 3.1 times higher (depending on cultivar) when plants were grown under approximately 1000 $\mu mol \cdot m^{-2} \cdot s^{-1}$ compared to approximately 450 $\mu mol \cdot m^{-2} \cdot s^{-1}$ during the flowering stage. Although these studies provide some insight into specific yield increase scenarios, the response of cannabis yield to a wide range of LIs is necessary to create a model for cannabis inflorescence yield response to increasing LI (i.e., a yield LRC). Eaves et al. (2020) found that cannabis yield increased linearly as PPFD increased from approximately 500 to 1500 $\mu mol \cdot m^{-2} \cdot s^{-1}$ (i.e., yield was on average 2.5 times higher) during the flowering stage, although there were no data between 1000 and 1500 $\mu mol \cdot m^{-2} \cdot s^{-1}$, and PPFD data were reported based on the height the plants were expected to be at harvest rather than their actual lighting environments in each LI treatment. These studies support the contention that cannabis has very high saturating PPFD on a yield basis relative to other crops. Currently, there is a lack of peer-reviewed literature for commercial growers to refer to when deciding on optimal LI for production (Backer et al., 2019; Eichhorn Bilodeau et al., 2019). Therefore, studies elucidating cannabis inflorescence yield response to increasing LI (i.e., yield LRCs) are required to add to the current literature and guide commercial growers to make informed decisions on optimal LI for cannabis production.

1.5 ULTRAVIOLET RADIATION IN PLANT PRODUCTION

Ultraviolet (UV) radiation in the solar spectrum is divided into three wavelength ranges: UVA (315 to 400 nm), UVB (280 to 315 nm), and UVC (100 to 280 nm). The ozone layer of Earth's atmosphere absorbs the harmful wavelengths of UVC and some wavelengths in the UVB band but allows UVA and some UVB wavelengths to reach ground level (De Gruijl and Van der Leun, 2000). The ozone layer began thinning in the 1970s, allowing some of the shorter, more harmful UV wavelengths to reach ground level. Upon the discovery of ozone depletion, researchers sought to identify the risks that shorter wavelength UV radiation might have on life on Earth. While the stratospheric ozone layer has recovered in most locations, the research efforts identifying the effects of UV on agricultural plants uncovered its potential benefits. Using horticultural science to test for optimal UV treatments in different species, UV radiation can be used to manipulate crops to attain desirable traits.

Photomorphogenic responses to UV radiation are achieved through the activation of gene expression (Jenkins, 2017), such as that of the UV resistant phytoreceptor-8 (UVR8) (Huché-Thélier et al., 2016; Yin and Ulm, 2017) or through UV-induced oxidative damage (Tossi et al., 2019). UV radiation activates UVR8, allowing it to bind to the protein called constitutively photomorphogenic 1 (COP1), which initiates UV signalling (Huché-Thélier et al., 2016; Yin and Ulm, 2017). The UV dependent interaction between UVR8 and COP1 is required for the expression of *ELONGATED HYPOCOTYL 5* (*HY5*) transcription factor (Jenkins, 2017). UV radiation regulates the expression of many genes through UVR8-independent pathways as well. UVR8-independent pathways may be triggered under more severe UV treatments (i.e., long-term exposure, exposure to short wavelength radiation such as UVC) that induce oxidative damage. Oxidative damage includes DNA mutagenesis through the formation of a dimer that inhibits transcription and replication (Tossi et al., 2019), or through disruption resulting from UV-induced reactive oxygen species (ROS) (Czégény et al., 2016). Overall, UV radiation can modulate the expression of hundreds of genes, leading differential expression of plant metabolism, morphology and physiology (Jenkins, 2017).

Biological responses to UV radiation are more sensitive to the shorter-wavelength (e.g., UVC) radiation within the UV waveband (i.e., more energetic UV spectra) than to the longer wavelength radiation (e.g., UVA) (Flint and Caldwell, 2003). Since the biological effects of UV radiation are highly wavelength specific, many studies express UV treatments by multiplying spectral irradiance at each wavelength by a Biological Spectral Weighting Function (BSWF). Applying a BSWF specifically for plant growth responses to UV radiation treatments provides a more accurate depiction of how the spectra will affect plant growth (Flint and Caldwell, 2003). Although UV is only present in sunlight in small quantities relative to PAR, its shorter wavelengths are disproportionately effective in plant response, which is accounted for with the BSWF. Even after weighting each wavelength, the severity of the UV radiation treatment applied to a crop is dependent on the intensity, the photoperiod (i.e., hours of UV radiation per day) and number of days of exposure throughout the crop life cycle. Long-term UV exposure can cause plant stress, whereas short-term exposure can induce minimal stress that elicits a beneficial outcome to the organism (Robson et al., 2019; Wargent and Jordan, 2013). Under stronger

exposure levels, UV radiation can induce damage to the cellular DNA of a plant, leading to genome instability and abnormalities in plant development (Friedberg, 2002; Manova and Gruszka, 2015). DNA damage can be induced directly from the absorption of UV photons or by the UV-driven production of ROS, which disrupts the balance between ROS production and ROS scavenging, ultimately leading to oxidative stress (Robson et al., 2019). This oxidative stress can damage DNA, lipids and proteins. On the other hand, other minor stress responses may include the UV stimulated expression of genes involved in flavonoid biosynthesis and antioxidant activity, which may be desirable secondary metabolites in crop production (Robson et al., 2019). Since the shorter wavelengths in the UV waveband have stronger biological effects (Flint and Caldwell, 2003), and amount of time of treatment impacts the biological effects of UV radiation, it is important to consider not only intensity, but also wavelength and time when evaluating the UV radiation treatments as reported in the literature. However, there is a lack of consistency with the use of BSWFs in the current literature relating to plant responses to UV radiation, where recent studies often refer to BSWF by Flint and Caldwell (2003) and older studies refer to the BSWF by Caldwell (1971). There is also a lack of consistency when reporting of UV intensity, photoperiod, and wavelength (Huché-Thelier et al., 2016). Therefore, caution is required when analyzing data on plant responses to UV radiation, and it may be most relevant to compare the current literature in relative terms rather than absolute UV treatments.

Although there is a large body of literature focused on the effects of UV radiation on agronomic and horticultural crops, the UV exposure conditions are highly variable between research groups. Experimental designs typically include versions of 1) low compared to high UV radiation treatments using UV lamps, or 2) UV radiation exclusion treatments compared to ambient sunlight UV exposure. Many of these experiments have variable UV to PAR ratios, and use UV lamps that may contain shorter or longer wavelengths than reported (e.g., UVC or UVA). Some studies are conducted using sunlight as the source of PAR, while others use various indoor production lighting methods, with variable spectrums. There are often large differences between plant UV response in controlled indoor environments compared to outdoor field environments (Robson et al., 2019). Plants exhibit higher sensitivity to UV radiation as UV:PAR increases (Behn et al., 2010; Dou et al., 2018), and other spectra present within the treatments can

influence the plant sensitivity to UV radiation as well (Palma et al., 2021). Often, the units of reported UV treatments between studies are highly variable (Huché-Thélier et al., 2016). Given the wide range of variability between UV exposure conditions, the effects of UV radiation on plant growth, yield, physiology, and secondary metabolites are highly variable as well.

Despite the variability in the effects of UV radiation on plant morphology and physiology, there has been a well-established understanding of the "UVB phenotype" (Robson et al., 2019; Jansen et al., 2017). UVB exposure has been shown to decrease plant stem length in a variety of monocotyledons and dicotyledons (Barnes et al., 1990; Liu et al., 2013) and increase number of branches (e.g., in dicotyledons such as bean and rose) and tillers (e.g., in monocotyledons such as oat and wheat) (Barnes et al., 1990; Torre et al., 2012) leading to reduced internode lengths and an overall more compact phenotype. Leaf area is highly affected by UVB exposure with decreases at higher vs. lower levels of UVB in wheat and wild oat, rapeseed, four cultivars of cucumber, three cultivars of rose and two cultivars of soya (Barnes et al., 1990; Cen and Bornman, 1993; Krizek et al., 1997; Terfa et al., 2014; Zhang et al., 2014). Other commonly reported impacts of UVB exposure include increased specific leaf weight (SLW; $g \cdot cm^{-2}$), a proxy for leaf thickness (Cen and Bornman, 1993; Zhang et al., 2014), a reduction in total leaf number (Krizek et al., 1997), a reduction in petiole length (Krizek et al., 1997; Zhang et al., 2014), and changes in leaf shape (i.e., leaf length:width) (Hectors et al., 2010; Klem et al., 2012; Robson and Aphalo, 2012). Less frequently reported responses to UVB exposure include epicuticular wax accumulation, which may decrease UVB penetration by reflectance (Cen and Bornman, 1993) and leaf epinasty, which is when tissue between leaf venation concaves away from incident light (Fierro et al., 2015; Jansen, 2002).

Some studies have reported bumpy leaf surfaces and necrotic spots on leaves that were exposed to UVB (Klem et al., 2012; Torre et al., 2012). In *Lactuca sativa* L. and *Cucumis sativus* L. excluded from UV exposure, higher total dry weight (DW) relative to the UVB exposure treatment has been reported (Krizek et al., 1997). However, morphological responses to UVB, such as reduced plant height and increased branching, can occur without alterations to carbon assimilation and total shoot DW (Barnes et al., 1990). UVB exposure induces early flowering in poinsettia (Torre et al., 2012), but *Setaria* and *Amaranthus* species exposed to UVB

demonstrated increases in biomass allocation to main shoot reproductive tissues (Barnes et al., 1990). UVB radiation also has the potential to reduce disease incidence for cannabis diseases such as powdery mildew (Austin and Wilcox, 2012; Demkura and Ballaré, 2012). Although there are many studies reporting the effects of UVB on a variety of species, there are many potential impacts of UVB on plant morphology, which may be variable depending on the UVB exposure conditions (e.g., UVB lamps versus sunlight exposure), treatments (e.g., hours per day and days per growing cycle).

UVB exposure in many plants can impact leaf stress and physiology. Gas exchange parameters (such as NCER and A_{sat}) are often lower in leaves that are exposed to supplemental UVB (Dou et al., 2018; Hoffmann et al., 2015; Pacher et al., 2006; Yang et al., 2008; Zhang et al., 2014), which could indicate damage to the photosystems. Hoffman et al. (2015) also found that supplemental UVB radiation induced stress in pepper leaves demonstrated by a decline in dark-adapted chlorophyll fluorescence (F_v/F_m). Chlorophyll content has been found to either increase or decrease in a wide range of other dicotyledons and monocotyledons in response to UVB radiation (Neugart and Schreiner, 2018). Plants demonstrate a higher sensitivity to UVB under higher UV:PAR with respect to total chlorophyll content (Chl $a + b$; µg cm^{-2}), A_{sat} and F_v/F_m (Klem et al., 2012). Such variations in physiological and morphological responses to UVB may be attributed to the highly variable UVB exposure conditions and differences in UV:PAR. For cannabis production, understanding the effects of UVB exposure on whole plant morphology and leaf physiology is relevant to production when it comes to establishing a UVB exposure damage threshold.

1.5.1 EFFECTS OF ULTRAVIOLET RADIATION ON CANNABIS PHOTOSYNTHESIS, GROWTH AND SECONDARY METABOLITES

The application of UV radiation during cultivation is an area of interest in the cannabis industry for its purported potential to increase cannabinoid concentration in mature female cannabis inflorescences tissues (hereafter, inflorescences). It has been shown that cannabis plants with higher Δ^9-THC to CBD ratios typically originated from equatorial regions (i.e., latitudes between the equator and 30°N or S, whereas plants with low Δ^9-THC and high CBD concentrations typically originate from latitudes north of 30°N or south of 30°S) (Small & Beckstead, 1973;

Small & Cronquist, 1976). Pate (1983) proposed a protective function model suggesting that Δ^9-THC protects cannabis tissue (i.e., leaves and inflorescences) from UV radiation. Factors proposed to contribute to this hypothetical model include: high Δ^9-THC production in plants grown in areas with high UV irradiation (e.g., high altitudes, low latitudes), the UV absorbing properties of Δ^9-THC, and high Δ^9-THC production in the female floral tissues which are responsible for reproductive success and must endure longer UV exposure than the male flowers. The findings by Pate (1983) showed that Δ^9-THC concentration in cannabis inflorescences is higher in plants with origins that have high UV exposure [in watt-sec·cm^{-2}, 302.5-312 nm, according to the world distribution map of UV exposure by Schulze and Grafe (1969)] and conversely there is a negative correlation between CBD concentration and high UV exposure.

UV application may be a useful tool to increase Δ^9-THC concentration in indoor production of modern drug-type cannabis genotypes. Horticultural researchers have evaluated plant responses to UV in indoor cannabis production settings. Early controlled-environment studies postulate there is a potential for UV radiation to increase Δ^9-THC concentration in cannabis leaf and inflorescence tissues (Fairbairn and Liebmann, 1974; Lydon et al., 1987), however the concentration of Δ^9-THC in typical inflorescences has increased over time where modern cannabis genotypes have ≈10× higher Δ^9-THC concentration in inflorescence tissue compared to the older genotypes used in older studies (Dujourdy and Besacier, 2017). It is possible that modern cannabis genotypes are near their maximum genetic ability to produce Δ^9-THC, impeding their ability to further increase inflorescence Δ^9-THC concentration in response to UV radiation, relative to older genotypes. Giupponi et al. (2020) found that CBD-dominant cannabis inflorescences exposed to high UV (i.e., higher altitudes) had greater CBD and terpene concentrations compared to plants exposed to low UV (i.e., lower altitudes), suggesting that Δ^9-THC may not be the only cannabinoid upregulated in response to UV radiation. Cannabinoid concentration has also been shown to vary with temperature conditions (Bazzaz et al., 1975), sub-optimal nutrient availability (Caplan et al., 2017; Haney and Kutscheid, 1973; Yep et al., 2020) and drought stress (Caplan et al., 2019; Haney and Kutscheid, 1973; Latta and Eaton, 1975). In general, there is potential for beneficial responses as a result of environmental changes in even in modern cannabis genotypes.

Currently, there are a few studies that demonstrate the potential to increase cannabinoid yields in cannabis inflorescences with the application of UV radiation during production (Giupponi et al., 2020; Lydon et al., 1987; Marti et al., 2014). However, there are no reliable studies demonstrating an increase in cannabis inflorescence cannabinoid concentration with reproducible, clearly defined UV treatments (i.e., hours of application, days of application, intensity in either radiant flux or photon flux units, peak wavelengths) that are relevant to modern cannabis production (i.e., using supplemental UV lamps in an indoor production facility and modern cannabis genotypes). There are no studies in the current literature that determine the effect of UV radiation on cultivars with balanced Δ^9-THC:CBD, which would indicate differences between cannabinoid responses.

1.6 THESIS STRUCTURE AND OBJECTIVES

Considering the limited scientific research on LI and UV radiation in cannabis production and the economic and medicinal importance of this crop, the goal of this thesis was to determine the effects of these treatments on cannabis photosynthesis, growth, inflorescence yield, and cannabinoid concentrations. Determining how cannabis responds to various lighting strategies in the flowering stage will provide insight into the optimization of cannabis production.

The specific objectives were to develop descriptive models can be used widely in the Cannabis industry and future research relating:

1. LI and cannabis leaf-level photosynthesis, and inflorescence yield and quality.

2. UV exposure levels and cannabis morphology, physiology, and inflorescence yield and quality via photoprotection mechanism.

Note: Chapter 2 and 3 follow the Frontiers' style guidelines and have been submitted to Frontiers in Plant Science, under the research topic entitled 'Smoke and Mirrors: Reflections on Improving Cannabis Production and Investigating Medical Potential'. Chapter 2 has been accepted and published:

Rodriguez-Morrison, V., Llewellyn, D. and Zheng, Y. (2021). Cannabis yield, potency, and leaf photosynthesis respond differently to increasing light levels in an indoor environment. Front. Plant Sci. 12:646020. doi: 10.3389/fpls.2021.646020.

CHAPTER TWO

CANNABIS YIELD, QUALITY, AND LEAF PHOTOSYNTHESIS RESPOND DIFFERENTLY TO INCREASING LIGHT LEVELS IN AN INDOOR ENVIRONMENT

ABSTRACT

Since the recent legalization of medical and recreational use of cannabis in many regions worldwide, there has been high demand for research to improve yield and quality. With the paucity of scientific literature on the topic, this study investigated the relationships between LI and photosynthesis, inflorescence yield, and inflorescence quality of cannabis grown in an indoor environment. After growing vegetatively for 2 weeks under a canopy-level PPFD of ≈425 $\mu mol \cdot m^{-2} \cdot s^{-1}$ and an 18-h light/6-h dark photoperiod, plants were grown for 12 weeks in a 12-h light/12-h dark "flowering" photoperiod under canopy-level PPFDs ranging from 120 to 1800 $\mu mol \cdot m^{-2} \cdot s^{-1}$ provided by LEDs. Leaf LRCs varied both with localized (i.e., leaf-level) PPFD and temporally, throughout the flowering cycle. Therefore, it was concluded that the leaf light response is not a reliable predictor of whole-plant responses to LI, particularly crop yield. This may be especially evident given that dry inflorescence yield increased linearly with increasing canopy-level PPFD up to 1800 $\mu mol \cdot m^{-2} \cdot s^{-1}$, while leaf-level photosynthesis saturated well below 1800 $\mu mol \cdot m^{-2} \cdot s^{-1}$. The density of the apical inflorescence and harvest index also increased linearly with increasing LI, resulting in higher-quality marketable tissues and less superfluous tissue to dispose of. There were no LI treatment effects on cannabinoid concentration, while there were minor LI treatment effects on terpene concentration. Commercial cannabis growers can use these light response models to determine the optimum LI for their production environment to achieve the best economic return; balancing input costs with the commercial value of their cannabis products.

2.1 INTRODUCTION

Drug-type cannabis (i.e., genotypes grown for their high cannabinoid content; hereafter, cannabis) is often produced indoors to allow complete control of environmental conditions, which is important for producing consistent medicinal plants and products (UNODC, 2019;

Zheng, 2020). Total reliance on electrical lighting for plant production gives growers the capability to manipulate crop morphology, yield, and quality using light. However, lighting-related costs comprise ≈60% of total energy used for indoor cannabis production (Evergreen Economics, 2016; Mills, 2012); making crop lighting one of the most substantial input costs for growing cannabis indoors. With recent nationwide legalization in Canada (among many other regions worldwide), energy demand for indoor cannabis production is expected to increase rapidly as the industry intensifies production to address rising demand (Sen and Wyonch, 2018).

There are many factors that govern the cost of producing PAR for indoor cannabis production. These factors include: the capital and maintenance costs of lighting fixtures and related infrastructure, efficiency of converting electricity into PAR [usually referred to as PAR efficacy; in units of $\mu mol_{(PAR)} \cdot J^{-1}$], management of excess heat and humidity, and uniformity of PAR distribution within the plant canopy. The most common lighting technologies used for indoor cannabis production are high intensity discharge (e.g., HPS) and LED (Evergreen Economics, 2016; Mills, 2012). These technologies have widely varying spectrum, distribution, PAR efficacy, and capital costs. However, regardless of the lighting technology used, the dominant factor that regulates the cost of crop lighting is the target canopy-level LI.

One common precept in controlled-environment agriculture production is that crop yield responds proportionally to increasing LI; i.e., the so-called "1% rule" whereby 1% more PAR equals 1% greater yield (Marcelis et al., 2006). On a per-leaf basis, this principle is clearly limited to lower light intensities, since light use efficiency [i.e., maximum quantum yield; QY, $\mu mol_{(CO_2)} \cdot \mu mol^{-1}_{(PAR)}$] of all photosynthetic tissues begins to decline at LI well below their LSPs (Posada et al., 2012). However, in indoor-grown cannabis, it is conceivable that whole-plant photosynthesis will be maximized when LI at the upper canopy leaves are near their LSP. This is partly attributable to the inter-canopy attenuation of PAR from self-shading; allowing lower-canopy foliage to function within the range of LIs where their respective light use efficiencies are optimized (Terashima and Hikosaka, 1995). This may be especially relevant to indoor production, where relatively small changes in distance from the light source can impart substantial differences in foliar LI (Niinemets and Keenan, 2012). Further, distinguished from

many other indoor-grown crops, cannabis foliage appears to tolerate very high LI, even when exposed to PPFDs that are much higher than what they have been acclimated to (Chandra et al., 2015).

There is a paucity of peer-reviewed studies that have related LI to cannabis cannabinoid concentration and yield (e.g., mass of dry, mature inflorescence per unit area and time). Perhaps the most referenced studies report aspects of single-leaf photosynthesis of several cultivars and under various PPFD, CO_2 concentration, and temperature regimes (Chandra et al., 2011; 2015; Lydon et al., 1987). These works have demonstrated that cannabis leaves have very high photosynthetic capacity. However, they have limited use in modeling whole canopy photosynthesis or predicting yield because single-leaf photosynthesis is highly variable; depending on many factors during plant growth such as: leaf age, their localized growing environments (e.g., temperature, CO_2, and lighting history), and ontogenetic stage (Bauerle et al., 2020; Carvalho et al., 2015; Murchie et al., 2002; Zheng et al., 2006). While lighting vendors have long relied on cannabis leaf photosynthesis studies to sell more light fixtures to cannabis growers, their models are only tangentially related to whole-canopy photosynthesis, growth, and ultimately yield (Kirschbaum, 2011).

Some forensic studies have utilized various methods to develop models to estimate crop yield from illicit indoor cannabis production (Backer et al., 2019; Potter and Duncombe, 2012; Toonen et al., 2006; Vanhove et al., 2011). These models use an array of input parameters (e.g., planting density, growing area, crop nutrition factors) but, rely on "installed wattage" (i.e., $W \cdot m^{-2}$) as a proxy for LI. It is notable that reporting yield as $g \cdot W^{-1}$ (i.e., $g \cdot m^{-2} / W \cdot m^{-2}$) overlooks the instantaneous time factor inherent in power units (i.e., $W = J \cdot s^{-1}$). A more appropriate yield metric would also account for the length of the total lighting time throughout the production period (i.e., $h \cdot d^{-1} \times d$), thus factoring out the time units resulting in yield per unit energy input (e.g., $g \cdot kWh^{-1}$). Furthermore, area-integrated power does not directly correlate to the canopy-level light environment due to a myriad of unknowns, such as hang height, light distribution, and fixture efficacy. It is therefore impossible to accurately ascertain canopy-level LI in these models. Eaves et al. (2020) reported linear relationships between canopy-level LI (up to 1500

μmol·m^{-2}·s^{-1}) and yield; however, they had only one LI treatment above 1000 μmol·m^{-2}·s^{-1}. Furthermore, they reported substantial inter-repetition variability in their yield models, which indicates that factors other than LI may have limited crop productivity in some circumstances. While methodological deficiencies in these studies may limit the confident quantitative extrapolation of their results to production environments, it is striking that none of these studies reported evidence of saturation of inflorescence yield at very high LI.

These studies all demonstrate the exceptionally high capacity that cannabis has for converting PAR into biomass. However, there are also clear knowledge gaps in cannabis' photosynthesis and yield responses to increasing LI. In addition, cannabis products are very high-value commodities relative to other crops grown in indoor environments. This means that producers may be willing to accept substantially higher lighting-related input costs in order to promote higher yields in limited growing areas. However, maximizing yield regardless of cost is not a feasible business model for most cannabis producers; rather there is a trade-off between input costs and crop productivity by selecting the optimum canopy-level LI (among other inputs) that will maximize net profits. Further complicating matters, producers must balance fixed costs which do not vary with crop productivity (such as property tax, lease rates, building security, and maintenance, etc.) and variable costs (such as the aforementioned lighting-related costs among other crop inputs) which can have dramatic impacts on crop productivity and yield (Vanhove et al., 2014). Since indoor crop lighting is a compromise between input costs and crop productivity, it is critical for growers to select the optimum LI for their respective production environment and business models.

The objectives of this study were to establish the relationships between canopy-level LI, leaf-level photosynthesis, and yield and quality of drug-type cannabis. We investigated how plant growth stage and localized foliar PPFD (LPPFD; i.e., instantaneous PPFD at leaf-level) affected photosynthetic parameters and leaf morphology, and how growing cannabis at average canopy-level PPFDs (APPFD; i.e., lighting history) ranging from 120 to 1800 μmol·m^{-2}·s^{-1} affected plant morphology, yield, and quality of mature marketable inflorescence. The results of this study will assist the indoor cannabis industry to determine how much PAR cannabis growers

should be providing to the crop canopy in order to maximize profits while minimizing energy use within their specific production scenarios.

2.2 MATERIALS AND METHODS

The trial area consisted of 2 adjacent deep-water culture basins (CB) located in an indoor cannabis production facility in southern Ontario, Canada. Each CB (14.6 × 2.4 m) consisted of 24 parallel polystyrene rafts (0.6 × 2.4 m), each containing holes for 16 plant pots, oriented in 2 rows with 30-cm spacing both within- and between-rows. This spacing provided for 384 plants to be evenly spaced within each CB, at a density of 0.09 m^2/plant.

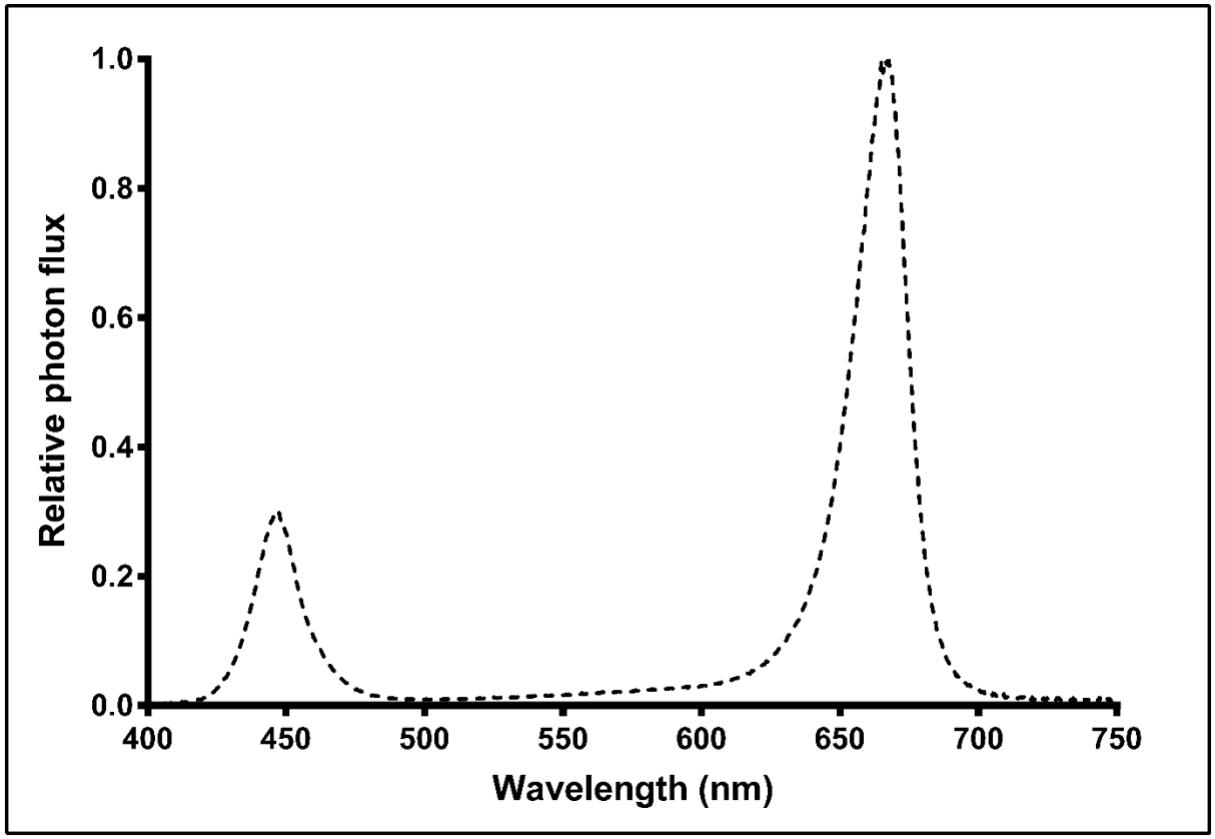

Figure 2.1. Relative spectral photon flux distribution of Pro-650 (Lumigrow) LED fixtures.

Above each CB were 3 racks of LED fixtures (Pro-650; Lumigrow, Emeryville, CA, USA), with each rack consisting 2 rows of 4 fixtures each; arranged such that all 24 fixtures were uniformly-

spaced (1.2 m apart, on-center) relative to each other and centered over the footprint of the CB. Each rack of fixtures was height-adjustable via a system of pulleys and cables, such that the hang-height of the 8 fixtures in each rack could be adjusted in unison. Each fixture contained dimmable spectrum channels for blue (B, peak 455 nm), white (broad-spectrum 5000K) and red (R, peak 660 nm) which could be individually controlled, wirelessly, through Lumigrow's SmartPAR software. The photon flux ratio of B (400-500 nm), green (G, 500-600 nm), and R (600-700 nm) was B18:G5:R77. Relative spectral photon flux distribution (**Figure 2.1**) was measured using a radiometrically calibrated spectrometer (UV-VIS Flame-S-XR; Ocean Optics, Dunedin, FL, USA) coupled to a CC3 cosine-corrector attached to a 1.9 m × 400 µm UV-Vis optical fiber.

2.2.1 EXPERIMENTAL DESIGN

The experiment was conducted using a gradient design, whereby plants grown in a common environment were exposed to a broad range of canopy-level PPFDs with a high level of spatial variability across the CB. Individual plants were assigned APPFD levels based on rigorous spatial and temporal evaluations of LI (explained below). Gradient designs can outperform traditional "treatment × replication" experimental designs when evaluating plants' responses to a continuous variable such as LI (Kreyling et al., 2018). Despite the fact they are arduous to setup and monitor, gradient designs have been successfully used to establish LI effects within other controlled-environment production scenarios (Bredmose, 1993, 1994; Jones-Baumgardt et al., 2019).

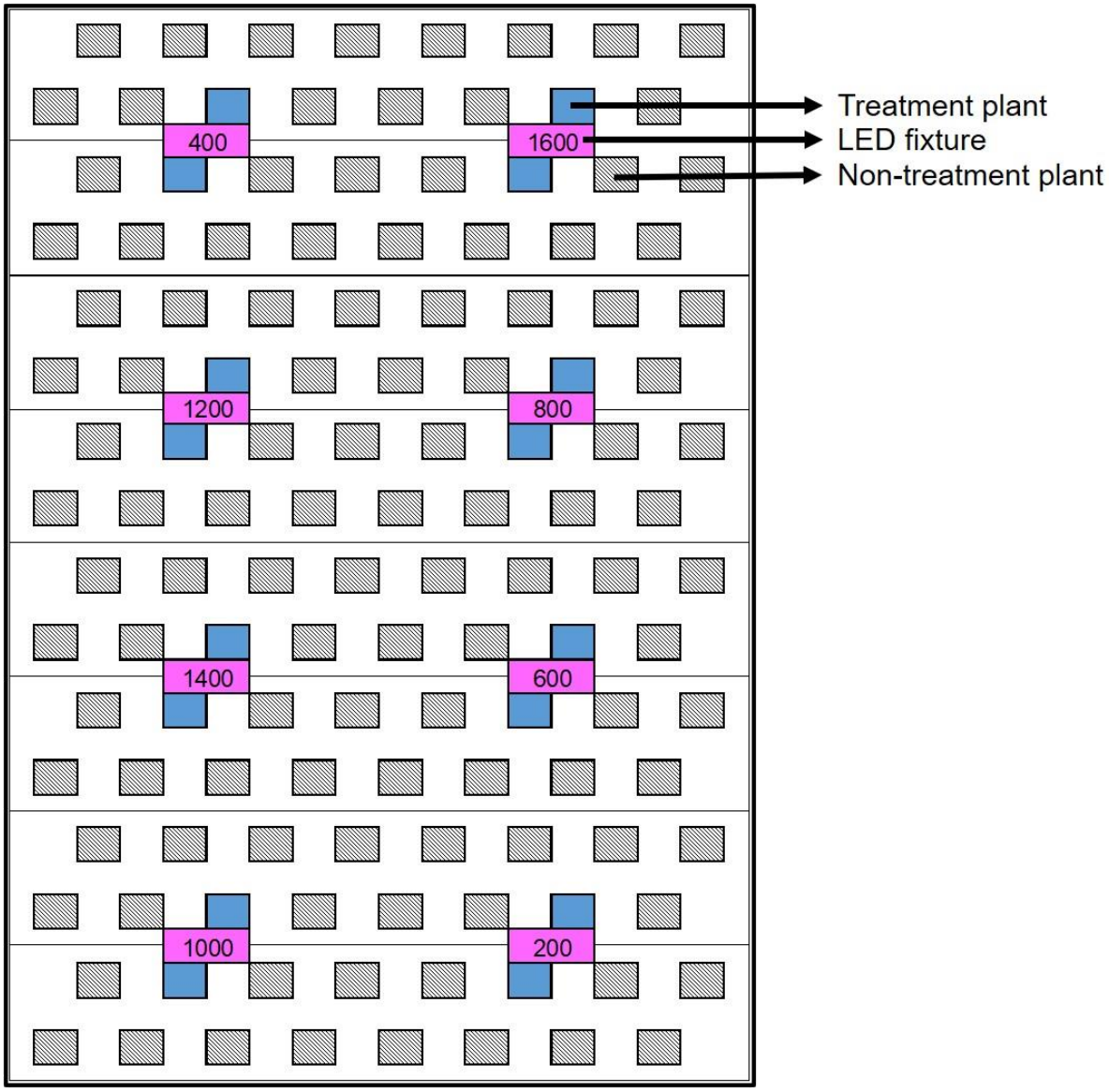

Figure 2.2. Schematic of a single light rack (8 LED fixtures, in magenta) above one third of a deep-water culture basins (CB). The entire growing area consists of 6 of these light racks. Within each light rack, each of the 8 target PPFD levels (i.e., the "treatments") were randomly assigned to one fixture (i.e., plot). This resulted in a randomized complete block type of experimental layout, comprised of 8 treatments × 6 replications. However, each treatment plant (in blue) was assigned an average photosynthetic photon flux density (APPFD) as LI treatment levels, reflecting the average canopy-level light intensity measured throughout the trial. The APPFD levels were used as the independent variable in subsequent analyses of plant growth, physiology and harvest metrics. Each plot was surrounded by non-treatment plants (diagonal lines) to ensure uniform growing environment and normal planting density.

To facilitate setup, the experiment was initially arranged as a randomized complete block type of design with 6 blocks (i.e., 3 blocks per CB) of 8 PPFD target levels: 200, 400, 600, 800, 1000, 1200, l400, and 1600 μmol·m^{-2}·s^{-1}. Each block consisted of a single rack of LED fixtures, with the PPFD target levels randomly assigned to individual fixtures (i.e., plots) within each rack. The two plants located most directly below each fixture were assessed experimentally (**Figure 2.2**). PPFD was measured at the apex of each plant using a portable spectroradiometer (LI-180; LI-COR Biosciences, Lincoln, NE, USA). The initial hang height of each rack was determined by the maximum height whereby approximately 1600 μmol·m^{-2}·s^{-1} could be achieved at the apical meristem of the tallest plant in the highest LI plot. The other treatment levels were subsequently achieved through dimming; targeting the prescribed PPFD at the apical meristem of the tallest plant in each plot while maintaining a uniform photon flux ratio of B18:G5:R77 in the entire CB. Plant height and apical meristematic PPFD were measured twice weekly until vegetative growth ceased (five weeks after the start of the 12-h photoperiod), and weekly thereafter until harvest. The prescribed intensity levels in each block were reset each time plant height was measured, first by raising the rack of fixtures to achieve the target PPFD at the apical meristem of the tallest plant in the 1600 μmol·m^{-2}·s^{-1} plot and then adjusting the intensity settings of the remaining plots accordingly. The trial ran from the beginning of the flowering stage (i.e., when the 12-h flowering photoperiod was initiated) until harvest, for a total of 81 days (nearly 12 weeks). While the underlying experimental arrangement was based on a RCBD organization, all analyses were performed as regressions with LI as the continuous, independent variable.

2.2.2 PPFD LEVELS

Although the prescribed target PPFD levels were maintained at the apical meristem position for the tallest plant within each plot on regular intervals, these values were not accurate proxies for the actual PPFD intensity dynamics experienced by each plant throughout the trial due to variability in individual plant height (on intra- and inter-plot bases), growth rates, and the lengths of the time periods between PPFD measurements. To account for these temporal dynamics in apical meristematic PPFD, total light integrals (TLIs, mol·m^{-2}) were calculated for each plant over the total production time and then back-calculated to APPFD or daily light integral (DLI, mol·m^{-2}·d^{-1}). The TLIs were based on the product of the PPFD level measured at the start and

end of each measurement interval and the length of time the lights were on during each measurement interval. These interim light integrals were then aggregated to form a TLI for each plant and divided by the total production time in seconds (i.e., the product of the daily photoperiod and the number of days). The resulting APPFD levels were then used as the independent variable (i.e., X-axis) in regressions of LI vs. various growth, yield and quality parameters. TLI can also be used in yield evaluations whereby the relationship between yield and TLI becomes a direct measure of production efficacy on a quantum basis (e.g., $g \cdot mol^{-1}$). This relationship can be converted to an energy-basis ($g \cdot kWh^{-1}$), if the fixture efficacy ($\mu mol \cdot J^{-1}$) and spatial distribution efficiency (i.e., proportion of photon output from fixtures that reach the target growing area) are known.

2.2.3 PLANT CULTURE

Cuttings were taken from mother plants of the 'Stillwater' cultivar, a CBD-dominant cultivar, on August 1 and 15 2019. Cuttings were rooted in stone wool cubes under 100 $\mu mol \cdot m^{-2} \cdot s^{-1}$ of fluorescent light for 14 d and then transplanted into a peat-based medium in 1-gallon plastic pots and grown under ≈425 $\mu mol \cdot m^{-2} \cdot s^{-1}$ of LED light, comprised of a mixture of Pro-325 (Lumigrow) and generic phosphor-converted white LEDs (unbranded) for an additional 14 d. The apical meristems were removed (i.e., "topped") from the first batch of clones, 10 d after transplant, and the second batch were not topped. Propagation and vegetative growth phases both had 18-h photoperiods. The first CB (CB1) was populated from the first batch of clones on August 20 2019 and the second CB (CB2) was populated from the second batch of clones on September 12 2019. In each case, 48 uniform and representative plants were selected from the larger populations of clones and placed in the plots to be evaluated experimentally. In CB1, the experimental plants initially had either 9 or 10 nodes and ranged in height (from growing medium surface to shoot apex) from 34 to 48 cm. In CB2 the experimental plants initially had either 12 or 13 nodes and ranged in height from 41 to 65 cm. Once the plants were moved to the CBs, the daily photoperiod switched to 12 h, from 06:30 HR to 18:30 HR.

Plant husbandry followed the cultivator's standard operating procedures except for the differences in canopy-level PPFD. Canopy-level air temperature, relative humidity (RH), and

CO_2 concentration were monitored at 600-s intervals throughout the trial with a data logger (Green Eye model 7788; AZ Instrument Corporation, Taiwan). Throughout the experiment, the air temperature, RH, and CO_2 concentrations were (mean ± SD) 25.3 ± 0.4°C, 60.5 ± 4.8%, and 437 ± 39 ppm during the day (i.e., lights on) and 25.2 ± 0.3°C, 53.1 ± 3.3%, and 479 ± 42 ppm during the night. A common nutrient solution was circulated through both CBs. The nutrient concentrations in the aquaponic solution supplying both CBs were sampled weekly (for 11 weeks) and analyzed at an independent laboratory (A&L Canada; London, ON, Canada). The nutrient element concentrations ($mg \cdot L^{-1}$) in the aquaponic system were averaged across the weekly sampling (mean ± SD): 170 ± 22 Ca, 86 ± 8.2 S, 75 ± 15 N, 57 ± 5 Mg, 32 ± 4 P, 23 ± 8 K, 250 ± 32 Cl, 0.27 ± 0.1 Fe, 0.18 ± 0.07 Zn, 0.050 ± 0.02 Mn, 0.031 ± 0.006 B, and 0.028 ± 0.004 Cu. Mo was reported as below detection limit (i.e., <0.02 $mg \cdot L^{-1}$) throughout the trial. The concentrations ($mg \cdot L^{-1}$) of non-essential nutrient elements were 170 ± 18 Na and 6.7 ± 0.7 Si. The aquaponic solution was aerated with an oxygen concentrator and the pH and EC were 6.75 ± 0.2 and 1.77 ± 0.15 $mS \cdot cm^{-1}$, respectively.

2.2.4 LEAF PHOTOSYNTHESIS

Quantifications of leaf-level gas exchange of leaflets on the youngest, fully-expanded fan leaves were performed on 64 plants (32 plants per CB) each, in weeks 1, 5, and 9 after the initiation of the 12-h photoperiod using a portable photosynthesis machine (LI-6400XT; LI-COR Biosciences, Lincoln, NE, USA), equipped with the B and R LED light source (6400-02B; LI-COR Biosciences). The Light Curve Auto-Response subroutine was used to measure NCER [$\mu mol_{(CO_2)} \cdot m^{-2} \cdot s^{-1}$] at PPFD levels of: 2000, 1600, 1400, 1200, 1000, 800, 600, 400, 200, 150, 100, 75, 50, 25, and 0 $\mu mol \cdot m^{-2} \cdot s^{-1}$. Since cannabis leaves are palmately compound, the middle leaflet was used to cover the 6 cm^2 chamber of the LI-COR 6400XT for photosynthesis measurements, because the middle leaflet is the largest. Occasionally, two leaflets of the same leaf were inserted to ensure the whole chamber was covered, similar to the methods used for oak seedlings (Goodman et al., 2007). Leaflets were exposed to 2000 $\mu mol \cdot m^{-2} \cdot s^{-1}$ for 180 s prior to starting each light response curve (LRC) and then progressed sequentially from highest to lowest PPFD to ensure stomatal opening was not a limitation of photosynthesis (Singsaas et al., 2001). The leaf chamber setpoints were 26.7°C (block temperature), 400 ppm CO_2, and 500 $\mu mol \cdot s^{-1}$

airflow. The localized PPFD (LPPFD) at each leaflet was measured immediately prior to the LRC measurement using the LI-180. A_{sat} [$\mu mol_{(CO_2)} \cdot m^{-2} \cdot s^{-1}$], localized NCER (LNCER), maximum QY [$\mu mol_{(CO_2)} \cdot \mu mol^{-1}_{(PAR)}$], and LSP [$\mu mol_{(PAR)} \cdot m^{-2} \cdot s^{-1}$] were determined for each measured leaflet using Prism (Version 6.01; GraphPad Software, San Diego, CA, USA) with the asymptotic LRC model: $y = a + b \cdot e^{(c \cdot x)}$ (Delgado et al., 1993) where y, x, a, and *e* represent NCER, PPFD, A_{sat}, and Euler's number, respectively. The LNCER of each leaflet was calculated by substituting the measured LPPFD into its respective LRC model. The QY was calculated as the slope of the linear portion of the LRC (i.e., at PPFD ≤200 $\mu mol \cdot m^{-2} \cdot s^{-1}$). The LSP is defined as the PPFD level where increasing LI no longer invokes a significant increase in NCER. The LSP for each LRC was determined using the methods described by Lobo et al. (2013) by evaluating the change in NCER (ΔNCER) over 50 $\mu mol_{(PAR)} \cdot m^{-2} \cdot s^{-1}$ increments, continuously along the LRC, until the ΔNCER reached a threshold value, which was determined from the prescribed measurement conditions and performance specifications of the LI-6400XT. Briefly, the minimum significant difference in CO_2 concentration between sample and reference measurements is 0.4 ppm (LI-COR Biosciences, 2012). Therefore, given the setup parameters of the leaf chamber, a ΔNCER of ≤0.33 $\mu mol_{(CO_2)} \cdot m^{-2} \cdot s^{-1}$ over a 50 $\mu mol_{(PAR)} \cdot m^{-2} \cdot s^{-1}$ increment indicated the LSP.

The ratio of variable to maximum fluorescence (F_v/F_m) emitted from photosystem II in dark-acclimated leaves exposed to a light-saturating pulse is an indicator of maximum quantum yield of photosystem II photochemistry (Murchie and Lawson, 2013). Immediately after each LRC, the leaflet was dark acclimated for ≈900 s and then F_v/F_m was measured with a fluorometer (FluorPen FP 100; Drasov, Czech Republic). Chlorophyll content index (CCI) was measured on three fan leaflets from leaves at the bottom and top of each plant in weeks 1, 5, and 9 using a chlorophyll meter (CCM-200; Opti-Sciences, Hudson, NH, USA). The CCI measurements from upper and lower tissues, respectively, were averaged on a per-plant basis for each measurement period.

2.2.5 LEAF MORPHOLOGY

On day 35 of the experiment, one leaf from each plant was removed from node 13 (counting upwards from the lowest node) in CB1 and node 15 from CB2, ensuring that the excised leaves developed under their respective LPPFD. A digital image of each leaf was taken using a scanner (CanoScan LiDE 25; Canon Canada Inc., Brampton, ON, Canada) at 600 dpi resolution and then the leaves were oven-dried (Isotemp Oven Model 655G; Fisher Scientific, East Lyme, CT, USA), singly, to constant weight at 65°C. The images were processed using ImageJ 1.42 software (National Institute of Health; https://imagej.nih.gov/ij/download.html) to determine leaf area (LA). The DW of scanned leaves were measured using an analytical balance (MS304TS/A00; Mettler-Toledo, Columbus, OH, USA). Specific leaf weight (SLW; $g \cdot m^{-2}$) was determined using the following formula: DW / LA. See **Appendix A** for plant growth methodology, and **Appendix B** for additional visual observations.

2.2.6 YIELD AND QUALITY

After 81 d of the experiment, the stems of each plant were cut at substrate level and the aboveground biomass of each plant was separated into three parts: apical inflorescence, remaining inflorescence, and stems and leaves (i.e., non-marketable biomass), and weighed using a digital scale (Scout SPX2201; OHAUS Corporation, Parsippany, NJ, USA). Since the plants from CB2 had the apical meristem removed, the inflorescence from the tallest side branch was considered the apical inflorescence. The length (L) and circumference (C; measured at the midpoint) of each apical inflorescence were also measured. Assuming a cylindrical shape, the density of the apical inflorescence ($g \cdot cm^{-3}$) was calculated using the formula: apical inflorescence density = fresh weight/$\{\pi \cdot [C/(2 \cdot \pi)^2] \cdot L\}$. The apical inflorescences from 22 representative plants (selected to ensure evenly distributed APPFD) from CB1 were air dried at 15°C and 40% RH for 10 d until they reached marketable weight (i.e., average moisture content of ≈11%), determined using a moisture content analyzer (HC-103 Halogen Moisture Analyzer; Mettler-Toledo, Columbus, OH, USA). This ensured that the apical inflorescence tissues selected for analysis of secondary metabolites followed the cultivator's typical post-harvest treatment. The apical inflorescences from CB1 were homogenized on a per-plant basis and ≈2-g sub-samples from each plant was processed by an independent laboratory (RPC Science &

Engineering; Fredericton, NB, Canada) for concentration [$mg \cdot g^{-1}_{(DW)}$ using solvent extraction followed by ultra-high-performance liquid chromatography with variable wavelength detection (HPLC-VWD) for cannabinoids and gas chromatography with mass spectrometry detection (GC-MSD) for terpenes]. Total equivalent Δ^9-THC, CBD, and CBG concentrations were determined by assuming complete carboxylation of the acid-forms of the respective cannabinoids, whose concentrations were adjusted by factoring out the acid-moiety from the molecular weight of each compound [e.g., total Δ^9-THC = (Δ^9-THCA × 0.877) + Δ^9-THC]. The separated aboveground tissues from 16 representative plants in each CB were oven-dried (Isotemp Oven Model 655G) to constant weight at 65°C to determine LI treatment effects on moisture content, which were then used to determine DW of all harvested materials. The harvest index was calculated as the ratio of total inflorescence DW (hereafter, yield) to the total aboveground DW, on a per-plant basis.

2.2.7 DATA PROCESSING AND ANALYSIS

Although the initial experimental setup was arranged as a randomized complete block type of design, blocking played no part in the statistical analysis of the results. Data were analyzed for random (i.e., blocks) and fixed (i.e., APPFD) effects, which revealed that the variation attributed to the random effects were not significantly different from 0. On per-CB and per-week bases, each model from the leaf photosynthesis measurements (i.e., A_{sat}, LSP, LNCER, and QY) were subjected to non-linear regression using the PROC NLMIXED procedure (SAS Studio Release 3.8; SAS Institute Inc., Cary, NC), with the LPPFD of each measured leaf as the independent variable, to determine the best-fit models after outliers were removed. In each case, best-fit models were selected based on the lowest value for the Akaike information criterion (AICc). If there were no LI treatment effects on a given parameter, then means (± SD) were calculated. Best-fit models for F_v/F_m and CCI were similarly determined, using LPPFD and APPFD (from the start of the trial up to the time of measurement), respectively, as the independent variable. On a per-week basis, A_{sat}, LSP, LNCER, QY, F_v/F_m, and CCI data from CB1 and CB2 were pooled if the 95% confidence intervals (95% CI) of each element of the respective best-fit models for the two CBs overlapped, and best-fit models for pooled datasets were then recalculated. The PROC GLIMMIX Tukey-Kramer test was used ($P \leq 0.05$) on means to determine if there were differences between the measurement periods (i.e., weeks). If there were any measurement

period effects on any element in the models, then weekly models for the respective parameters were reported.

Computed parameters from single-time measurements (SLW, apical inflorescence density, yield, and harvest index) were grouped per CB, using the APPFD (at the time of measurement) to define each datapoint within each CB and PROC NLMIXED was used to evaluate the best fit model for each parameter using the AICc. Parameter means were computed (on per-CB bases) when there were no LI treatment effects. If there were LI treatment effects on a given parameter, datasets from CB1 and CB2 were pooled if the 95% CI of each element of the respective best-fit models for the two CBs overlapped and best-fit models for pooled datasets were then recalculated. For parameters with no LI treatment effects, differences between CBs were evaluated using the 95% CIs of their respective means. For a given parameter, if the 95% CIs the parameter means for the 2 CBs overlapped, then the data were pooled, and new parameter means were calculated and presented. Cannabinoids and terpenes from CB1 were modeled, with APPFD as the independent variable, using PROC NLMIXED to evaluate the best-fit model for each parameter using the AICc. Best-fit models or parameter means were reported.

2.3 RESULTS

No CB effects were found in any leaf photosynthesis, leaf morphology, and postharvest parameters; therefore, CB1 and CB2 data were pooled for the development of all models except secondary metabolites, which were only measured in CB1. In contrast, many of the parameters that were repeated over time (i.e., in weeks 1, 5, and 9 of the experiment) showed differences between weeks; whereby the different weeks were modeled separately. Note also that the week-over-week ranges of LPPFD varied as the plants progressed through their ontogeny, since self-shading from upper tissues resulted in decreases in maximum LPPFD of leaves selected for photosynthesis measurements. Nevertheless, a consistent range of APPFDs was maintained throughout the trial.

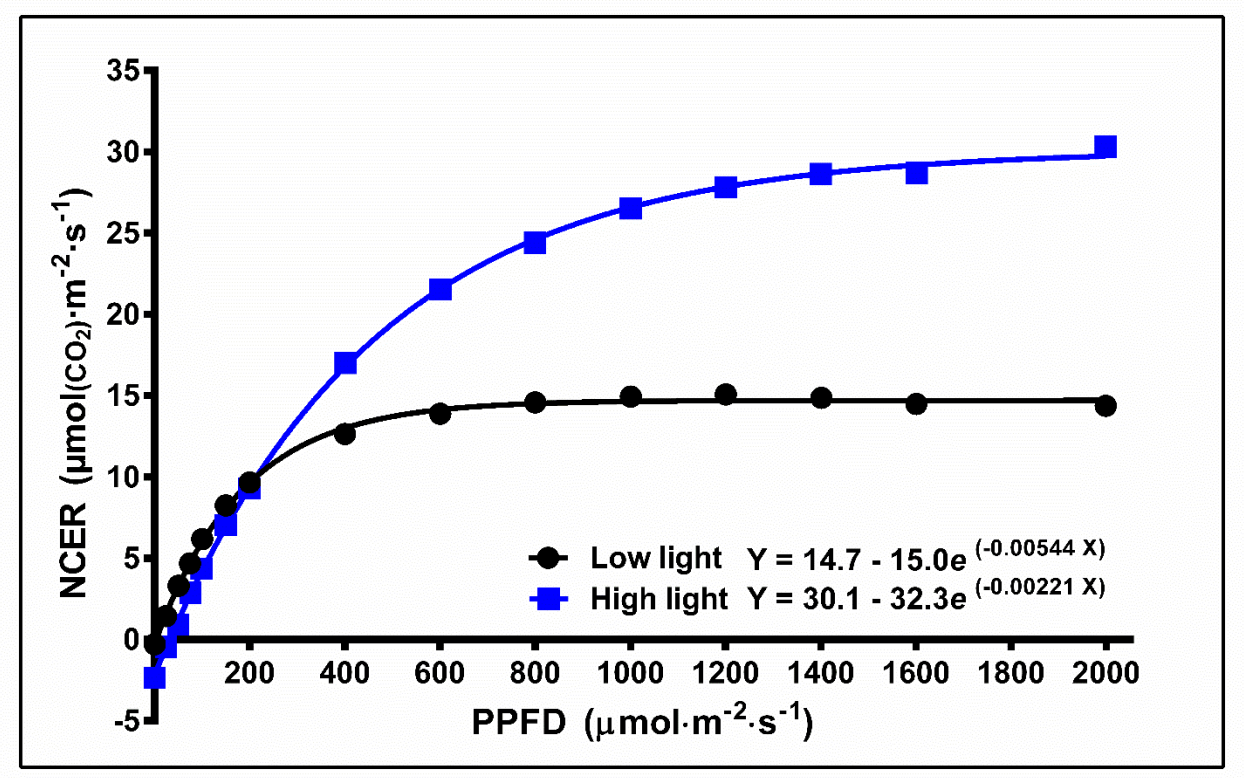

Figure 2.3. Typical light response curves [net CO_2 exchange rate (NCER) response to light intensity] of two youngest fully-expanded fan leaves of *Cannabis sativa* L. 'Stillwater' grown under either low or high localized photosynthetic photon flux densities (LPPFD). The low and high LPPFD were 91 and 1238 $\mu mol \cdot m^{-2} \cdot s^{-1}$, respectively. Measurements were made during week 5 after the initiation of the 12-h photoperiod.

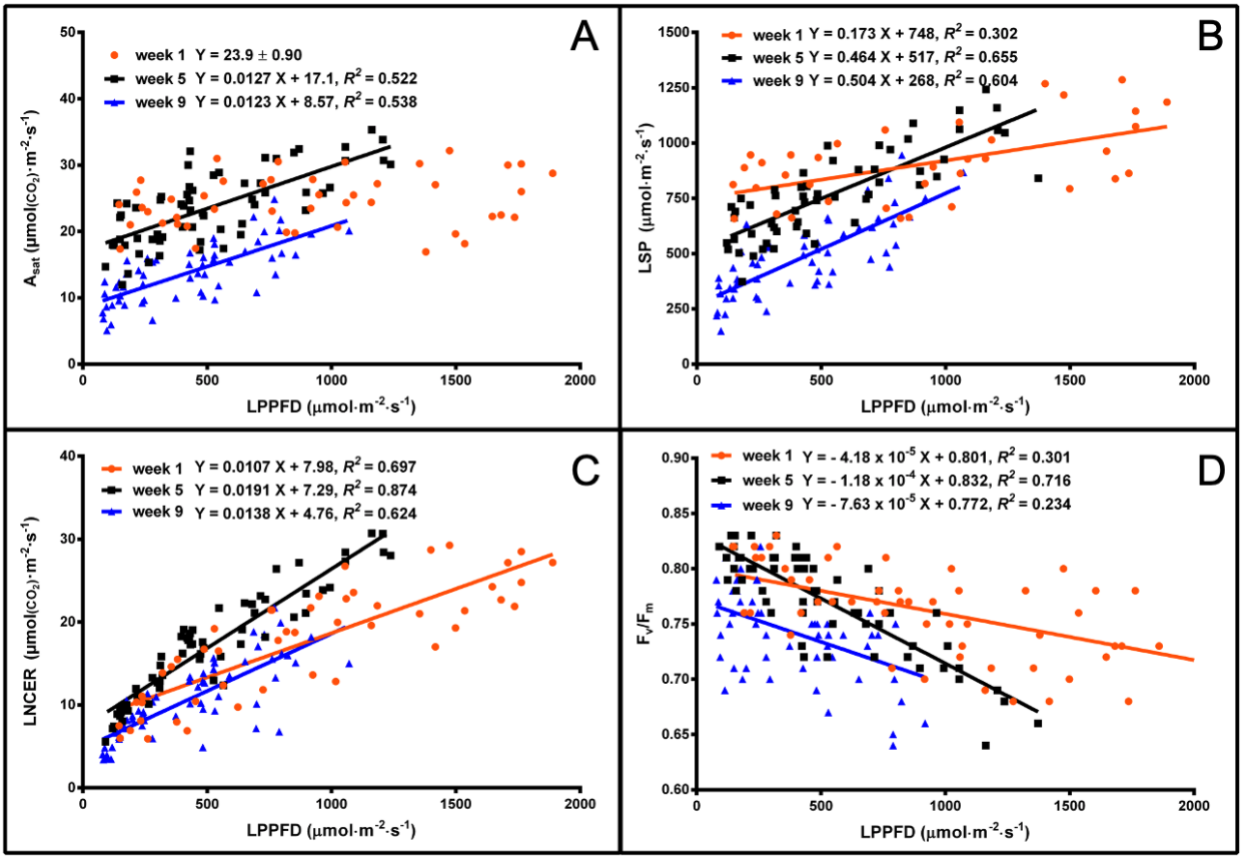

Figure 2.4. The light-saturated net CO_2 exchange rate (A_{sat}) **(A)**, the light saturation point (LSP) **(B)**, the localized net CO_2 exchange rate (LNCER) **(C)**, and the F_v/F_m **(D)** of the youngest fully-expanded fan leaves of *Cannabis sativa* L. 'Stillwater' at the localized photosynthetic photon flux densities (LPPFD) that the respective leaves were growing under when the measurements were made, during weeks 1, 5, and 9 after initiation of the 12-h photoperiod. Each datum is a single plant. Regression lines are presented when $P \leq 0.05$.

2.3.1 LEAF PHOTOSYNTHESIS

Leaf light response curves constructed under different LI and at different growth stages (week 1, 5, and 9) generally demonstrated the trends that the A_{sat} and LSP were higher for plants grown under high vs. low LPPFD (**Figures 2.3, 2.4A-B**), especially after the plants had acclimated to their new lighting environments (i.e., weeks 5 and 9). There were no LPPFD effects on A_{sat} in week 1, with a mean (± SE, n = 52) of 23.9 ± 0.90 $\mu mol_{(CO_2)} \cdot m^{-2} \cdot s^{-1}$ (**Figure 2.4A**). The A_{sat} in weeks 5 and 9 (**Figure 2.4A**) and LSP in weeks 1, 5, and 9 (**Figure 2.4B**) increased linearly with increasing LPPFD. At low LPPFD, the highest LSP was in week 1. The slopes of the A_{sat} and LSP models were similar in weeks 5 and 9, but the Y-intercepts for both parameters were

approximately twice as high in week 5 vs. week 9. LNCER increased linearly with increasing LPPFD in weeks 1, 5, and 9 (**Figure 2.4C**) with the steepest and shallowest slopes apparent at weeks 5 and 1, respectively. The LNCER model in week 9 had a substantially lower Y-intercept than the other two weeks. As evidenced by the projected intersection of the A_{sat} and LNCER models in week 5 (i.e., at LPPFD of 1532 $\mu mol \cdot m^{-2} \cdot s^{-1}$), the maximum LPPFD in week 5 (i.e., 1370 $\mu mol \cdot m^{-2} \cdot s^{-1}$) was nearly sufficient to saturate the photosynthetic apparatus at the top of the canopy. There were no LPPFD effects on QY, but the mean QY in weeks 1 and 5 were higher than week 9. The mean (± SE) QY were 0.066 ± 0.0013 (*n* = 54), 0.068 ± 0.0005 (*n* = 60), and 0.058 ± 0.0008 (*n* = 63) $\mu mol_{(CO_2)} \cdot \mu mol^{-1}_{(PAR)}$ in weeks 1, 5, and 9 respectively. The F_v/F_m decreased linearly with increasing LPPFD in all three measurement periods (**Figure 2.4D**).

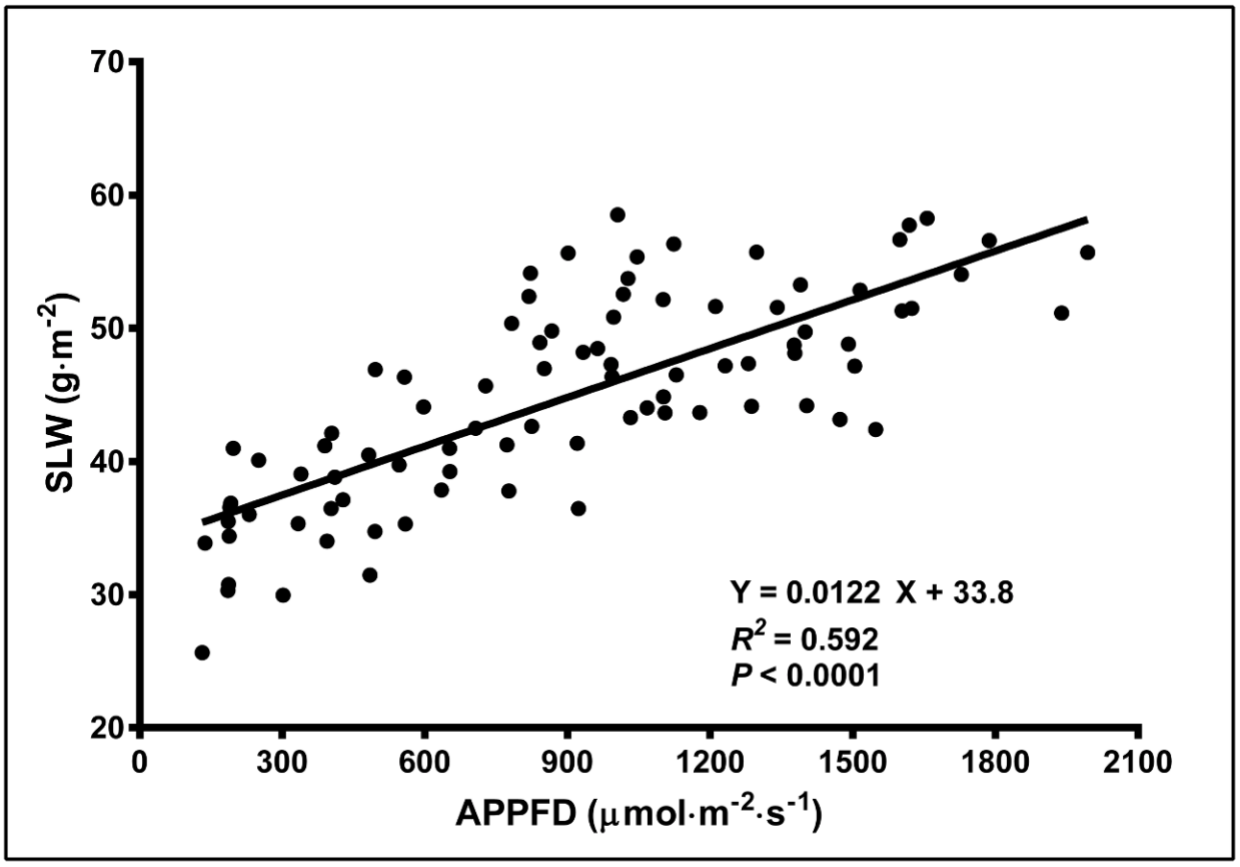

Figure 2.5. The specific leaf weight (SLW; on a dry weight basis) of young, fully-expanded *Cannabis sativa* L. 'Stillwater' leaves in response to the average photosynthetic photon flux density (APPFD), measured on day 35 after initiation of the 12-h photoperiod. Each datum represents one fan leaf from a single plant.

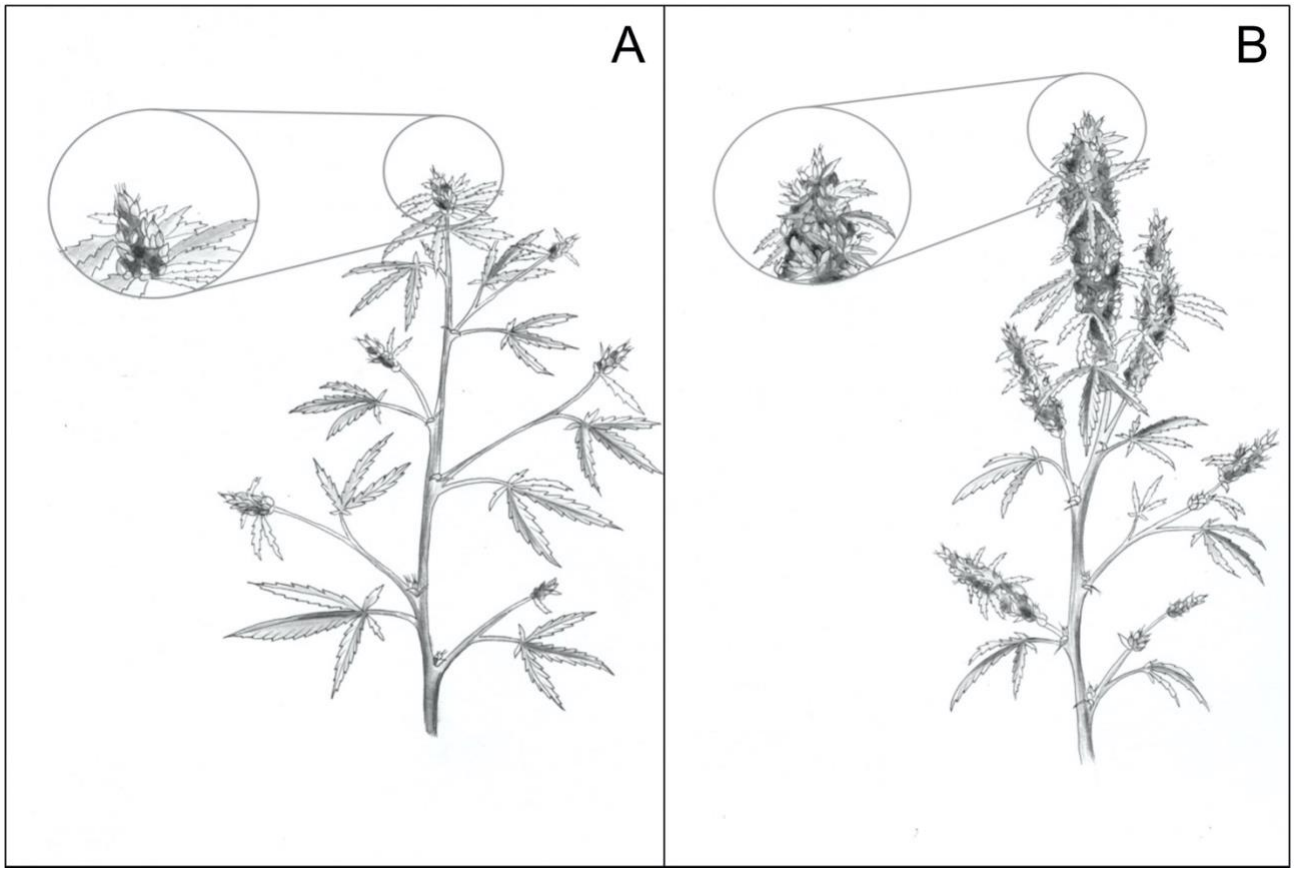

Figure 2.6. Sketches of *Cannabis sativa* L. 'Stillwater' plants grown under low **(A)** and high **(B)** photosynthetic photon flux density (APPFD), 9 weeks after initiation of 12-h photoperiod (illustrated by Victoria Rodriguez Morrison).

2.3.2 CHLOROPHYLL CONTENT INDEX AND PLANT MORPHOLOGY

There were no LI treatment effects on CCI either at the top or bottom of the canopy. However within in each week, the upper canopy CCI were higher than the lower canopy. Additionally, the CCI in the upper and lower canopy was higher in week 1 vs. weeks 5 and 9. The CCI was assessed for 91 plants per week. The mean CCI (± SE) were 67.1 ± 0.80, 55.8 ± 2.2, and 52.0 ± 2.1 in the upper canopy and 46.3 ± 1.1, 31.1 ± 0.86, and 31.5 ± 1.1 in the lower canopy, in weeks 1, 5, and 9 respectively. The SLW increased linearly from 35.4 to 58.1 $g \cdot m^{-2}$ as APPFD (calculated based on the respective plants' accumulated PAR exposures up to day 35 of the flowering stage) increased from 130 to 1990 $\mu mol \cdot m^{-2} \cdot s^{-1}$ (**Figure 2.5**). Plants grown under low

vs. high APPFD were generally shorter and wider, with thinner stems, larger leaves, and fewer, smaller inflorescences (**Figure 2.6**).

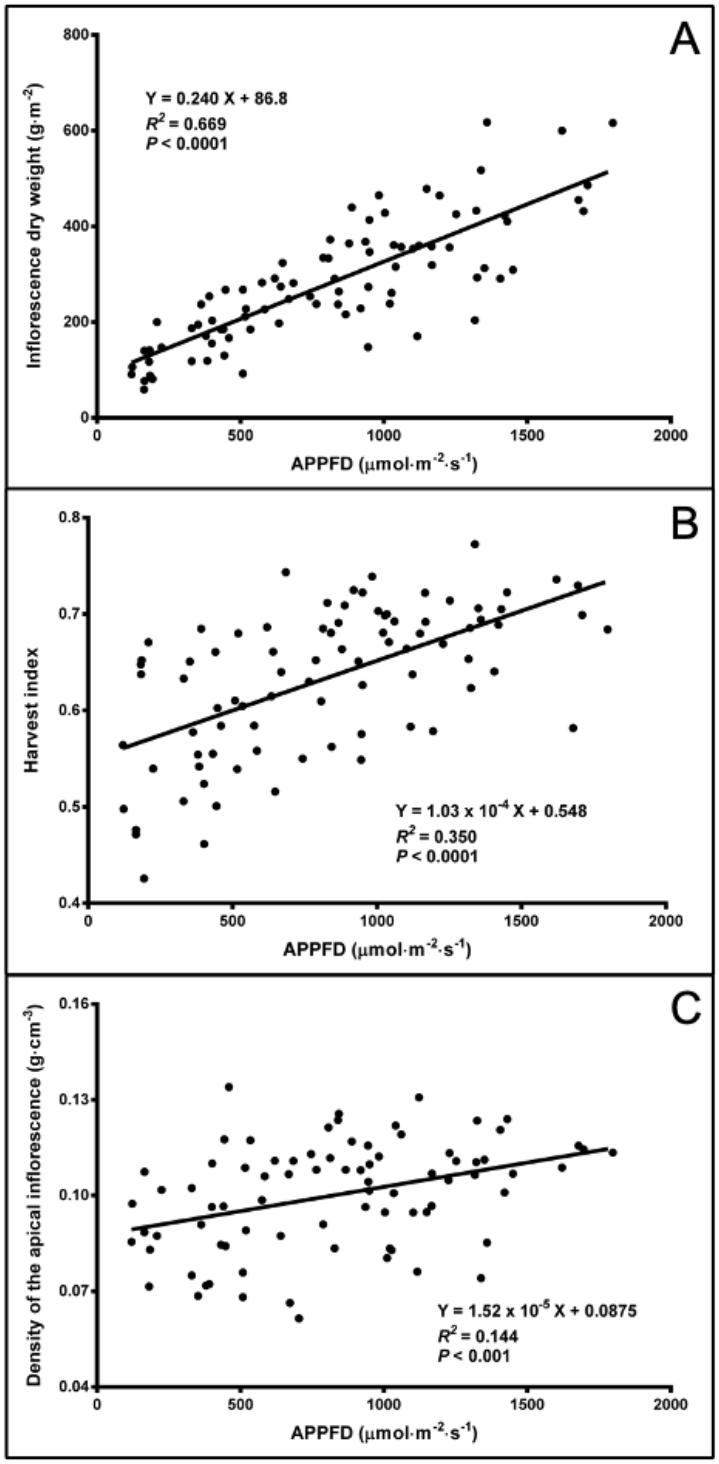

Figure 2.7. The relationship between average apical photosynthetic photon flux density (APPFD) applied during the flowering stage (81 days) and inflorescence dry weight **(A)**, harvest index (total inflorescence dry weight / total aboveground dry weight) **(B)**, and apical

inflorescence density (based on fresh weight) **(C)** of *Cannabis sativa* L. 'Stillwater'. Each datum is a single plant.

Table 2.1. Cannabinoid concentration in apical inflorescences of *Cannabis sativa* L. 'Stillwater'.

Cannabinoid	**Concentration (mg·g^{-1} of inflorescence dry weight)**
Δ-9-tetrahydrocannabinol (Δ^9-THC)	UDL[z]
Δ-9-tetrahydrocannabinolic acid (Δ^9-THCA)	12.9[y] ± 0.03
Total equivalent Δ^9-tetrahydrocannabinol (TΔ^9-THC)	11.3 ± 0.02
Cannabidiol (CBD)	5.53 ± 0.01
Cannabidiolic acid (CBDA)	214 ± 0.4
Total equivalent cannabidiol (TCBD)	193 ± 0.4
Cannabigerol (CBG)	UDL
Cannabigerolic acid (CBGA)	4.76 ± 0.01
Total equivalent cannabigerol (TCBG)	4.45 ± 0.009
Cannabinol (CBN)	UDL

[z]under detection limit of 0.5 mg·g^{-1} of inflorescence dry weight
[y]data are means ± SE of 22 representative inflorescences across all of the APPFDs in CB1

Table 2.2. The relationships between average photosynthetic photon flux density (APPFD) applied during the flowering stage (81 days) and terpene concentration in apical inflorescences of myrcene, limonene and total terpenes, and the mean concentration for terpenes with no APPFD treatment effects, of *Cannabis sativa* L. 'Stillwater'.

Terpene	Terpene concentration ($mg \cdot g^{-1}$ of inflorescence dry weight)		
	Mean [z]	Regression equation [y]	R^2
Total terpenes		Y = 0.00230 X + 8.57	0.320
Myrcene		Y = 0.00142 X + 2.34	0.464
Limonene		Y = 0.000326 X + 1.01	0.246
Alpha pinene	0.16[z] ± 0.01		
Beta pinene	0.22 ± 0.01		
Terpinolene	UDL[x]		
Linalool	0.53 ± 0.01		
Terpineol	0.32 ± 0.02		
Caryophyllene	2.9 ± 0.2		
Humulene	0.65 ± 0.04		
3-carene	UDL		
Cis-ocimene	UDL		
Eucalyptol	UDL		
Trans-ocimene	UDL		
Fenchol	0.22 ± 0.01		
Borneol	0.03 ± 0.01		
Valencene	UDL		
Cis-nerolidol	UDL		
Trans-nerolidol	UDL		
Guaiol	UDL		
Alpha-bisabolol	0.38 ± 0.03		
Sabinene	UDL		

[z]when there were no APPFD treatment effects on terpene concentration, the means ± SE of 22 representative inflorescences across all of the PPFDs in CB1 are presented

[y]linear regression models for the APPFD treatment effects on terpene concentration when $P \leq 0.05$

[x]under detection limit of 0.5 $mg \cdot g^{-1}$ of inflorescence dry weight

2.3.3 YIELD AND QUALITY

Cannabis yield was 4.5 times higher for plants grown at APPFD of 1800 μmol·m^{-2}·s^{-1} relative to those grown at 120 μmol·m^{-2}·s^{-1} (**Figure 2.7A**). Note that yields in the present study are true oven-DWs. Since fresh cannabis inflorescences are typically dried to 10 to 15% moisture content to achieve optimum marketable quality (Leggett, 2006), yields in the present study can be easily adjusted upwards to be comparable any desirable moisture level (e.g., by multiplying the DW by the FW:DW to determine the additional FW). The harvest index was 1.3 times higher as APPFD increased from 120 to 1800 μmol·m^{-2}·s^{-1} (**Figure 2.7B**). The apical inflorescence density increased 1.3 times as APPFD increased from 120 to 1800 μmol·m^{-2}·s^{-1} (**Figure 2.7C**).

Cannabidiolic acid (CBDA) was the dominant cannabinoid in the dried inflorescences; however, there were no APPFD treatment effects on the concentration of any of the measured cannabinoids (**Table 2.1**). Due to linear increases in inflorescence yield with increasing LI, cannabinoid yield (g·m^{-2}) increased by 4.5 times as APPFD increased from 120 to 1800 μmol·m^{-2}·s^{-1}. Myrcene, limonene, and caryophyllene were the dominant terpenes in the harvested inflorescences (**Table 2.2**). The concentration of total terpenes, myrcene, and limonene were 1.4, 2.0 and 1.5 times higher at APPFD of 1800 μmol·m^{-2}·s^{-1} relative to those detected in plants grown at 120 μmol·m^{-2}·s^{-1}. There were no APPFD effects on the concentration of the other individual inflorescence terpenes.

2.4 DISCUSSION

2.4.1 CANNABIS INFLORESCENCE YIELD IS PROPORTIONAL TO LIGHT INTENSITY

It was predicted that cannabis yield would exhibit a saturating response to increasing LI, thereby signifying an optimum LI range for indoor cannabis production. However, the yield results of this experiment demonstrated cannabis' immense plasticity for exploiting the incident lighting environment by efficiently increasing marketable biomass up to extremely high – for indoor production – LIs (**Figure 2.7A**). Even under ambient CO_2, the linear increases in yield indicated that the availability of PAR photons was still limiting whole-canopy photosynthesis at APPFD levels as high as ≈1800 μmol·m^{-2}·s^{-1} (i.e., DLI ≈78 mol·m^{-2}·d^{-1}). These results were generally

consistent with the trends of other studies reporting linear cannabis yield responses to LI (Eaves et al., 2020; Potter and Duncombe, 2012; Vanhove et al., 2011), although there is considerable variability in both relative and absolute yield responses to LI in these prior works. The present study covered a broader range of LI, and with much higher granularity, compared with other similar studies.

The lack of a saturating yield response at such high LI is an important distinction between cannabis and other crops grown in controlled environments (Beaman et al., 2009; Fernandes et al., 2013; Oh et al., 2009; Faust, 2003). This also means that the selection of an "optimum" LI for indoor cannabis production can be made somewhat independently from its yield response to LI. Effectively, within the range of practical indoor PPFD levels – the more light that is provided, the proportionally higher the increase in yield will be. Therefore, the question of the optimum LI may be reduced to more practical functions of economics and infrastructure limitations: basically, how much lighting capacity can a grower afford to install and run? This becomes a trade-off between fixed costs which are relatively unaffected by yield and profit (e.g., building lease/ownership costs including property tax, licensing, and administration) and variable costs such as crop inputs (e.g., fertilizer, electricity for lighting) and labor. Variable costs will obviously increase with higher LI but the fixed costs, on a per unit DW basis, should decrease concomitantly with increasing yield (Vanhove et al., 2014). Every production facility will have a unique optimum balance between facility costs and yield; but the yield results in the present study can help cannabis cultivators ascertain the most suitable LI target for their individual circumstances. Readers should be mindful that this study reports yield parameters as true DWs; marketable yield can be easily determined by factoring back in the desirable moisture content of the inflorescence. For example, for a 400 $g \cdot m^{-2}$ of dry yield, the corresponding marketable yield would be 444 $g \cdot m^{-2}$ at 10% moisture content [i.e., 400 $g \cdot m^{-2}$ + (400 $g \cdot m^{-2}$ × 10% FW / 90% DW)].

It is also important to appreciate that PPFD, which represents an instantaneous LI level, does not provide a complete accounting of the total photon flux incident on the crop canopy throughout the entire production cycle. While this LI metric is ubiquitous in the horticulture industry and

may be most broadly relatable to prior works, there is value in relating yield to the total photon flux received by the crop. Historically, this has been done by relating yield to installed wattage on per area bases, resulting in $g \cdot W^{-1}$ metric (Potter and Duncombe, 2012), which can be more fittingly converted to yield per unit electrical energy input ($g \cdot kWh^{-1}$) by factoring in the photoperiod and length of the production cycle (EMCDDA, 2013). However, since photosynthesis is considered a quantum phenomenon, crop yield may be more appropriately related to incident (easily measured) or absorbed photons and integrated over the entire production cycle (i.e., TLI, $mol \cdot m^{-2}$), in a yield metric that is analogous to QY: $g \cdot mol^{-1}$. Unlike installed wattage, this metric has the advantage of negating the effects of different fixture efficacy ($\mu mol \cdot J^{-1}$), which continues its upward trajectory, especially with LEDs (Kusuma et al., 2020; Nelson and Bugbee, 2014). The present study did not directly measure lighting-related energy consumption; however, installed energy flux ($kWh \cdot m^{-2}$) can be estimated from TLI using the Lumigrow fixture's efficacy rating: 1.29 and 1.80 $\mu mol \cdot J^{-1}$, from Nelson and Bugbee (2014) and Radetsky (2018), respectively. Using the average of these values (1.55 $\mu mol \cdot J^{-1}$), the conversion from TLI to energy flux becomes: $mol \cdot m^{-2} \times 5.6 = kWh \cdot m^{-2}$. At an APPFD of 900 $\mu mol \cdot m^{-2} \cdot s^{-1}$ (i.e., TLI of 3149 $mol \cdot m^{-2}$), the model in **Figure 2.7A** predicts a yield of 303 $g \cdot m^{-2}$ which corresponds to an energy use efficacy of 0.54 $g \cdot kWh^{-1}$. For comparison, doubling the LI to the highest APPFD used in this trial increases the yield by 70% but results in a ≈15% reduction in energy use efficacy. It is up to each grower to determine the optimum balance between variable (e.g., lighting infrastructure and energy costs) and fixed (e.g., production space) costs in selecting a canopy level LI that will maximize profits.

2.4.2 INCREASING LIGHT INTENSITY ENHANCES INFLORESCENCE QUALITY

Beyond simple yield, increasing LI also raised the harvest quality through higher apical inflorescence (also called "cola" in the cannabis industry) density – an important parameter for the whole-bud market – and increased ratios of inflorescence to total aboveground biomass (**Figure 2.7B and 2.7C**). The linear increases in harvest index and apical inflorescence density with increasing LI both indicate shifts in biomass partitioning more in favor of generative tissues; a common response in herbaceous plants (Poorter et al., 2019) including cannabis (Hawley et al., 2018; Potter and Duncombe, 2012). The increases in these attributes under high

LI may also indirectly facilitate harvesting, as there is correspondingly less unmarketable biomass to be processed and discarded, which is an especially labour-intensive aspect of cannabis harvesting.

The terpene composition of the inflorescence – comprised mainly of myrcene, limonene, and caryophyllene – increased by approximately 25%, as APPFD increased from 120 to 1800 $\mu mol \cdot m^{-2} \cdot s^{-1}$ (**Table 2.2**), which could lead to enhanced aromas and higher quality extracts (McPartland and Russo, 2001; Nuutinen, 2018). Conversely, total cannabinoid yield increased in proportion with increasing inflorescence yield since there were no LI treatment effects on cannabinoid concentration (**Table 2.1**). Similarly, Potter and Duncombe (2012) and Vanhove et al. (2011) found no LI treatment effects on cannabinoid concentration (primarily Δ^9-THC in those studies) and attributed increasing cannabinoid yield to enhanced biomass apportioning towards generative tissues at higher LI. Other studies had contradictory results on the effects of LI on cannabinoid concentration. Hawley et al. (2018) did not find canopy position effects on Δ^9-THC or CBD levels in a subcanopy lighting (SCL) trial, but they did find slightly higher CBG concentration in the upper canopy in the control (HPS top-lighting only) and the Red-Green-Blue SCL treatment, but not in the Red-Blue SCL treatment. While it is not possible to unlink spectrum from LI in their results, the magnitude of the reported chemical profile differences, both between canopy positions and between lighting treatments, were relatively minor. Conversely, Namdar et al. (2018) reported what appeared to be a vertical stratification on cannabis secondary metabolites, with highest concentrations generally found in the most distal inflorescences (i.e., closest to the light source, PPFD $\approx$600 $\mu mol \cdot m^{-2} \cdot s^{-1}$). They attributed this stratification to the localized LI at different branch positions, which were reportedly reduced by $\geq$60% at lower branches vs. at the plant apex. However, given the lack of LI treatment effects (over a much broader range of PPFDs) on cannabinoid levels in the present study, it is likely that other factors were acting on higher-order inflorescences, such as delayed maturation and reduced biomass allocation, that reduced the concentrations in these tissues (Diggle, 1995; Hemphill et al., 1980).

2.4.3 PLASTICITY OF CANNABIS LEAF MORPHOLOGY AND PHYSIOLOGY RESPONSES TO LI AND OVER TIME

The objectives of the photosynthesis and leaf morphology investigations in this study were two-fold: 1) to address the knowledge gap in the relationships between localized cannabis leaf photosynthesis and yield and 2) observe and report changes in physiology as the plant progresses through the flowering ontogeny.

General morphological, physiological, and yield responses of plants are well documented across LI gradients ranging from below compensation point to DLIs beyond 60 $mol \cdot m^{-2} \cdot d^{-1}$. Recently, the LI responses of a myriad of plant attributes were compiled across a tremendous range species, ecotypes and growing environments, and concisely reported them in the excellent review paper by Poorter et al. (2019). The trends in their LI models align well with primary attributes measured in the present study, including morphological parameters such as plant height and internode length, SLW (discussed below), and physiological parameters such as F_v/F_m, $_L$NCER (i.e., photosynthesis at growth light; Phot/A^{GL}), and A_{sat} (i.e., photosynthesis at saturating light; Phot/A^{SL}). In general, cannabis photosynthesis and yield responses to localized LI were linear across the $_A$PPFD range of 120 to 1800 $\mu mol \cdot m^{-2} \cdot s^{-1}$. Although these results are in agreement with the contemporary literature on cannabis (Bauerle et al., 2020; Chandra et al., 2008; 2015; Eaves et al., 2020; Potter and Duncombe, 2012), we also showed substantial chronological dependencies on leaf photosynthetic indices.

By surveying the photosynthetic parameters of the upper cannabis canopy across a broad range of $_L$PPFDs and over multiple timepoints during the generative phase, we saw evidence of both acclimation and early senescence as the crop progressed through its ontogeny. At the beginning of the trial, the plants were abruptly transitioned from a uniform PPFD (425 $\mu mol \cdot m^{-2} \cdot s^{-1}$) and 18-h photoperiod (i.e., 27.5 $mol \cdot m^{-2} \cdot d^{-1}$) and subjected to a much shorter photoperiod (12-h) and an enormous range of LI (120 to 1800 $\mu mol \cdot m^{-2} \cdot s^{-1}$), resulting in DLIs ranging from 5.2 to 78 $mol \cdot m^{-2} \cdot d^{-1}$. Furthermore, on a DLI-basis, approximately 1/3 of the plants were exposed to lower LIs in the flowering vs. vegetative phase (i.e., $_A$PPFD <640 $\mu mol \cdot m^{-2} \cdot s^{-1}$). These sudden transitions in both LI and photoperiod resulted in substantive changes in the plants' lighting environment at the start of the trial, stimulating various morphological and physiological

adaptations with differing degrees of plasticity. The leaves measured in week 1 developed and expanded during the prior vegetative phase under a different lighting regimen (LI and photoperiod). The leaves measured in week 5 were developed under their respective LPPFDs during a period characterized by slowing vegetative growth and transitioning to flower development. The leaves measured in week 9 would have also developed under their respective LPPFDs, but since cannabis vegetative growth greatly diminishes after the first five weeks in 12-h days (Potter, 2014), these tissues were physiologically much older than the leaves measured in week 5, with concomitant reductions in photosynthetic capacity (Bauerle et al., 2020; Bielczynski et al., 2017).

These differences in leaf physiological age, plant ontogeny, and localized lighting environments during leaf expansion vs. measurement resulted in notable temporal variability in leaf-level LI responses. In week 1, there were no LI treatment effects on A_{sat} and the slopes of the LSP, LNCER, and F_v/F_m were shallower in weeks 5 and 9. The comparatively lower LI responses in week 1 were likely due to the reduced adaptive plasticity that mature foliar tissues have vs. leaves that developed under a new lighting regime (Sims and Pearcy, 1992). In addition, Y-intercepts for the A_{sat}, LSP, and LNCER models were higher in week 1 than weeks 5 and 9, which may be partly due to the higher LI (amplified by the longer photoperiod) that the leaves developed under, during the latter part of the vegetative phase. Further, the A_{sat}, LSP, and LNCER models in weeks 5 and 9 have comparable slopes, but there is a vertical translation in the respective models, resulting week 9 models having substantially lower Y-intercepts (i.e., approximately half) for these parameters. The interplay of physiological age of foliage and plant ontogeny (i.e., onset of senescence) on the diminished photosynthetic capacity of the leaves in week 9 is unknown, but the dynamic temporal nature of cannabis photosynthesis (during flowering) is manifest in these models.

Given these impacts of physiological age and light history, we posit that cannabis leaf photosynthesis cannot be used as a stand-alone gauge for predicting yield. Chandra et al. (2008) and Chandra et al. (2015) provided insight into the substantial capacity for drug-type strains of indoor grown cannabis leaves to respond to LI; and the results of these trials are much lauded in the industry as evidence that maximum photosynthesis and yields will be reached under canopy-

level PPFDs of ≈1500 μmol·m^{-2}·s^{-1}. However, the 400 to 500 μmol·m^{-2}·s^{-1} increments in LPPFD does not provide sufficient granularity (particularly at low LI) to reliably model the LRCs, thus no models were provided. Further, the LRCs were made on leaves of varying and unreported physiological ages, from plants exposed to a vegetative photoperiod (18-h), and acclimated to unspecified localized LI (a canopy-level PPFD of 700 μmol·m^{-2}·s^{-1} was indicated in Chandra et al., 2015). The strong associations between a tissue's light history and its photosynthesis responses to LI, demonstrated in this trial and by others (Björkman, 1981), represent a major shortcoming of using leaf LI response models to infer crop growth and yield. To illustrate, **Figure 2.3** shows LRCs of leaves from a single cultivar, at similar physiological ages (week 5 after transition to 12-h photoperiod) but acclimated to disparate LPPFDs: 91 and 1238 μmol·m^{-2}·s^{-1}. The relative difference in LNCER at higher LIs (≈50%) between these two curves is representative of the potential uncertainty due to just one of the uncontrolled parameters (LNCER) in these prior works. Differing physiological ages of tissues at the time of measurement may have conferred an even larger degree of uncertainty in the magnitude of leaf responses to LI (Bauerle et al., 2020) than leaf light history. Consideration must also be given to the different life stages of a photoperiodic crop (i.e., vegetative vs. generative) and the inherent impact that day length imbues on the total daily PAR exposure (i.e., DLI) which can correlate better to crop yield than PPFD. Furthermore, for a given DLI, yields are higher under longer photoperiod (Vlahos et al., 1991; Zhang et al., 2018), ostensibly due to their relative proximity to their maximum QY (Ohyama et al., 2005). A final distinction between leaf photosynthesis and whole plant yield responses to LI is the saturating LI: the LSP for leaf photosynthesis were substantially lower than the LSP for yield, which remains undefined due to the linearity of the light response model.

Newly-expanded leaves, especially in herbaceous species, are able to vary their leaf size, thickness and chlorophyll content in response to LPPFD in order to balance a myriad of factors such as internal and leaf surface gas exchange (CO_2 and H_2O), internal architecture of the light-harvesting complexes, and resistance to photoinhibition (Björkman, 1981). In the present study, the effects of LI on leaf morphology were only evaluated in week 5, when the crop was still actively growing vegetative biomass. Reductions in SLW (i.e., increases in specific leaf area,

SLA) in response to increasing LI are abundant in the literature (Fernandes et al., 2013; Gratani, 2014; Sims and Pearcy, 1992). In particular, Poorter et al. (2019) reported a saturating response of SLW [also known as leaf mass (per) area; LMA] to LI across 520 species (36% of which were herbaceous plants), however much of their data was at DLIs lower than the minimum DLI in the present study (5.2 $mol \cdot m^{-2} \cdot d^{-1}$), which affected the shape of their SLW response model to LI. Across similar DLI ranges, the average increase in SLW across 520 species was 1.7× in Poorter et al., (2019) vs 1.6× in the present study, indicating that cannabis SLW responses to LI are consistent with normal trends for this parameter.

The lack of LI treatment effects on CCI are also consistent with other studies that have shown that area-based chlorophyll content is fairly stable across a broad range of LIs (Poorter et al., 2019; Björkman, 1981), despite substantial variability in photosynthetic efficiency. However, since there were LI treatment effects on SLW, chlorophyll content on leaf volume or mass bases would likely have reduced under higher LI. The positional effects on CCI (i.e., higher in upper vs. lower canopy) were probably due to the interplay between self-shading and advancing physiological age of the lower leaves (Bauerle et al., 2020). The temporal effects on CCI, which was higher in week 1 vs. weeks 5 and 9, in both upper and lower leaves, may have been due to changes in QY over the life-cycle of the crop. Bugbee and Monje (1992) presented a similar trend; high QY during the active growth phase of a 60-d crop cycle of wheat, followed by a reduction in QY at the onset of senescence (i.e., shortly before harvest). The decline in chlorophyll content in the latter phase of the production cycle probably contributed to the reductions in the photosynthetic parameters (e.g., A_{sat}, LSP, LNCER) of the tissues measured in week 9 vs. week 5.

Overall, the impact that increasing LI had on cannabis morphology and yield were captured holistically in the plant sketches in **Figure 2.6**, which shows plants grown under higher LIs had shorter internodes, smaller leaves, and much larger and denser inflorescences (resulting in higher harvest index), especially at the plant apex, compared to plants grown under lower LIs. Like many other plant species, we have found that cannabis has immense plasticity to rapidly acclimate its morphology and physiology, both at leaf- and whole plant-levels, to changes in the

growing lighting environment. Therefore, in order reliably predict cannabis growth and yield to LI, it is necessary to grow plants under a broad range of LIs through their full ontological development, as was done in this study. Without knowing the respective tissues' age and light history, instantaneous light response curves at leaf-, branch-, or even canopy-levels cannot reliably predict yield.

2.5 CONCLUSIONS

We have shown an immense plasticity for cannabis to respond to increasing LI; in terms of morphology, physiology (over time), and yield. The temporal dynamics in cannabis leaf acclimations to LI have also been explored, addressing some knowledge-gaps in relating cannabis photosynthesis to yield. The results also indicate that the relationship between LI and cannabis yield does not saturate within the practical limits of LI used in indoor production. Increasing LI also increased harvest index and the size and density of the apical inflorescence; both markers for increasing quality. However, there were no and minor LI treatment effects on the concentrations of cannabinoids and terpenes, respectively. This means that growers may be able to vastly increase yields by increasing LI but maintain a relatively consistent secondary metabolite profile in their marketable products. Ultimately, the selection of the economic optimum canopy-level LI for a given commercial production system depends on many interrelated factors.

Future research should expand to multiple cultivars of different biotypes. Further, since plant yield responses to elevated CO_2 can mirror the responses to elevated LI, the combined effects of CO_2 and LI should be investigated on cannabis yield with an in-depth cost-benefit analysis of the optimum combination of these two input parameters.

CHAPTER THREE

CANNABIS INFLORESCENCE YIELD AND CANNABINOID CONCENTRATION IS NOT IMPROVED WITH LONG-TERM EXPOSURE TO UV RADIATION

ABSTRACT

It is commonly believed that exposing cannabis plants to UV radiation can enhance Δ^9-THC concentrations in female inflorescences and associated foliar tissues. However, a lack of published scientific studies has left knowledge-gaps in the effects of UV on cannabis; these must be elucidated before UV can be utilized as a horticultural management tool in commercial cannabis production. In this study we investigated the effects of UV exposure level on photosynthesis, growth, inflorescence yield, and secondary metabolite composition of two indoor-grown cannabis cultivars: 'Low Tide' (LT) and 'Breaking Wave' (BW). After growing vegetatively for 2 weeks under a canopy-level PPFD of ≈225 $\mu mol \cdot m^{-2} \cdot s^{-1}$ in an 18-h light/6-h dark photoperiod, plants were grown for 9 weeks in a 12-h light/12-h dark "flowering" photoperiod under a canopy-level PPFD of ≈400 $\mu mol \cdot m^{-2} \cdot s^{-1}$ and 3.5 $h \cdot d^{-1}$ of supplemental UV radiation with photon flux densities (PFD) ranging from 0.01 to 0.8 $\mu mol \cdot m^{-2} \cdot s^{-1}$ provided by LEDs with a peak wavelength of 287 nm (i.e., biologically-effective UV doses of 0.2 to 13 $kJ \cdot m^{-2} \cdot d^{-1}$). The severity of UV-induced morphology (e.g., whole-plant size and leaf size reductions, leaf malformations, and stigma browning) and physiology (e.g., reduced leaf photosynthetic rate and reduced F_v/F_m) symptoms worsened as UV exposure level increased. Dry inflorescence yield decreased with increasing UV exposure level in LT, but not in BW. In LT, total equivalent Δ^9-THC and total equivalent CBD concentrations decreased with increasing UV exposure level, whereas there were no UV treatment effects on total equivalent concentrations of individual cannabinoids in BW. Total inflorescence terpene concentrations decreased linearly with increasing UV exposure level in both cultivars however, relative concentrations of individual terpenes varied by cultivar. The potential for using UV to enhance cannabis quality must still be confirmed before it can be used as a production tool for modern, indoor-grown cannabis cultivars.

3.1 INTRODUCTION

Cannabis is a short-day plant commonly cultivated for its unique secondary metabolites (e.g., cannabinoids) that are used both medicinally and recreationally (Small, 2017). Cannabis is often grown in controlled-environment facilities that are illuminated solely with electrical lighting to accommodate its photoperiod specificity and produce uniform plants by maintaining prescribed environmental parameters. Popular sole-source lighting technologies used in the flowering stage of cannabis production include HPS and, increasingly, LEDs (Cannabis Business Times, 2020); both technologies normally have little to no UV radiation in their spectra (Radetsky, 2018). In the natural environment, cannabis plants are exposed a small fraction of UVB radiation relative to the amount of PAR in sunlight. However, the higher-energy photons in the UVB vs. PAR spectra are disproportionately effective in evoking plant responses (Flint and Caldwell, 2003), including changes in morphology, physiology, and metabolism (Huché-Thélier et al., 2016; Robson et al., 2019). UVC photons have even higher energy than UVB, but solar UVC is absorbed by the ozone layer and therefore does not reach the Earth's surface (McElroy and Fogal, 2008). While UVC is used to inactivate microorganisms such as waterborne pathogens in recirculating irrigation systems (Younis et al., 2019), UVC is only rarely directly applied to foliage – to inactivate foliar pathogens through short-term exposures (Aarrouf and Urban, 2020) – since UVC can cause tissue damage (Stapleton, 1992).

UV radiation can affect many aspects of plant morphology, physiology, and metabolism (Jenkins, 2017). Plant responses to UV exposure are either induced through pathways mediated by UVR8 (a UVB-specific photoreceptor) or by UV-induced oxidative cellular damage, including to DNA (Czégény et al., 2016, Tossi et al., 2019). Typical plant responses to UV stress include stunted growth, reduced leaf area, increased leaf thickness (Robson et al., 2019), epicuticular wax accumulation (Cen and Bornman, 1993), and foliar necrosis (Klem et al., 2012; Torre et al., 2012). From an ecological standpoint, it has been speculated that Δ^9-THC (the most economically valuable psychoactive cannabinoid) production is upregulated in cannabis tissues under UV exposure to serve as photoprotection. This concept arose from studies that found comparatively higher Δ^9-THC concentrations in cannabis ecotypes that grow in global regions with relatively high solar UV exposure, such as at low latitudes and high altitudes (Small and

Beckstead, 1973; Pate, 1983). However, despite the focus on Δ^9-THC in the literature, other cannabinoids have similar UV absorbing properties (Hazekamp et al., 2005), which may challenge an ecological explanation for upregulating Δ^9-THC over other cannabinoids. Preliminary controlled-environment studies that were done about three decades ago alluded to the potential for UV to increase Δ^9-THC concentration in cannabis foliar and floral tissues (Fairbairn and Liebmann, 1974; Lydon et al., 1987). However, the concentration of Δ^9-THC in inflorescence tissues has increased substantially over the past decades, with contemporary genotypes having ≈10-fold higher Δ^9-THC concentrations than the genotypes used these older studies (Dujourdy and Besacier, 2017). Therefore, modern cannabis genotypes may function nearer to their maximum capacity for producing Δ^9-THC; which could impede their ability to further increase Δ^9-THC production under UV exposure, relative to older genotypes.

Studies on modern cannabis genotypes have shown that environmental stimuli can modify the cannabinoid composition. For example, inflorescences in CBD-dominant genotypes had greater CBD concentrations when grown at high vs. low altitude, which may have been a response to increased UV exposure at higher elevation (Giupponi et al., 2020). Drought-stress and salt-stress have also been shown to alter the inflorescence cannabinoid composition in modern genotypes (Caplan et al., 2019; Yep et al., 2020). Therefore, the potential for UV exposure to provoke changes in the secondary metabolite composition in inflorescences of modern cannabis genotypes grown in controlled-environments merits scientific investigation. Evaluating the effects of UV on modern genotypes with relatively balanced concentrations of Δ^9-THC and CBD [i.e., chemotype II; a cultivar with a ratio of Δ^9-THC to CBD of ≈1 (Small and Beckstead, 1973)] would provide insight into whether UV impacts individual cannabinoids differently.

The objectives of this study were to: 1) characterize morphological and physiological responses of indoor-grown cannabis to UV exposure, and 2) investigate the relationships between UV exposure levels during the flowering stage and inflorescence yield and secondary metabolite composition of cannabis genotypes with disparate growth habits and moderate concentrations of both Δ^9-THC and CBD.

3.2 MATERIALS AND METHODS

3.2.1 PLANT CULTURE

Cuttings were taken from mother plants of LT and BW, both of which are classified as chemotype II. After growing for 13 d under humidity domes and fluorescent light (F32T8/TL850; Philips, Amsterdam, Netherlands) providing ≈100 µmol·m^{-2}·s^{-1}, rooted cuttings were transferred to 1-gallon pots containing a peat-based substrate, and placed under LED light comprised of a mixture of Pro-325 (Lumigrow; Emeryville, CA, USA) and generic (unbranded) white LEDs providing ≈225 µmol·m^{-2}·s^{-1}, for an additional 9 d. Both the propagation and vegetative growth stages had 18-h photoperiods. The potted plants were subsequently transferred to a single deep-water CB, where they were placed in floating polystyrene rafts in an indoor cannabis production facility in southern Ontario, Canada (described in Chapter 2 of this thesis). There were 384 evenly-spaced plants in the CB at a density of 0.09 m^2/plant. The daily photoperiod was reduced to 12 h on the day the plants were transferred to the CB.

3.2.2 EXPERIMENTAL SETUP

PAR was supplied by 24 LED fixtures (Pro650; Lumigrow Inc. Emeryville, Ca, USA) arranged evenly over the CB (i.e., 2 rows of 12 PAR fixtures). The LED composition and spectrum of the PAR fixtures was described in Chapter 2 and the relative photon flux distribution is provided in **Figure 3.1A.** Single UV LED fixtures were centered between adjacent PAR fixtures (within each row), resulting in 2 rows of 11 UV fixtures. The 22 UV LED fixtures had consistent spectrum output (peak wavelength of 287 nm; **Figure 3.1B**), but adjustable intensity (with analog dimmers). According to the conventional definitions of the different UV wavebands (described above), the photon flux ratio of UVB to UVC was UVB(93):UVC(7). The UV treatments (described below) were applied daily, in the last 3.5 hours (from 16:00 HR to 19:30 HR) of the PAR photoperiod (from 07:30 HR to 19:30 HR), from the day that the plants were transferred to the CB. The plants were exposed to the UV treatments for 60 d (≈9 weeks) and then harvested.

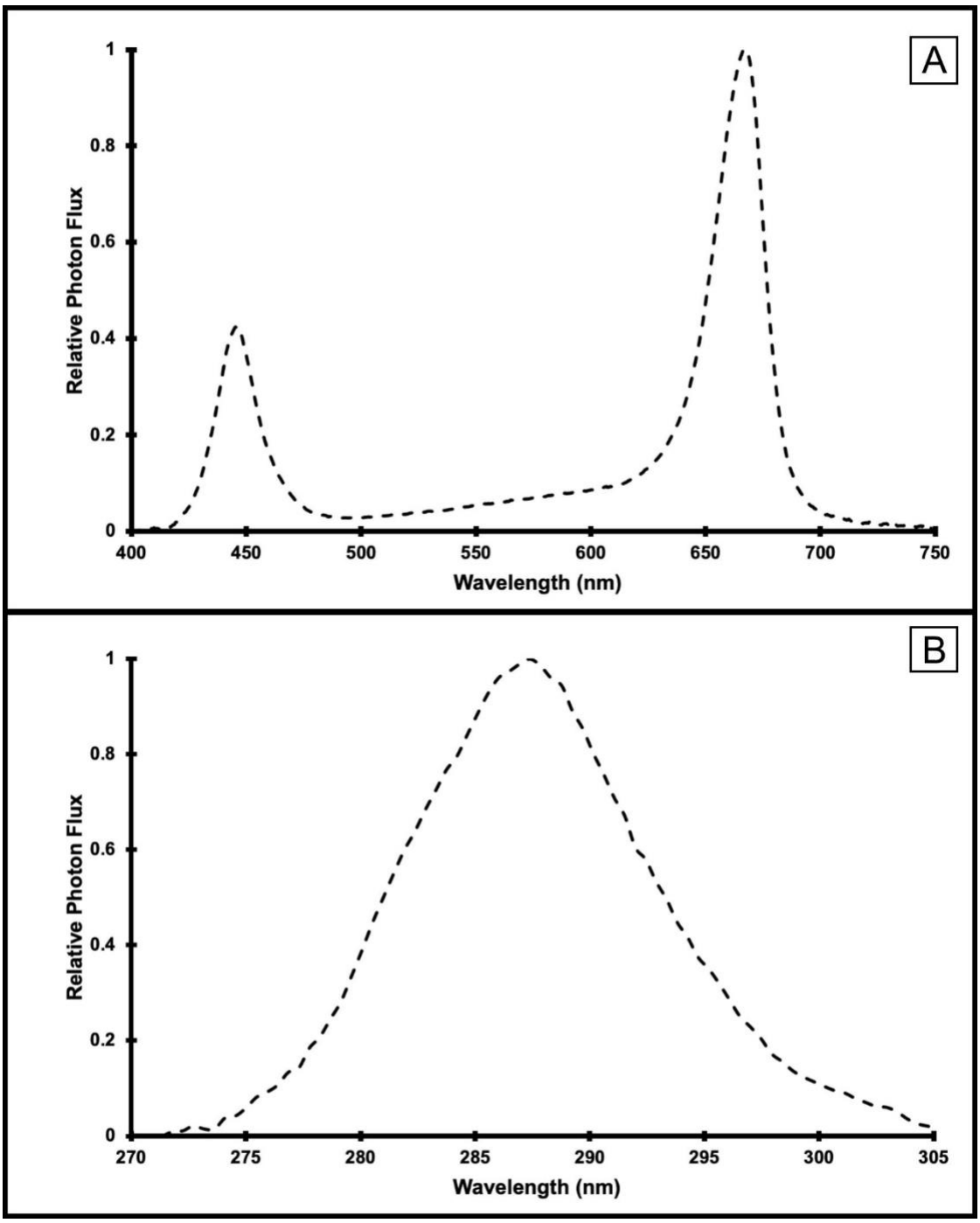

Figure 3.1. Relative spectral photon flux distribution of **(A)** Pro-650 (Lumigrow) LED fixtures and **(B)** UV LED fixtures.

For each cultivar, 44 representative uniform plants were selected from the larger populations to be experimentally evaluated. Plots, each consisting of 4 plants, were arranged where 2 plants were directly underneath each UV LED fixture, and 2 plants were adjacent. There were 3 UV LED fixture settings that were randomly assigned (within each cultivar) to each plot: off, half power, and full power. Within each plot, the 2 plants closer to the UV LED fixture were exposed to relatively higher UV exposure than the 2 adjacent plants. This configuration allowed for a wide range of evenly-distributed UV exposure levels; ranging from 0.01 to 0.8 $\mu mol \cdot m^{-2} \cdot s^{-1}$.

At the start of the UV treatments, experimental plants of LT all had 7 nodes, with heights (from the substrate surface to the shoot apex) ranging from 14 to 23 cm. Experimental plants of BW had 8 nodes, with heights ranging from 14 to 20 cm. Experimental plants were surrounded by plants of the same cultivar to maintain canopy uniformity. The LT cultivar populated the south half of the CB, while BW populated the north half.

Average hang height (i.e., distance from the bottom of the fixtures to the top of the canopy) was maintained at 50.5 cm by adjusting the height of the light racks weekly using a system of pulleys and cables. Canopy-level PPFD (400 to 700 nm) and UV-PFD (270 to 320 nm) were measured at the apex of each plant weekly, after the light rack height adjustment, using a PAR meter (LI-180; LI-COR Biosciences, Lincoln, NE, USA) and a radiometrically-calibrated spectrometer (XR-Flame-S, Ocean Optics, Dunedin, Florida), respectively. A MS Excel tool developed by Mah et al. (2019) was used to integrate spectrometer data into UV-PFD, biologically-effective UV-PFD [$UV\text{-}PFD_{BE}$; Flint and Caldwell (2003)], and daily biologically-effective UV dose ($kJ \cdot m^{-2} \cdot d^{-1}$) (**Table 3.1**). At the end of the trial, average PPFD and average UV-PFD were calculated for each treatment plant by determining the corresponding TLI ($mol \cdot m^{-2}$) as described in Chapter 2. The experiment-wise average (± SE, n = 88) PPFD was 408 ± 6.5 $\mu mol \cdot m^{-2} \cdot s^{-1}$. The average UV-PFD for each plant was used as the independent variable (i.e., X-axis) in regressions of UV exposure vs. the measured growth, yield and quality parameters.

Table 3.1. Range of canopy-level UV photon flux density, UV biologically-effective photon flux density and daily UV biologically-effective dose from UV LEDs with a peak wavelength of 287 nm and a daily 3.5 h photoperiod.

UV exposure target	UV photon flux density ($\mu mol \cdot m^{-2} \cdot s^{-1}$)	UV biologically effective[z] photon flux density ($\mu mol \cdot m^{-2} \cdot s^{-1}$)	Daily UV biologically-effective dose ($kJ \cdot m^{-2} \cdot d^{-1}$)
Minimum	0.01	0.032	0.16
Low	0.1	0.32	1.6
Medium	0.5	1.6	8.3
Maximum	0.8	2.5	13

[z] weighted using the BSWF for Plant Growth by Flint and Caldwell (2003)

Plant husbandry and environmental controls followed the cultivator's standard operating procedures except for the UV radiation. The air temperature and relative humidity set points were: 25°C and 60%. There was no CO_2 supplementation, with typical concentrations of ≈400 ppm when lights were on. The aquaponic solution was maintained within normal levels of nutrient concentrations, pH, electrical conductivity and dissolved oxygen, as described in Chapter 2.

3.2.3 GROWTH MEASUREMENTS

The number of nodes (i.e., primary branches), height (i.e., length of main stem from substrate surface to the highest point) and widths (i.e., the widest part and its perpendicular width) of each experimental plant were measured in week 6. Plant height and widths were used to calculate growth index [(height × $width_1$ × $width_2$) / 300 (Ruter, 1992)] for each plant.

3.2.4 LEAF CHLOROPHYLL AND FLUORESCENCE MEASUREMENTS

CCI [% transmission at 931 nm / % transmission at 653 nm (Parry et al., 2014)] was measured in upper and lower canopy leaves in week 3. Triplicate measurements from the center leaflet of the three youngest fully-expanded fan leaves and from three fan leaves at the bottom of each plant, were taken using a chlorophyll meter (CCM-200; Opti-Sciences, Hudson, NH, USA). The triplicate measurements were averaged per plant for the upper and lower canopy leaves, respectively.

The ratio of variable to maximum fluorescence (F_v/F_m) emitted from photosystem II in dark-acclimated leaves exposed to a light-saturating pulse is an indicator of maximum quantum yield of photosystem II photochemistry (Murchie and Lawson, 2013). During the first 8.5 h of the PAR photoperiod (i.e., before daily UV exposure), the middle leaflet of the youngest, fully-expanded fan leaf from each plant was dark acclimated for 15 min and then F_v/F_m measurements were taken with a fluorometer (FluorPen FP 100; Drasov, Czech Republic). The F_v/F_m measurements were done weekly on each cultivar, from the start of the trial until evidence of stress (i.e., reduction of F_v/F_m with increasing UV-PFD) was seen.

3.2.5 LEAF GAS EXCHANGE MEASUREMENTS, LEAF SIZE AND SPECIFIC LEAF WEIGHT

Quantifications of leaf gas exchange of the middle leaflet of the youngest, fully-expanded fan leaf on each plant was performed in week 5 during the first 8.5 h of the PAR photoperiod using a portable photosynthesis machine (LI-6400XT; LI-COR Biosciences, Lincoln, NE, USA) equipped with the B and R LED light source (6400-02B; LI-COR Biosciences). *In situ* NCER was measured with the leaf chamber environmental conditions set to: PPFD of 500 $\mu mol \cdot m^{-2} \cdot s^{-1}$, block temperature of 26.7°C, CO_2 concentration of 400 ppm, and air flow rate of 500 $\mu mol \cdot s^{-1}$. If the leaflet did not cover the entire 6 cm^2 chamber, the section of the leaflet that was clamped in the chamber gasket was marked along the outside of the gasket so that leaf area inside the chamber could be calculated post hoc (described below). After removing the leaflets from the leaf chamber, whole leaves were excised from the plant and scanned (CanoScan LiDE 25; Canon Canada Inc., Brampton, ON, Canada) at 600 dpi resolution. Each leaf was oven dried to constant weight at 65°C (Isotemp Oven 655G; Fisher Scientific, East Lyme, CT, USA). The scanned images were processed using ImageJ 1.42 software (National Institute of Health; https://imagej.nih.gov/ij/download.html) to determine the leaflet area within the gas exchange chamber and the total individual leaf size. The DW of each scanned leaf was measured using an analytical balance (MS304TS/A00; Mettler-Toledo, Columbus, OH, USA) to determine SLW [leaf DW / leaf size ($g \cdot m^{-2}$)].

3.2.6 VISUAL OBSERVATIONS

Weekly observations were performed on each plant to evaluate other visual parameters, including: upward curling of the leaflet margins, leaf shine, leaf-drop, browning of inflorescence stigmas, leaf epinasty (i.e., concaved leaf tissue between veins), leaf necrotic patches, and appearance of powdery mildew on the adaxial sides of the leaves. Except for week 1 observations, which occurred 4 d after the start of the UV treatments, all weekly observations occurred on 7-d intervals. Leaf-drop was recorded as the occurrence of fallen leaves observed on each plant's substrate surface. The absence or presence of each respective parameter was evaluated for each plant, weekly. While these are observational data, weekly minimum UV-PFDs where parameters were observed were reported, regardless of whether or not all plants above these UV levels displayed the observed responses.

At various points throughout the trial, representative photos of each cultivar under different UV exposure levels were taken with a digital camera (iPhone XR iOS 14.4.1; Cupertino, CA, USA). In week 2, photos of whole plants exposed to minimum and maximum UV exposure, of each cultivar, were taken. Photos of whole plants in week 3 and whole plants and apical inflorescences at harvest (i.e., week 9), exposed to minimum, low, moderate and maximum UV exposure levels (described in **Table 3.1**) were taken for each cultivar. Photos of the inflorescences grown under minimum and maximum exposure levels, of each cultivar, were taken in week 4. In week 5 [i.e., approximately when vegetative growth in cannabis ceases (Rodriguez-Morrison et al., 2021)], fully-expanded leaves from plants under minimum, moderate, and high UV exposure were excised from the plants and scanned (CanoScan LiDE 25) at 600 dpi resolution. All photos were processed using ImageJ 1.42 software to add scale bars.

3.2.7 YIELD AND QUALITY

The FWs of total inflorescence, stems, and leaves were separately weighed for each plant using a precision balance (EG 2200-2NM; Kern, Balingen, Germany). The separated aboveground tissues of all plants were oven-dried at 65°C to constant weight (Isotemp Oven 655G) and the DW (i.e., yield) of the respective tissues were recorded. The apical inflorescences of 18 plants from each cultivar that were representative of the entire range of UV-PFD exposure levels were

air dried at 15°C and 40% relative humidity for 7 d before 2 g sub-samples from each plant were submitted to an independent laboratory (RPC Science & Engineering; Fredericton, NB, Canada) for analysis of concentrations [reported in $mg \cdot g^{-1}_{(DW)}$] of cannabinoids using ultra-high-performance liquid chromatography and variable wavelength detection (HPLC-VWD) and terpenes using gas chromatography and mass spectrometry detection (GC-MSD). Total equivalent Δ^9-THC, CBD, and CBG concentrations were determined by assuming complete carboxylation of the acid-forms (i.e., Δ^9-THCA, CBDA and CBGA) of the respective cannabinoids, whose concentrations were adjusted by factoring out the acid-moiety from the molecular weight of each respective compound [e.g., total equivalent Δ^9-THC = (Δ^9-THCA × 0.877) + Δ^9-THC].

3.2.8 STATISTICAL ANALYSIS

The treatments in this experiment were continuous, independent variables based on the calculated UV-PFDs for each individual plant, each week. On per cultivar bases, the best-fit models (linear or quadratic) for parameters with continuous dependent variables were selected based on the lowest value for the Akaike Information Criterion (AICc) using UV-PFD as the independent variable using the PROC NLMIXED procedure (SAS Studio Release 3.8; SAS Institute Inc., Cary, NC). Analyses also revealed that each dataset had a normal distribution. For parameters that were measured prior to harvest, UV exposure was determined based on the weekly UV measurements made until the parameter was measured. If there were no LI treatment effects on a given parameter, then parameter means (± SD) were calculated.

3.3 RESULTS

The measured canopy-level range of average UV-PFDs (based on the weekly UV measurements) was 0.01 to 0.8 $\mu mol \cdot m^{-2} \cdot s^{-1}$. The average (± SE) step change, relative to the maximum UV-PFD, between adjacent UV-PFD levels was 2.3 ± 0.43% for both cultivars. For models presented below, this range was used to contextualize the results since all measured parameters fit within this range.

3.3.1 UV-INDUCED CANNABIS MORPHOLOGY AND PHYSIOLOGY CHANGES

While each entire plant was observed for UV-induced changes in morphology, the recorded effects occurred primarily in recently developed tissues. Where UV effects were also seen in older tissues has been highlighted in the text. The data in **Table 3.2** are provided to show the temporal trends in how the parameters relate to each other and how UV sensitivity increases over time.

The UV-induced changes in cannabis morphology appeared within the first few days of the initiation of the UV treatments (i.e., in week 1), where the leaflet margins on leaves that had developed in the vegetative stage (i.e., prior to the initiation of the UV exposure) curled upwards under UV-PFDs ≥0.33 and ≥0.37 $\mu mol \cdot m^{-2} \cdot s^{-1}$ in the LT and BW cultivars, respectively (**Table 3.2**). Leaves appeared to accumulate epicuticular wax, as demonstrated by the increase in shiny appearance of adaxial surfaces, shortly after UV exposure began and persisted henceforth. Leaf shine also appeared to be more prevalent in plants exposed to higher UV-PFDs, more so in BW vs. LT. In week 2 there were no changes in the extent of upward curling in the leaves that had developed during the vegetative stage (i.e., older, mid-canopy leaves) however, newly expanded leaves did not present this symptom (**Figure 3.2**). In week 3 (about a week after the first appearance of inflorescences), stigmas of terminal inflorescences began to turn from white to brown on LT plants exposed to UV-PFDs ≥0.69 $\mu mol \cdot m^{-2} \cdot s^{-1}$ and ≥0.30 $\mu mol \cdot m^{-2} \cdot s^{-1}$ in BW (**Figure 3.3, Table 3.2**). In week 3, early symptoms of upper leaf epinasty started to appear in upper canopy leaves of plants grown under the highest UV-PFDs (**Figure 3.3**); observational measurements on leaf epinasty were initiated in week 5. Leaf-drop occurred in week 3 on plants under UV-PFDs ≥0.14 and ≥0.23 $\mu mol \cdot m^{-2} \cdot s^{-1}$ in LT and BW, respectively (**Table 3.2**). Fallen leaves appeared to be predominantly the same leaves that showed upward curling in week 1.

There were no treatment effects on the CCI of the upper canopy leaves of LT in week 3, but the CCI of the upper canopy leaves of BW decreased linearly and with a 42% reduction from lowest to highest UV-PFD. The CCI in the lower canopy leaves decreased linearly with the increase of UV-PFD in week 3, with 60% and 46% reductions from lowest to highest UV-PFD in LT and BW, respectively (**Table 3.3**). In week 4, the minimum UV-PFD at which plants exhibited

stigma browning (0.22 and 0.14 µmol·m^{-2}·s^{-1} in LT and BW, respectively) and leaf-drop (0.013 and 0.050 µmol·m^{-2}·s^{-1} in LT and BW, respectively) were lower than the previous week (**Table 3.2**). The onset of UV treatment effects on F_v/F_m were observed in week 4 for BW and in week 5 for LT. Both cultivars presented quadratic relationships between UV-PFD and F_v/F_m (**Table 3.3**). However, the F_v/F_m values were within 1% (i.e., low stress) of their respective vertices (both ≈0.79, at 0.084 and 0.12 µmol·m^{-2}·s^{-1} for LT and BW, respectively) from the lowest UV-PFD up to ≈0.25 µmol·m^{-2}·s^{-1}, followed by an increasing rate of reduction in F_v/F_m with increasing UV-PFD thereafter. At the highest UV-PFD, the F_v/F_m values were 10% and 21% lower than the respective vertices for LT (in week 5) and BW (in week 4), respectively. The severity of UV-induced epinasty was higher in plants exposed to higher UV-PFDs, demonstrated by images of whole plants (in week 3) of LT (**Figure 3.4A**) and BW (**Figure 3.4B**) and single-leaf scans (in week 5) of LT and BW (**Figure 3.5**) grown under various UV exposure levels. In week 5, leaves (particularly in the upper canopy) showed upward curling under minimum UV-PFDs of 0.16 and 0.34 µmol·m^{-2}·s^{-1} in LT and BW, respectively (**Table 3.2, Figure 3.5**). In week 5, brown stigmas were observed at the minimum UV-PFD in LT and 0.14 µmol·m^{-2} in BW (**Table 3.2**). Leaf-drop was observed at very low UV-PFDs of 0.013 µmol·m^{-2}·s^{-1} in LT and 0.015 µmol·m^{-2}·s^{-1} in BW (**Table 3.2**).

Leaf epinasty was evident in week 5, predominantly in youngest fully-expanded leaves, exposed to minimum UV-PFDs of 0.13 µmol·m^{-2}·s^{-1} in LT and 0.14 µmol·m^{-2}·s^{-1} in BW (**Table 3.2**). In week 5, the size of the youngest fully-expanded leaf on each plant decreased linearly by almost half in both cultivars, while SLW increased by 27% and 21% in LT and BW under highest vs. lowest UV-PFD (**Table 3.3**). In week 5, the *in situ* NCER of the youngest fully-expanded leaves decreased 31% and 27% in LT and BW, respectively, at highest vs. lowest UV-PFD (**Table 3.3**). Brown stigmas and leaf-drop were observed in all experimental plants starting in week 6 (**Table 3.2**). Starting in in week 7, upper canopy leaves on a few plants grown under intermediate UV-PFDs (i.e., ranging from 0.12 to 0.69 µmol·m^{-2}·s^{-1} in LT) began to show brown (necrotic) patches (**Table 3.2**, see **Appendix C**). The minimum UV-PFDs under which leaf epinasty was evident were marginally lower in week 7 vs. week 5, and substantially lower in week 8 vs. week 7 (**Table 3.2**). The prevalence of leaves exhibiting necrotic patches increased in BW in week 8

vs. week 7 (**Table 3.2**). While investigating the UV exposure effects on foliar powdery mildew was not one of the designed objectives of this study, treatment differences were observed and recorded. In week 9, powdery mildew was visible on the adaxial leaf surfaces on plants exposed to lower UV-PFDs but was not observed on any plants exposed to UV-PFDs ≥0.076 µmol·m^{-2}·s^{-1} in LT and ≥0.090 µmol·m^{-2}·s^{-1} in BW (**Table 3.2, Figure 3.6**).

Figure 3.2. (A) The side view and **(B)** top view of *Cannabis sativa* L. plants in week 2 after the initiation of the UV treatments. 'Low Tide' under **(1)** minimum and **(2)** maximum UV exposure and 'Breaking Wave' under **(3)** minimum and **(4)** maximum UV exposure levels. The black scale bar at the lower right of each image is 5.0 cm.

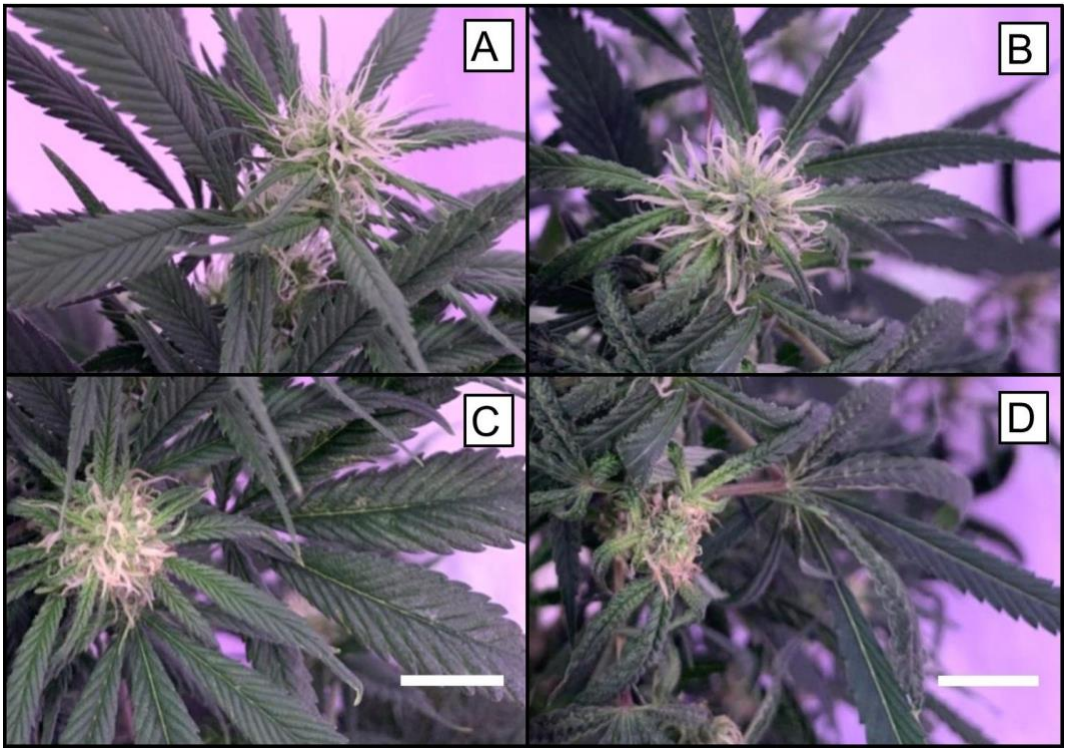

Figure 3.3. (A) 'Low Tide' (LT) and **(B)** 'Breaking Wave' (BW) *Cannabis sativa* L. stigmas under minimum UV exposure levels and **(C)** LT and **(D)** BW under maximum UV exposure levels, in week 3 after the initiation of the UV treatments. The white scale bar at the lower right of (C) applies to (A), and at the lower right of (D) applies to (B). Both scale bars are 1.0 cm.

Figure 3.4. (A) ‘Low Tide’ and **(B)** ‘Breaking Wave’ *Cannabis sativa* L. plants demonstrating (from left to right) minimum, low, moderate, and high UV exposure levels. The images were taken in week 3 after the initiation of the UV treatments. The black scale bar at the lower right of each image is 5.0 cm.

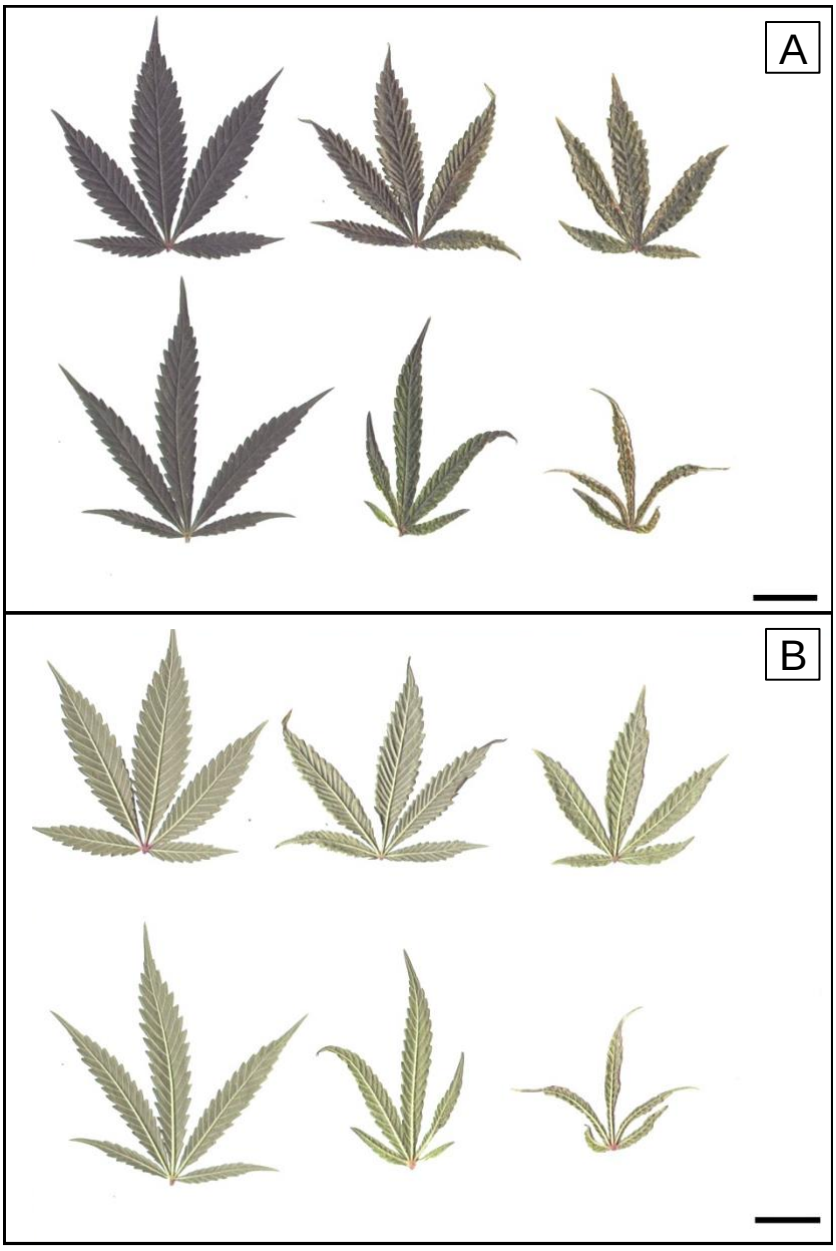

Figure 3.5. (A) Adaxial and **(B)** abaxial sides of youngest, fully-expanded *Cannabis sativa* L. fan leaves of 'Low Tide' (top row in each image) and 'Breaking Wave' (bottom row in each image) demonstrating UV induced leaf morphology effects with increasing UV-PFDs. Leaves from plants under minimum UV exposure are on the left, moderate UV exposure in the middle, and high UV exposure on the right. Scans were taken in week 5 after the initiation of UV treatments. The black scale bar at the lower right of each image is 2.0 cm.

Table 3.2. Minimum UV-PFD (µmol·m^{-2}·s^{-1}) where symptoms were observed in *Cannabis sativa* L. 'Low Tide' (LT) and 'Breaking Wave' (BW) cultivars (CV) in each week after the initiation of UV treatments, regardless of whether or not all plants above the minimum UV-PFD presented the observed symptom.

		Leaf symptoms					Flower Symptoms
Week[z]	CV	Upward curling	Epinasty	Leaf-drop	Necrotic patches	Powdery mildew	Stigma browning
1	LT	0.33	NI[y]	NI	NI	NI	NI
	BW	0.37					
2	LT	NIE[x]	NI	NI	NI	NI	NI
	BW						
3	LT	NIE	NI	0.14	NI	NI	0.69
	BW			0.23			0.30
4	LT	NIE	NI	0.013	NI	NI	0.22
	BW			0.050			0.14
5	LT	0.16	0.13	0.013	NI	NI	0
	BW	0.34	0.14	0.015			0.14
6	LT	0.13	NIE	0[w]	NI	NI	0
	BW	0.33		0			0
7	LT	NIE	0.10	0	0.12 to 0.69[v]	NI	0
	BW		0.13	0	0.32		0
8	LT	NIE	0.018	0	0.12 to 0.70	NI	0
	BW		0.034	0	0.20 to 0.51		0
9	LT	NIE	NIE	0	NIE	0 to 0.076	0
	BW			0		0 to 0.090	0

[z]except for observations in week 1, which occurred 4 d after the start of the UV treatments, all weekly observations occurred on 7-d intervals

[y]NI: symptom was not investigated

[x]NIE: no increase in extent of crop sensitivity to UV exposure level was observed

[w]zero indicates that the symptom was observed at the lowest UV-PFD

[v]ranges are provided when the symptom was observed in only intermediate UV-PFDs

Table 3.3. The effects of UV-PFD ($\mu mol \cdot m^{-2} \cdot s^{-1}$) applied during the flowering stage on physiological, morphological and yield parameters of *Cannabis sativa* L. 'Low Tide' and 'Breaking Wave'.

Parameter	Unit	Regression equation[z], R^2 or mean ± SD[y]	
		'Low Tide'	'Breaking Wave'
CCI[x] of upper canopy leaves in week 3	–	42.0 ± 8.11	y = –19.0x + 36, 0.28
CCI of lower canopy leaves in week 3	–	y = –30.6x + 41, 0.39	y = –18.7x + 32, 0.27
Net CO_2 exchange rate (NCER) in week 5	$\mu mol_{(CO_2)} \cdot m^{-2} \cdot s^{-1}$	y = –7.52x + 19, 0.35	y = –6.78x + 20, 0.32
F_v/F_m in week 2	–	0.78 ± 0.0269	0.78 ± 0.0338
F_v/F_m in week 3	–	0.80 ± 0.0154	0.77 ± 0.0329
F_v/F_m in week 4	–	0.78 ± 0.0224	$y = –0.364x^2 + 0.0839x + 0.79$, 0.87
F_v/F_m in week 5	–	$y = –0.152x^2 + 0.0255x + 0.79$, 0.41	–
Individual leaf size in week 5	cm^2/leaf	y = –15.7x + 28, 0.46	y = –10.4x + 18, 0.45
Specific leaf weight (SLW) in week 5	$g_{(leaf)} \cdot m^{-2}{}_{(leaf)}$	y = 15.4x + 45, 0.34	y = 12.3x + 46, 0.32
Growth index in week 6	–	y = –210x + 275, 0.25	y = –145x + 350, 0.11
Increase in height until week 6	cm	y = –13.7x + 35, 0.14	y = –11.9x + 36, 0.13
Increase in number of nodes until week 6	–	y = –3.42x + 10.0, 0.11	y = –3.15x + 9.7, 0.11
Inflorescence moisture content	%	79.0 ± 1.27	79.3 ± 1.01
Leaf moisture content	%	69.5 ± 3.59	72.0 ± 2.31
Stem moisture content	%	72.4 ± 2.93	74.5 ± 2.17
Apical inflorescence dry weight (DW)	$g \cdot m^{-2}$	y = –55.8x + 57, 0.43	y = –22.5x + 26, 0.45
Total inflorescence DW	$g \cdot m^{-2}$	y = –95.6x + 235, 0.11	236 ± 63
Leaf DW	$g \cdot m^{-2}$	y = –26.0x + 111, 0.14	y = –40.5x + 100, 0.28
Stem DW	$g \cdot m^{-2}$	49.2 ± 26.5	46.1 ± 21.6

[z]parameters with UV treatment effects ($P \leq 0.05$) are presented as linear or quadratic models and the R^2

[y]the means ± SD are presented for parameters without UV treatment effects

[x]chlorophyll content index

3.3.2 GROWTH RESPONSES TO UV

Exposure to UV radiation suppressed plant growth, which was recorded after the cessation of the majority of vegetative growth (i.e., week 6). Growth indices were 61% and 33% lower in plants grown under the highest vs. lowest UV-PFDs in LT and BW, respectively (**Table 3.3**, **Figure 3.6**). Increases in height were 31% and 26% lower in plants grown under the highest vs. lowest UV-PFDs in LT and BW, respectively. Increases in numbers of nodes were 27% and 26% lower in plants grown under the highest vs. lowest UV-PFDs in LT and BW, respectively (**Table 3.3**).

There were no UV treatment effects on moisture content of aboveground tissues in either cultivar (**Table 3.3**).

Figure 3.6. Gross plant morphology of **(A)** 'Low Tide' and **(B)** 'Breaking Wave' *Cannabis sativa* L. plants grown under (from left to right) minimum, low, moderate, and high UV exposure levels. Images were taken just prior to harvest (i.e., 9 weeks after the initiation of UV treatments). Note the white spots (powdery mildew) on the adaxial sides of leaves on the far-left plants. The black scale bar at the upper left of each image is 5.0 cm.

3.3.3 RESPONSES OF INFLORESCENCE YIELD, QUALITY AND CANNABINOID AND TERPENE CONCENTRATIONS TO UV

The most discernable UV exposure effects on inflorescences were the differences in size (**Figure 3.7**) of the apical inflorescences. The apical inflorescence DW was reduced linearly by 78% and 69% in LT and BW, respectively, from the lowest to highest UV-PFDs. However, the reduction in apical inflorescence DW under increasing UV exposure only translated to reductions in total inflorescence DW in LT, which was 32% lower under the highest vs. lowest UV-PFDs. Approximately 60% of the difference in the total LT inflorescence DW in lowest vs. highest UV exposure levels arose from the decreases in the DW of apical inflorescences. The leaf DW were 19% and 32% lower under highest vs. lowest UV-PFD in LT and BW, respectively. There were no UV treatment effects on stem DW.

The effects of UV exposure on the apical inflorescence secondary metabolite composition varied between the two cultivars. In LT, the concentrations of Δ^9-THCA, CBDA and CBGA decreased linearly by 15%, 21% and 31%, respectively, as UV-PFD increased from lowest to highest (**Table 3.4**); with concomitant reductions in the total equivalent concentrations of these cannabinoids. However, there were no UV treatment effects on Δ^9-THC, CBD, CBG or cannabinol (CBN) concentrations, or the ratio of total equivalent Δ^9-THC to total equivalent CBD (hereafter, Δ^9-THC:CBD) in LT. As UV-PFD increased from lowest to highest, the concentrations of myrcene, limonene, fenchol all decreased in LT, resulting in a combined 41% decrease in the total concentration of terpenes. In BW, the concentration of Δ^9-THC in the apical inflorescences was 1.6 times higher under highest vs. lowest UV-PFD, while there were no UV treatment effects on the concentrations of the other cannabinoids. However, the Δ^9-THC:CBD was 1.1 times higher in BW under highest vs. lowest UV-PFD. The concentration of myrcene and linalool in BW decreased while caryophyllene and guaiol concentrations increased, with increasing UV-PFD, resulting in a combined 24% decrease in the total concentration of terpenes at the highest vs. lowest UV-PFD.

Figure 3.7. The apical inflorescences of **(A)** 'Low Tide' and **(B)** 'Breaking Wave' *Cannabis sativa* L. plants grown under (from left to right) minimum, low, moderate, and high UV exposure levels. Images were taken at harvest (i.e., 9 weeks after the initiation of UV treatments). The black scale bar at the upper left of each image is 2.0 cm.

Table 3.4. The effects of UV-PFD ($\mu mol \cdot m^{-2} \cdot s^{-1}$) applied during the flowering stage on cannabinoid and terpene concentrations ($mg \cdot g^{-1}$) in the apical inflorescence of *Cannabis sativa* L. 'Low Tide' and 'Breaking Wave'.

Parameter ($mg \cdot g^{-1}$)	Regression equation[z], R^2 or mean ± SD[y]	
	'Low Tide'	'Breaking Wave'
Δ^9-tetrahydrocannabinol (Δ^9-THC)	1.66 ± 0.347	y = 1.02x + 1.35, 0.327
Δ^9-THC acid (Δ^9-THCA)	y = –15.9x + 84.3, 0.294	73.8 ± 12.2
Total equivalent Δ^9-THC (TΔ^9-THC)	y = –13.5x+ 75.5, 0.282	66.5 ± 11.1
Cannabidiol (CBD)	1.38 ± 0.447	1.47 ± 0.338
CBD acid (CBDA)	y = –33.9x + 130, 0.428	93.8 ± 13.8
Total equivalent CBD (TCBD)	y = –29.3x + 115, 0.408	83.7 ± 12.2
Cannabigerol (CBG)	0.657 ± 0.275	1.27 ± 0.217
CBG acid (CBGA)	y = –3.31x + 8.59, 0.576	6.04 ± 1.07
Total equivalent CBG (TCBG)	y = –2.93x+ 8.21, 0.435	6.85 ± 1.07
Total equivalent Δ^9-THC: total equivalent CBD	0.678 ± 0.0387	y = 0.0980x + 0.755, 0.262
Cannabinol (CBN)	UDL[x]	UDL
Alpha pinene	UDL	0.214 ± 0.0593
Beta pinene	0.235 ± 0.0672	0.440 ± 0.124
Myrcene	y = –4.16x + 6.21, 0.376	y = –2.47x + 3.45, 0.363
Limonene	y = –0.788x + 1.26, 0.341	1.57 ± 0.423
Linalool	0.274 ± 0.0703	y = –0.147x + 0.222, 0.528
Terpineol	0.254 ± 0.0655	0.379 ± 0.108
Caryophyllene	2.42 ± 0.746	y = 0.520x + 1.13, 0.354
Humulene	0.892 ± 0.324	0.403 ± 0.0842
Fenchol	y = –0.118x + 0.219, 0.321	0.257 ± 0.0653
Guaiol	0.801 ± 0.100	y = 0.251x + 0.457, 0.313
Alpha-bisabolol	0.677 ± 0.181	0.355 ± 0.104
Total terpenes	y = –7.25x + 14.0, 0.383	y = –2.72x + 9.21, 0.222

[z]cannabinoids and terpenes with UV treatment effects ($P \leq 0.05$) are presented as equations and R^2

[y]the means ± SD are presented for cannabinoids and terpenes without UV treatment effects

[x]under detection limit of 0.5 $mg \cdot g^{-1}$ of inflorescence DW

3.4 DISCUSSION

Both LT and BW cultivars would be categorized as chemotype II because they have relatively balanced total Δ^9-THC and total CBD concentrations (Small and Beckstead, 1973). However, they demonstrated disparate morphological attributes: LT had a relatively compact phenotype with wide leaflets and dense branching and BW had a relatively spindly phenotype with narrow leaflets and sparse branching. Each cultivar responded to UV exposure with different magnitudes of severity, but in the majority of the parameters that had UV treatment effects, increasing UV exposure resulted in distress responses [i.e., damage to plant growth and health following a strong stress event (Hideg et al., 2013)] that are generally unfavorable for commercial cannabis production.

3.4.1 UV RADIATION ALTERS CANNABIS MORPHOLOGY AND PHYSIOLOGY

Cannabis leaf morphology demonstrated substantial plasticity in response to UV radiation exposure throughout the 9-week flowering stage. The first observed morphological response to UV was upward curling of leaflet margins during the first week of treatment in plants exposed UV-PFDs as low as 0.33 $\mu mol \cdot m^{-2} \cdot s^{-1}$ in LT and 0.37 $\mu mol \cdot m^{-2} \cdot s^{-1}$ in BW. Upward leaf curling was most evident under higher UV-PFDs, and it occurred primarily on the youngest leaves (i.e., that developed just prior to UV exposure). Conversely, leaves that expanded in subsequent weeks (i.e., under UV exposure) exhibited more typical UV-induced morphology responses such as reduced leaf size and increased SLW, which were more prominent in plants grown under higher UV exposure levels (Searles et al., 2001; Zlatev et al., 2012). Further, by week 5, leaves of both cultivars exhibited similar responses of increasing epinasty with increasing UV-PFD. Leaves in BW demonstrated more plasticity in terms of epinasty than LT (**Figure 3.5**), which may be acclimations for leaf protection by reducing foliar exposure to UV stress (Wilson, 1998; Fierro et al., 2015). The apparent increase in leaf shine shortly after the initiation of UV exposures indicates an accumulation of epicuticular wax, which is a common response to UV exposure in other crops (Steinmüller and Tevini, 1985; Cen and Bornman, 1993; Fukuda et al., 2008; Valenta et al., 2020). Since epicuticular wax may reflect UV radiation (Cen and Bornman, 1993; Valenta et al., 2020), upregulating epicuticular wax production may reduce the potential for damage to the photosynthetic machinery.

UV radiation accelerated plant senescence symptoms (i.e., symptoms associated with deterioration with age), including signs of foliar stress. Female inflorescence maturation can be characterized by carpel swelling and the transition from white stigmas to a reddish-brown colour in the final days before harvest (Punja and Holmes, 2020). Although the number of days until the appearance of inflorescences after moving to the 12-h photoperiod was unaffected by UV exposure (data not shown), plants exposed to higher UV-PFDs exhibited earlier stigma browning without carpel swelling (**Figure 3.3**). It is unknown if premature stigma senescence has any knock-on effects on other inflorescence development parameters, such as production of secondary metabolites. However, since stigma browning was observed in different weeks

depending on UV exposure levels, this attribute could not be used reliably to determine the "optimum harvest maturity".

Foliar chlorophyll content is often negatively correlated to UV exposure level (Neugart and Schreiner, 2018), which could have negative effects on photosynthesis (Singsaas et al., 2004). While increasing UV-PFD decreased CCI in the upper canopy leaves of BW and there were no UV treatment effects on CCI in LT, CCI is an area-based metric that is not directly indicative of leaf chlorophyll concentration on a biomass basis (i.e., $mg \cdot g^{-1}$). Chlorophyll concentration in the upper canopy leaves in both cultivars would probably have been reduced under increasing UV-PFD due to the trends of increasing SLW (i.e., leaf thickness) under higher UV exposure. Reduced lower canopy CCI was manifested through higher leaf chlorosis (e.g., **Figure 3.6**) and earlier leaf-drop, a phenomenon also seen in sweet basil exposed to UVB radiation (Dou et al., 2019). Nitrogen from lower canopy leaves is normally remobilized to more active upper canopy foliage (Havé et al., 2017) as plants age; this appeared to be accelerated by UV exposure given the reduction in CCI. Foliar necrosis is also a commonly-observed symptom of UV damage in many species (Maffei and Scannerini, 2000; Zhao et al., 2003; Dou et al., 2019). While the severity of most of the observed UV stress responses increased with increasing UV exposure, necrotic patches were observed on upper canopy leaves exposed to intermediate UV-PFDs (primarily in LT) in the latter weeks of the trial. The acclimation (e.g., epinasty, curling, small size) of leaves exposed to the highest UV-PFDs may have mitigated foliar necrosis, while the leaves grown under intermediate UV-PFDs may not have been sufficiently acclimated for long-term UV exposure. Upper canopy leaves (in week 5 for LT and week 4 for BW) exposed UV-PFDs <0.25 $\mu mol \cdot m^{-2} \cdot s^{-1}$ had F_v/F_m values of ≈0.8, which is normal for unstressed leaves (Björkman and Demmig, 1987). The reduction in F_v/F_m at higher UV exposure levels in both cultivars indicates that UV radiation may have induced a stress response in the photosynthetic machinery of upper canopy leaves.

Lydon et al. (1987) reported no UV treatment effects on measured cannabis morphology and physiology parameters, which is in stark contrast to the copious morphological and physiological UV-induced stress responses (outlined above) observed in the present study. While the reported maximum doses were similar in both studies, the plants in Lydon et al. (1987) may have

experienced lower than reported doses due to rapid aging of the cellulose acetate filters (used to eliminate UVA and PAR wavelengths from their UV spectrum treatments) when exposed to UVB (Middleton and Teramura, 1993), resulting in substantial reductions in UVB transmissivity. Additionally, their plants grew for several months under greenhouse conditions (likely including some UV) prior to exposure to UV treatments, whereas there was no UV exposure in the light history of the young vegetative plants prior to initiation of the UV treatments in the present study. Therefore, light history (e.g., spectrum and intensity) and plant age may affect plant responses to UV stress. Evidently, the plants in the present study were subjected to more efficacious UV radiation treatments than in Lydon et al. (1987).

3.4.2 UV RADIATION SUPPRESSES CANNABIS GROWTH AND YIELD

Increasing UV radiation exposure suppressed overall plant growth (e.g., height, number of nodes, plant size) in both cultivars; however, these UV exposure responses were generally more severe in LT than BW. The growth reductions in both cultivars could be partially attributed to the UV-induced alterations in leaf morphology that impede biomass accumulation. Reduced aboveground biomass and lower yields are common effects of exposure to UV radiation (Teramura et al., 1990; Fiscus and Booker, 1995; Caldwell et al., 2003; Liu et al., 2005). Reduced leaf area is a typical response to light stress [e.g., high intensity (Poorter et al., 2019) or UV radiation (Wargent and Jordan, 2013)]. In the present study, individual leaf size and total leaf biomass reduced with increasing UV exposure, limiting area available for light capture which reduces a plant's capacity to convert PAR into biomass (Zlatev et al., 2012). In addition to morphological changes that impede biomass accumulation, area-based NCER was reduced as UV exposure increased over the range of UV-PFDs evaluated in both cultivars, which could further reduce yields under higher UV exposure levels (Kakani et al., 2003).

Total inflorescence DW and the proportion of that DW which is comprised of apical tissues are two major considerations for commercial cannabis production. The apical proportion may be of particular interest since these tissues are normally considered premium quality due to their relatively large size and higher cannabinoid concentrations compared to higher-order (i.e., on lower branches) inflorescences (Namdar et al., 2018). Despite the UV-induced limitations to

foliar biomass accumulation seen in both cultivars, increasing UV exposure only reduced total inflorescence yield in LT. Within this context, the various growth habits of common indoor-grown cannabis cultivars may influence their yield responses to UV stress. In the present study, BW and LT had disparate whole-plant reproductive macro-morphology (i.e., the distribution of inflorescence biomass within the canopy) under normal indoor conditions. For example, under minimum UV exposure, the apical inflorescence comprised 24% of the total inflorescence DW in LT compared to only 11% in BW. Apparently, growth habit may have predisposed BW's mitigation of UV-induced yield reductions by partitioning relatively more inflorescence biomass to positions farther away (i.e., more protected) from the UV source. However, while this may be a self-protective response to reduce UV exposure to reproductively important (from an ecological sense) tissues, it also came at commercially-objectionable reductions in inflorescence quality, such as visually unappealing morphology (**Figure 3.7**).

To prevent UV-induced yield losses, such as are reported in the present study, it is conceivable that cannabis plants could be exposed to UV only after the majority of vegetative growth has completed [i.e., a few weeks after the visual appearance of inflorescences (Potter, 2014)]. This strategy may minimize UV-induced leaf alterations that could inhibit biomass accumulation.

3.4.3 UV RADIATION ALTERS THE SECONDARY METABOLITE COMPOSITION OF CANNABIS INFLORESCENCES

The most economically relevant cannabinoids (e.g., Δ^9-THC and CBD) are predominantly found in their acid forms in mature female inflorescence tissues, which are converted to the psychoactive and medicinal compounds through decarboxylation (Eichler et al., 2012; Zou and Kumar, 2018). The decarboxylated compounds also exist in relatively low quantities in the fresh inflorescences, for example, while Δ^9-THC concentration increased in BW with increasing UV-PFD, the concentration was a relatively small proportion of the total equivalent Δ^9-THC; maximized at 3.3% at the highest UV-PFD. Further, Δ^9-THC naturally converts to CBN, particularly under postharvest conditions and in the presence of oxygen and light. Since CBN was undetectable in the inflorescences, this is an indicator that the crop was not past peak maturity (in terms of cannabinoid concentrations) at the time of harvest (Russo, 2007; Aizpurua-Olaizola et al., 2016).

The present study found that there were no UV-induced enhancements to total equivalent concentrations of Δ^9-THC, CBD and CBG. These results are consistent with a recent study that found no UV treatment effects on Δ^9-THC content in a Δ^9-THC-dominant cultivar (Llewellyn et al. 2021), but contrast with studies on older genotypes (Pate, 1983; Lydon et al., 1987). For example, by exposing greenhouse-grown cannabis to UV_{BE} (based on Caldwell, 1971) doses up to 13.4 $kJ \cdot m^{-2} \cdot d^{-1}$, Lydon et al. (1987) found Δ^9-THC concentration increased linearly by 28% under the highest dose vs. control (i.e., 32 vs. 25 $mg \cdot g^{-1}$). These contrasting results may be due to the disparate growing conditions (both before and during UV exposure), plant age at the time of UV exposure and the relative magnitude of cannabinoid concentrations. While the proportional increases in Δ^9-THC content (28%) presented in Lydon et al. (1987) appeared to be substantial, the magnitude of their increase (e.g., 7 $mg \cdot g^{-1}$) is probably inconsequential in the context of cannabinoid composition in modern genotypes which can have Δ^9-THC concentrations that exceed 200 $mg \cdot g^{-1}$ (Dujourdy and Besacier, 2017).

Pate (1983) reported an increased Δ^9-THC:CBD under UV exposure, which suggests that the production of Δ^9-THC may be upregulated and CBD downregulated as temporal adaptations (i.e., over multiple generations) to the localized environment. However, the results of the present study do not support this trend, at least as a short-term acclimation response to UV stress. Additionally, de Meijer et al. (2003) showed that cannabinoid profiles are largely genetically predetermined, (e.g., a CBD-dominant cultivar is lacking the genetic predisposition to generate abundant Δ^9-THC). This could support the contention that the upregulation of Δ^9-THC under UV stress may be an adaptive response (i.e., over generations) rather than an acclimation response (i.e., during a single production cycle). Over the past few decades, there have been radical increases in inflorescence cannabinoid concentrations, which is often attributed to intensive breeding programs (Chouvy, 2015; Dujourdy and Besacier, 2017; Aliferis and Bernard-Perron, 2020) and the “sinsemilla” cultivation method that eliminates seeds and chiefly produces high potency female inflorescences (ElSohly et al., 2016). Thus, these factors may have a larger impact on cannabis inflorescence cannabinoid composition than environmental factors such as the UV exposure treatments in the present study.

While cannabinoids are the primary psychoactive and medicinal compounds in cannabis inflorescences, volatile terpenes are also economically valuable; both for the aromas that influence consumer preference and potential medicinal properties (Nuutinen, 2018; Booth and Bohlmann, 2019). UV radiation equivocally altered the terpene composition, with disparate responses within and between cultivars. However, total terpene concentrations in both cultivars decreased linearly with increasing UV exposure, which could depreciate the quality of aromas and extracts (McPartland and Russo, 2001; Nuutinen, 2018).

While UV exposure did not result in economically relevant increases in cannabinoid or terpene concentrations in cannabis inflorescences under the conditions of the present study, UV radiation has been shown to increase concentrations of UV-absorbing secondary metabolites (e.g., flavonoids and phenolic compounds) in many species (Huché-Thélier et al., 2016; Robson et al., 2019), including economically important essential oil producing crops (Schreiner et al., 2012; Neugart and Schreiner, 2018). However, UV-induced increases in secondary metabolite concentrations are often concurrent with biomass reductions (Fiscus and Booker, 1995; Caldwell et al., 2003). This paradox must be evaluated when considering the use UV radiation to manipulate secondary metabolite concentrations in indoor cannabis production, since the simultaneous yield reduction may offset any improvements in secondary metabolite composition.

Compared to the UV spectra employed in most other studies, the biologically effective doses in the present study were dramatically higher for a given photon flux density due to the very short peak wavelength of the UV LEDs. It is possible that the alternate UV treatment protocols, such as have been used in other studies, may have more positive results in cannabis production; for example: longer wavelength, less energetic spectra (Hikosara et al., 2010) and shorter-term (e.g., proximal to harvest maturity) exposure (Johnson et al., 1999; Martínez-Lüscher et al., 2013; Huarancca Reyes et al., 2018; Dou et al., 2019).

3.4.4 IMPLICATIONS OF UV IN INDOOR CANNABIS PRODUCTION AND FUTURE RESEARCH DIRECTIONS

This study provided insight into the sensitivity of cannabis to relatively short-wavelength UVB radiation (including a small proportion of UVC) and long-term UV exposure. Increasing UV

exposure levels generally had negative impacts on cannabis plant growth, inflorescence yield, quality, and secondary metabolite composition. The plants exhibited primarily distress responses to UV radiation, even at low exposure levels. No amount of UV exposure resulted in substantial increases of cannabinoid concentrations. Perhaps the UV exposure treatments protocol in the present study (i.e., short-wavelength and long-term exposure) were sufficiently stressful that any potential eustress responses [i.e., a positive response to mild stress (Hideg et al., 2013)] to increasing UV intensity were overwhelmed by more abject distress responses.

Many studies have investigated the effects of stratospheric ozone depletion on plant exposure to UV radiation (Searles et al., 2001; Caldwell et al., 2003) either through ecological or controlled-environment type research. The ratios between UV and PAR (hereafter, UV:PAR) in controlled-environment type investigations tend to be much higher than in the solar spectrum in terrestrial ecosystems (Robson et al., 2019), where plants may exhibit higher sensitivity to UV radiation including increased secondary metabolite accumulation and reduced photosynthesis and growth relative to lower UV:PAR responses (Behn et al., 2010; Dou et al., 2019). The other spectra within the lighting environment have also been shown to influence plant sensitivity to UV radiation, including biomass accumulation (Palma et al., 2021) and some spectra have even been shown to counteract UVB-induced damage (Krizek, 2004). Conceivably, through serendipity, researchers have discovered potential horticultural benefits for providing unnaturally stressful UV exposure conditions which can enhance pertinent traits in economically relevant crops, including increasing secondary metabolite concentrations (Huché-Thélier et al., 2016).

Any horticultural UV treatment protocol is comprised of a myriad of factors including: time of application in the plants' life cycle, number of days of application, number of hours per day (including pulsed methods), time of day with respect to the PAR photoperiod, spectrum, and intensity. While none of the UV exposure levels in the present study would have been commercially beneficial, results from studies in other species (Huché-Thélier et al., 2016; Neugart and Schreiner, 2018; Robson et al., 2019; Höll et al., 2019) indicate a strong potential for there being UV treatment protocols – as yet unidentified through rigorous scientific investigation and reporting – that could enhance secondary metabolite concentrations in cannabis.

There are other horticulturally relevant reasons, other than enhancing secondary metabolite concentrations, for having UV wavelengths present in the radiation spectrum in a cannabis production environment, such as pest management. In the present study there were visible reductions in powdery mildew on the adaxial foliar surfaces of plants exposed to UV-PFDs $\geq$0.10 $\mu mol \cdot m^{-2} \cdot s^{-1}$, with concomitant reductions in inflorescence yield of only 2-3% in LT (no yield reductions in BW) at this threshold UV exposure level. UV exposure has also been shown to reduce powdery mildew in other crops such as grape (Austin and Wilcox, 2012) and strawberry and rosemary (Suthaparan et al., 2016). UV exposure may also improve plant resistance to insect herbivory through changes in plant secondary metabolite composition that affect plant-insect interactions (Demkura et al., 2010).

When making the decision to utilize UV wavelengths (as with any production technology) in indoor cannabis production, the positive crop outcomes must outweigh factors related to the cost of deploying the technology including infrastructure and energy costs, fixture lifespan, and health risks that UV radiation could pose to employees. While UVB LEDs in particular (Kusuma et al., 2020) and UV lighting technologies in general are less energy efficient than modern horticultural PAR fixtures (Nelson and Bugbee, 2014; Radetsky, 2018), fluence rates in the UV spectrum are typically many times lower than the PAR spectrum. Typical functional lifespans of UVB LEDs are currently much lower (Kebbi et al., 2020) than common horticultural LEDs (Kusuma et al., 2020); potentially leading to relatively rapid degradation in fluence rates over time. Given that plant responses in the present study were closely tied to the UV exposure level, fixture degradation could lead to inconsistencies between sequential crops, which is an important parameter in the indoor cannabis production industry. Future research could seek to achieve UV application protocols that promote eustress responses in cannabis secondary metabolite concentrations while minimizing distress responses (e.g., yield reductions) by using less energetic UV spectra or shorter-term exposure than were used in the present study. Future research could also investigate how UV affects cannabis plants grown under different lighting histories, and seek to determine the ideal developmental stage for UV exposure to achieve the desired effects in both yield and quality.

3.5 CONCLUSIONS

Long-term exposure of various intensities of relatively short-wavelength UV radiation had generally negative impacts on cannabis growth, inflorescence yield, and inflorescence quality. By studying two cultivars with similar cannabinoid profiles, we found some differences in phenotypic plasticity in the temporal dynamics in morphology, physiology, yield, and quality responses to UV exposure level. Importantly, as it was applied in this study, UV radiation had substantially reduced yield in one cultivar and had no commercially relevant benefits to inflorescence secondary metabolite composition. Therefore, potential for UV radiation to enhance cannabinoid concentrations must still be confirmed before UV can be used as a tool in cannabis production.

CHAPTER FOUR

GENERAL DISCUSSION AND CONCLUSIONS

Light is a crucial resource for plant growth. It is well known that the manipulation of light environment (e.g., LI and spectrum) can substantially alter plant development. In indoor plant production, LI and spectrum can be manipulated to achieve desired plant traits. Determining optimal LI for indoor cannabis production is of particular interest, since the costs relating to light energy make up a large component of the total energy consumption. However, there was no reliable published research demonstrating the relationship between LI and cannabis floral yield to provide guidance for growers to optimize LI energy cost and yield return. Cannabis is unique in that it is cultivated not only for its floral yield, but also for the medicinal and recreational secondary metabolites (e.g., cannabinoids and terpenes) in the inflorescences. These two factors must be optimized to improve cannabis quality and profitability. Prior work suggests that wavelengths in the PAR spectrum may influence the secondary metabolite profile in cannabis. Early studies have alluded to the potential for increasing cannabinoid concentrations with UV radiation, which has made the UV spectrum a particular topic of current interest in the cannabis industry. However, this theory has yet to be validated with modern production systems and modern genotypes that have relevant baseline cannabinoid concentrations. The objectives of this thesis were to 1) establish the relationships between light intensity and cannabis leaf-level photosynthesis, and inflorescence yield and quality, and 2) establish the relationships between UV exposure levels and cannabis morphology, physiology, and inflorescence yield and quality.

To achieve the first objective, the impact of a refined range of LIs (from 120 to 1800 $\mu mol \cdot m^{-2} \cdot s^{-1}$ testing the lower and upper limits of practical LIs used in indoor crop production) on cannabis leaf-level photosynthesis, and inflorescence yield and quality was evaluated. Likewise, to achieve the second objective, the impact of various UV exposure levels of short-wavelength UV radiation (applied during the flowering stage) on morphology, physiology, and inflorescence yield and quality of two cultivars (LT and BW) was evaluated. The findings demonstrated the extraordinary plasticity of cannabis' physiological, morphological and yield responses to

increasing LI and UV radiation. In general, the effects of LI and UV radiation, as they were applied in this thesis, had drastically contrasting effects on cannabis plant health. Increasing LI in the cannabis growing environment during the flowering stage had an overwhelmingly positive impact on the cannabis plant, notably shown through the linear inflorescence yield increase up to 1800 $\mu mol \cdot m^{-2} \cdot s^{-1}$. In other words, the relationship between LI and cannabis yield did not saturate within the practical limits of LI used in indoor production. A general trend of stress was observed in the UV response of both cannabis cultivars, despite differences in phenotypic plasticity of crop morphology, physiology, yield and quality. Importantly, as it was applied in this study, UV radiation had no commercially relevant benefits to inflorescence cannabinoid content, and the total terpene concentrations decreased linearly over the range of UV-PFDs evaluated. Additionally, yield in LT decreased linearly as UV-PFD increased from the lowest to highest UV-PFD. The general trends of plant stress could be a result of the minimal UVC exposure, and the long-term exposure starting during vegetative development. Therefore, potential for UV radiation to enhance cannabinoid concentrations must still be validated before UV can be used as a tool in cannabis production.

There were no LI treatment effects on inflorescence cannabinoid concentrations therefore commercial cannabis growers can modify their LIs without altering the cannabinoid profile of their product. The quality of the inflorescences improved with increasing LI (in addition to the yield increases), including denser, larger apical inflorescences with increased concentrations of aromatic terpenes. Contrarily, UV radiation reduced total terpene concentrations and the size and proportion of apical inflorescences relative to other inflorescences on the plant in both cultivars. Cannabis growth (i.e., height increases and increases in number of nodes) was generally suppressed by UV radiation and increased by LI. The SLW (i.e., leaf thickness) increased linearly both as LI and UV exposure level increased over the ranges evaluated. Leaves that developed under UV radiation had abnormal morphology including leaf epinasty, upward curling of leaflet margins, and asymmetry. The severity of these symptoms worsened as UV exposure level increased.

On the physiological level, although plants exposed to high LIs showed some signs of light stress in the upper canopy leaves (i.e., through linear decreases in F_v/F_m), the A_{sat} and *in situ* NCER

increased with increasing canopy-level LI. The findings also demonstrated that leaf-level photosynthetic responses to LI vary substantially with leaf age and light history. Therefore, leaf- and plant-level photosynthetic responses cannot reliably predict cannabis yield responses to LI. Increasing cannabis exposure to UV radiation decreased NCER and induced physiological (i.e., linear decrease in F_v/F_m over the range of UV PFDs evaluated) and visible (necrotic spots on leaves) signs of stress. Exposure to UV radiation also accelerated the severity of symptoms related to plant senescence (e.g., lower canopy leaf-drop and stigma browning). Cannabis plants have a very capacity to utilize high photon densities (i.e., high LI) demonstrated through increased photosynthesis and concomitant yield increases. On the contrary, highly energetic photons (i.e., UV spectrum) trigger morphological and physiological stress in cannabis plants through UVR8 specific and non-specific pathways (Tossi et al., 2019).

This study has provided the first reliable models for lighting strategies in the flowering stage for indoor cannabis production. As evidenced through the research in this thesis, high LIs are beneficial for increasing cannabis yields, but further evaluations are required to establish a beneficial method of UV application. This research will assist growers in making informed decisions about the optimum LI to use for their specific production systems. Ultimately, the selection of the economic optimum canopy-level LI for a given commercial production system depends on many interrelated factors, including the infrastructure limitations of a particular cultivation operation. However, particularly since this is the forefront of cannabis horticulture research, many research questions remain. Since plant yield responses to elevated CO_2 can mirror the responses to elevated LI, the combined effects of CO_2 and LI should be investigated on cannabis yield with an in-depth cost-benefit analysis of the optimum combination of these two input parameters. The present study evaluated the effects of LI from red and blue LEDs. Since it is well documented that different light spectra impact plant development differently, further research is required to understand the impacts of LI of other spectra (e.g., full spectrum) on cannabis morphology, physiology, and inflorescence yield and quality. Previous studies have also shown that the PAR spectra influences plant responses to UV radiation, and that plants may be less sensitive to UV radiation when paired with high PAR intensities. Further investigations

are required to understand the interactive effects of UV and PAR radiation (e.g., spectrum and intensity) on cannabis responses to UV treatments.

Although the cannabis plants in the present study demonstrated stress responses to even the low UV exposure levels, given that there are various possible UV treatments (e.g., spectrum, intensity and temporal application), other UV application methods can be explored. Future research could seek to achieve a method to promote eustress responses in cannabis secondary metabolite concentration by using less energetic UV spectra than the present study. The plants in the present study were exposed to UV radiation for 60 days, including during some of the vegetative development, which could have been a sufficient amount of time to induce the observed distress responses. Given that studies on other essential-oil producing species have seen increases in secondary metabolite concentrations with shorter-term UV exposure, future research could also investigate how UV affects cannabis plants with different lighting histories, and the ideal development stage for UV exposure to achieve the desired effects in both yield and quality. This study evaluated the effects of LI on a CBD-dominant cultivar, and the effects of UV radiation on two balanced Δ^9-THC to CBD cultivars with disparate morphology. Future research on cannabis photobiology should also expand to evaluate multiple cultivars of all chemotypes.

REFERENCES

Aarrouf, J., Urban, L. (2020). Flashes of UV-C light: An innovative method for stimulating plant defences. PLoS One. 15:7. doi: 10.1371/journal.pone.0235918.

Ainsworth, E.A., Rogers, A. (2007). The response of photosynthesis and stomatal conductance to rising [CO_2]: mechanisms and environmental interactions. Plant Cell Environ. 30(3):258–270. doi: 10.1111/j.1365-3040.2007.01641.x. PMID: 17263773.

Aizpurua-Olaizola, O., Soydaner, U., Öztürk, E., Schibano, D., Simsir, Y., Navarro, P., Etxebarria, N., Usobiaga, A. (2016). Evolution of the cannabinoid and terpene content during the growth of *Cannabis sativa* plants from different chemotypes. J. Nat. Prod. 79:324–331. doi: 10.1021/acs.jnatprod.5b00949.

Aliferis, K.A., Bernard-Perron, D. (2020). Cannabinomics: Application of metabolomics in cannabis (*Cannabis sativa* L.) research and development. Front. Plant Sci. 11:554. doi: 10.3389/fpls.2020.00554.

Austin, C.N., Wilcox, W.F. (2012). Effects of sunlight exposure on grapevine powdery mildew development. Phytopathology. 102:857–866. doi: 10.1094/PHYTO-07-11-0205.

Barcott, B., Whitney, B. (2019). *Special report: Cannabis jobs count.* Leafly.

Barnes, P.W., Flint, S.D., Caldwell, M.M. (1990). Morphological responses of crop and weed species of different growth forms to ultraviolet-B radiation. Am. J. Bot. 77:1354–1360. doi: 10.2307/2444596.

Barthélémy, D., Caraglio, Y. (2007). Plant architecture: A dynamic, multilevel and comprehensive approach to plant form, structure and ontogeny. Ann. Bot. 99:375–407. doi: 10.1093/aob/mcl260.

Backer, R., Schwinghamer, T., Rosenbaum, P., McCarty, V., Eichhorn Bilodeau, S., Lyu, D., Ahmed, M.B., Robinson, G., Lefsrud, M., Wilkins, O., Smith, D.L. (2019). Closing the yield gap for cannabis: A meta-analysis of factors determining cannabis yield. Front. Plant Sci. 10:495. doi: 10.3389/fpls.2019.00495.

Bauerle, W.L., McCullough, C., Iversen, M., Hazlett, M. (2020). Leaf age and position effects on quantum yield and photosynthetic capacity in hemp crowns. Plants 9:271. doi: 10.3390/plants9020271.

Bazzaz, F.A., Dusek, D., Seigler, D.S., Haney, A.W. (1975). Photosynthesis and cannabinoid content of temperate and tropical populations of *Cannabis sativa*. Biochem. Syst. Ecol. 3:15–18. doi: 10.1016/0305-1978(75)90036-8.

Beaman, A.R., Gladon, R.J., Schrader, J.A. (2009). Sweet basil requires an irradiance of 500 $\mu mol \cdot m^{-2} \cdot s^{-1}$ for greatest edible biomass production. HortScience 44:64–67. doi: 10.21273/HORTSCI.44.1.64.

Behn, H., Albert, A., Marx, F., Noga, G., Ulbrich, A. (2010). Ultraviolet-B and photosynthetically active radiation interactively affect yield and pattern of monoterpenes in leaves of peppermint (*Mentha x piperita* L.). J. Agric. Food Chem. 58:7361–7367. doi: 10.1021/jf9046072.

Behr, M., Legay, S., Žižková, E., Motyka, V., Dobrev, P.I., Hausman, J.F., Lutts, S., Guerriero, G. (2016). Studying secondary growth and bast fiber development: The hemp hypocotyl peeks behind the wall. Front. Plant Sci. 7:1733. doi: 10.3389/fpls.2016.01733.

Bernacchi, C.J., Calfapietra, C., Davey, P.A., Witting, V.E., Scarascia-Mugnozza, G.E., Raines, C.A., Long, S.P. (2003). Blackwell Publishing Ltd. Photosynthesis and stomatal conductance responses of poplars to free-air CO_2 enrichment (PopFACE) during the first growth cycle and immediately following coppice. New Phytol. 159: 609–621. doi: 10.1046/j.1469-8137.2003.00850.x

Bielczynski, L.W., Łaçki, M.K., Hoefnagels, I., Gambin, A., Croce, R. (2017). Leaf and plant age affects photosynthetic performance and photoprotective capacity. Plant Physiol. 175:1634–1648. doi: 10.1104/pp.17.00904.

Björkman, O. (1981). "Responses to different quantum flux densities," in: Encyclopedia of Plant Physiology: New Series: Vol. 12A, Physiological Plant Ecology 1, eds. L. Lange, P.S. Nobel, C.B. Osmond, and H. Ziegler (Heidelberg, Berlin: Springer-Verlag), 57-107.

Booth, J.K., Bohlmann, J. (2019). Terpenes in *Cannabis sativa* – From plant genome to humans. Plant Sci. 284:67–72. doi: 10.1016/j.plantsci.2019.03.022.

Bredmose, N. (1993). Effects of year-round supplementary lighting on shoot development, flowering and quality of two glasshouse rose cultivars. Sci. Hortic. 54:69–85. doi: 10.1016/0304- 4238(93)90084-4.

Bredmose, N. (1994). Biological efficiency of supplementary lighting on cut roses the year round. Sci. Hortic. 59:75–82. doi: 10.1016/0304-4238(94)90094-9.

Bugbee, B., Monje, O. (1992). The limits of crop productivity. Bioscience. 42:494–502. doi: 10.2307/1311879.

Caldwell, M.M. (1971). Solar UV irradiation and the growth and development of higher plants. Photophysiology 6:131–177. doi: 10.1016/b978-0-12-282606-1.50010-6.

Caldwell, M.M., Ballaré, C.L., Bornman, J.F., Flint, S.D., Björn, L.O., Teramura, A.H.,

Kulandaiveli, G., Tevini, M. (2003). Terrestrial ecosystems, increased solar ultraviolet radiation and interactions with other climatic change factors. Photochem. Photobiol. Sci. 2:29–38. doi: 10.1039/b211159b.

Campbell, R.J., Marini, R.P., Birch, J.B. (1992). Canopy position affects light response curves for gas exchange characteristics of apple spur leaves. J. Am. Soc. Hortic. Sci. 117:467–472. doi: doi.org/10.21273/JASHS.117.3.467

Cannabis Business Times. (2021). 2020 State of the industry report. (2020) Valley View, OH: GIE Media, Inc.

Cannigma. (2019). *Cannabis regulation around the world.* The Cannigma.

Caplan, D., Dixon, M., Zheng, Y. (2017). Optimal rate of organic fertilizer during the flowering stage for cannabis grown in two coir-based substrates. HortScience 52:1796–1803. doi: 10.21273/HORTSCI12401-17.

Caplan, D., Dixon, M., Zheng, Y. (2019). Increasing inflorescence dry weight and cannabinoid content in medical cannabis using controlled drought stress. HortScience 54:964–969. doi: 10.21273/HORTSCI13510-18.

Carlini, E.A., Leite, J.R., Tannhauser, M., Berardi, A.C. (1973). Cannabidiol and *Cannabis sativa* extract protect mice and rats against convulsive agents. J. Pharm. Pharmacol. 25:664–665. doi: 10.1111/j.2042-7158.1973.tb10660.x.

Carvalho, F.E.L., Ware, M.A., Ruban, A. V. (2015). Quantifying the dynamics of light tolerance in *Arabidopsis* plants during ontogenesis. Plant Cell Environ. 38:2603–2617. doi: 10.1111/pce.12574.

Casal, J.J. (2013). Photoreceptor signaling networks in plant responses to shade. Annu. Rev. Plant Biol. 64:403–427. doi: 10.1146/annurev-arplant-050312-120221.

Cen, Y., Bornman, J.F. (1993). The effect of exposure to enhanced UV-B radiation on the penetration of monochromatic and polychromatic UV-B radiation in leaves of *Brassica napus*. Physiol. Plant. 87:249–255. doi: 10.1111/j.1399-3054.1993.tb01727.x.

Chandra, S., Lata, H., Khan, I.A., Elsohly, M.A. (2008). Photosynthetic response of *Cannabis sativa* L. to variations in photosynthetic photon flux densities, temperature and CO_2 conditions. Physiol. Mol. Biol. Plants 14:299–306. doi: 10.1007/s12298-008-0027-x.

Chandra, S., Lata, H., Khan, I.A., ElSohly, M.A. (2011). Photosynthetic response of *Cannabis sativa* L., an important medicinal plant, to elevated levels of CO_2. Physiol. Mol. Biol. Plants 17:291–295. doi: 10.1007/s12298-011-0066-6.

Chandra, S., Lata, H., Mehmedic, Z., Khan, I.A., ElSohly, M.A. (2015). Light dependence of photosynthesis and water vapor exchange characteristics in different high Δ9-THC yielding varieties of *Cannabis sativa* L. J. Appl. Res. Med. Aromat. Plants 2:39–47. doi: 10.1016/J.JARMAP.2015.03.002.

Chandra, S., Lata, H., ElSohly, M.A., Walker, L.A., Potter, D. (2017). Cannabis cultivation: Methodological issues for obtaining medical-grade product. Epilepsy Behav. 70:302–312. doi: 10.1016/j.yebeh.2016.11.029.

Chouvy, P.-A. (2015). The supply of hashish to Europe report prepared for the EMCDDA. Paris, France.

Clarke, R.C., Merlin, M.D. (2016). Cannabis domestication, breeding history, present-day genetic diversity, and future prospects. CRC. Crit. Rev. Plant Sci. 35:293–327. doi: 10.1080/07352689.2016.1267498.

Coco for Cannabis. (n.d.). How much light (ppf) do you need for indoor cannabis?. Coco Cannabis. Retrieved from: https://www.cocoforcannabis.com/how-much-light-ppf-do-you-need-for-indoor-cannabis/.

Cristiana Moliterni, V.M., Cattivelli, L., Ranalli, P., Mandolino, G. (2004). The sexual differentiation of *Cannabis sativa* L.: A morphological and molecular study. Euphytica 140:95–106. doi: 10.1007/s10681-004-4758-7

Czégény, G., Mátai, A., Hideg, É. (2016). UV-B effects on leaves-Oxidative stress and acclimation in controlled environments. Plant Sci. 248:57–63. doi: 10.1016/j.plantsci.2016.04.013.

Delgado, E., Parry, M.A.J., Lawlor, D.W., Keys, A.J., Medrano, H. (1993). Photosynthesis, ribulose-1,5-bisphosphate carboxylase and leaf characteristics of *Nicotiana tabacum* L. genotypes selected by survival at low CO_2 concentrations. J. Exp. Bot. 44:1–7. doi: 10.1093/jxb/44.1.1.

Demkura, P. V., Ballaré, C.L. (2012). UVR8 mediates UV-B-induced Arabidopsis defense responses against *Botrytis cinerea* by controlling sinapate accumulation. Mol. Plant. 5:642–652. doi: 10.1093/MP/SSS025.

Diggle, P.K. (1995). Architectural effects and the interpretation of patterns of fruit and seed development. Annu. Rev. Ecol. Syst. 26:531–552. doi: 10.1146/annurev.es.26.110195.002531.

Dou, H., Niu, G., Gu, M., Joseph G., M. (2018). Responses of sweet basil to different daily light integrals in photosynthesis, morphology, yield, and nutritional quality. HortScience. 53:496–503.

Downer, S. (2018). The ultimate lighting guide for cannabis cultivation. Medium. Retrieved from: https://medium.com/@sabinedowner/the-ultimate-lighting-guide-for-cannabis-cultivation-cc60b22df835.

Dujourdy, L., Besacier, F. (2017). A study of cannabis potency in France over a 25 years period (1992–2016). Forensic Sci. Int. 272:72–80. doi: 10.1016/j.forsciint.2017.01.007.

Eaves, J., Eaves, S., Morphy, C., Murray, C. (2020). The relationship between light intensity, cannabis yields, and profitability. Agron. J. 112:1466–1470. doi: 10.2139/ssrn.3310456.

Eichhorn Bilodeau, S., Wu, B.-S., Rufyikiri, A.-S., MacPherson, S., Lefsrud, M. (2019). An update on plant photobiology and implications for cannabis production. Front. Plant Sci. doi: 10.3389/fpls.2019.00296.

Eichler, M., Spinedi, L., Unfer-Grauwiler, S., Bodmer, M., Surber, C., Luedi, M., Drewe, J. (2012). Heat exposure of *cannabis sativa* extracts affects the pharmacokinetic and metabolic profile in healthy male subjects. Planta Med. 78:686–691. doi: 10.1055/s-0031-1298334.

ElSohly, M.A., Mehmedic, Z., Foster, S., Gon, C., Chandra, S., Church, J.C. (2016). Changes in cannabis potency over the last 2 decades (1995-2014): Analysis of current data in the United States. Biol. Psychiatry 79:613–619. doi: 10.1016/j.biopsych.2016.01.004.

ElSohly, M.A., Radwan, M.M., Gul, W., Chandra, S., Galal, A. (2017). Phytochemistry of *Cannabis sativa L.* Phytocannabinoids. 103:1-36. doi: 10.1007/978-3-319-45541-9_1. Springer, Cham.

European Monitoring Centre for Drugs and Drug Addiction. (2013). *Cannabis Production and Markets In Europe*. Lisbon, Portugal: EMCDDA Insights, No. 12.

Evergreen Economics. (2016). *Cannabis Agriculture Energy Demand Study Final Report*. San Diego, CA: San Diego Gas & Electric Company.

Fairbairn, J.W., Liebmann, J.A. (1974). The cannabinoid content of *Cannabis sativa* L. grown in England. J. Pharm. Pharmacol. 26:413–419. doi: 10.1111/j.2042-7158.1974.tb09306.x.

Faust, J.E. (2003). "Light," in Ball Redbook, ed. D. Hamrick (Batabia, IL: Ball Publishing), 71–84.

Farag, S., Kayser, O. (2015). Cannabinoids production by hairy root cultures of *Cannabis sativa* L. SciRes. Am. J. Plant Sci. 6:1874–1884. doi: 10.4236/ajps.2015.611188.

Fernandes, V.F., de Almeida, L.B., da Feijó, E.V.R.S., da Silva, D.C., de Oliveira, R.A., Mielke, M.S., do Costa, L.C.B. (2013). Light intensity on growth, leaf micromorphology and

essential oil production of *Ocimum gratissimum*. Brazilian J. Pharmacogn. 23:419–424. doi: 10.1590/S0102-695X2013005000041.

Fierro, A.C., Leroux, O., De Coninck, B., Cammue, B.P.A., Marchal, K., Prinsen, E., Van Der Straeten, D., Vandenbussche, F. (2015). Ultraviolet-B radiation stimulates downward leaf curling in *Arabidopsis thaliana*. Plant Physiol. Biochem. 93:9–17. doi: 10.1016/j.plaphy.2014.12.012.

Fiscus, E.L., Booker, F.L. (1995). Is increased UV-B a threat to crop photosynthesis and productivity?. Photosynth. Res. 43:81–92. doi: 10.1007/BF00042965.

Flint, S.D., Caldwell, M.M. (2003). A biological spectral weighting function for ozone depletion research with higher plants. Physiol. Plant. 117:137–144. doi: 10.1034/j.1399-3054.2003.1170117.x.

Flores-Sanchez, I.J., Verpoorte, R. (2008). PKS activities and biosynthesis of cannabinoids and flavonoids in *Cannabis sativa* L. plants. Plant Cell Physiol. 49:1767–1782. doi: 10.1093/pcp/pcn150.

Friedberg, E.C. (2002). The intersection between the birth of molecular biology and the discovery of DNA repair. DNA Repair. 1:855–867. doi: 10.1016/S1568-7864(02)00112-X.

Fukuda, S., Satoh, A., Kasahara, H., Matsuyama, H., Takeuchi, Y. (2008). Effects of ultraviolet-B irradiation on the cuticular wax of cucumber (*Cucumis sativus*) cotyledons. J. Plant Res. 121:179–189. doi: 10.1007/s10265-007-0143-7.

Gara, T., Darvishzadeh, R., Skidmore, A., Wang, T. (2018). Impact of vertical canopy position on leaf spectral properties and traits across multiple species. Remote Sens. 10:346. doi: 10.3390/rs10020346.

Giupponi, L., Leoni, V., Pavlovic, R., Giorgi, A. (2020). Influence of altitude on phytochemical composition of hemp inflorescence: A metabolomic approach. Molecules 25:1381. doi: 10.3390/molecules25061381.

Gonçalves, J., Rosado, T., Soares, S., Simão, A., Caramelo, D., Luís, Â., Fernández, N., Barroso, M., Gallardo, E., Duarte, A. (2019). Cannabis and its secondary metabolites: Their use as therapeutic drugs, toxicological aspects, and analytical determination. Medicines 6:31. doi: 10.3390/medicines6010031.

Goodman, R.C., Apostol, K.G., Jacobs, D.F., Wilson, B.C. (2007). Comparing cold-stored and freshly lifted water oak (*Quercus nigra*) seedlings based on physiological parameters. National Proceedings, Forest and Conservation Nursery Associations, 2006. Fort Collins, CO.

Government of Canada. (2015). *Canadian tobacco alcohol and drugs (CTADS): 2015 summary.* Retrieved from: https://www.canada.ca/en/health-canada/services/canadian-tobacco-alcohol-drugs-survey/2015-summary.html.

Government of Canada. (2016). *Understanding the new Access to cannabis for medical purposes regulations.* Retrieved from: https://www.canada.ca/en/health-canada/services/publications/drugs-health-products/understanding-new-access-to-cannabis-for-medical-purposes-regulations.html.

Government of Canada. (2019a). *Cannabis legalization and regulation.* Department of Justice. Retrieved from: https://www.justice.gc.ca/eng/cj-jp/cannabis/.

Government of Canada. (2019b). *What you need to know about cannabis.* Health Canada. Retrieved from: https://www.canada.ca/en/services/health/campaigns/cannabis/canadians.html.

Graham, S.D. (2004). Medical marijuana: Canada's regulations, pharmacology, and social policy. Can. Pharm. J. 137:23–27. doi: 10.1177/171516350413700104

Gratani, L. (2014). Plant phenotypic plasticity in response to environmental factors. Adv. Bot. 2014:1–17. doi: 10.1155/2014/208747.

De Gruijl, F.R., Van der Leun, J.C. (2000). Environment and health: 3. Ozone depletion and ultraviolet radiation. CMAJ. 163:851–855.

Guindon, J., Hohmann, A.G. (2009). The endocannabinoid system and pain. CNS Neurol. Disord. Drug Targets 8:403–21. doi: 10.2174/187152709789824660.

Haney, A., Kutscheid, B.B. (1973). Quantitative variation in the chemical constituents of marihuana from stands of naturalized *Cannabis sativa* L. in East-Central Illinois. Econ. Bot. 27:193–203. doi: 10.1007/BF02872989.

Havé, M., Marmagne, A., Chardon, F., Masclaux-Daubresse, C. (2017). Nitrogen remobilization during leaf senescence: Lessons from Arabidopsis to crops. J. Exp. Bot. 68:2513–2529. doi: 10.1093/jxb/erw365.

Hawley, D., Graham, T., Stasiak, M., Dixon, M. (2018). Improving cannabis bud quality and yield with subcanopy lighting. HortScience 53:1593–1599. doi: 10.21273/hortsci13173-18.

Hazekamp, A., Peltenburg, A., Verpoorte, R., Giroud, C. (2005). Chromatographic and spectroscopic data of cannabinoids from *Cannabis sativa* L. J. Liq. Chromatogr. Relat. Technol. 28:2361–2382. doi: 10.1080/10826070500187558.

Hectors, K., Jacques, E., Prinsen, E., Guisez, Y., Verbelen, J.P., Jansen, M.A.K., Vissenberg, K. (2010). UV radiation reduces epidermal cell expansion in leaves of *Arabidopsis thaliana*. J. Exp. Bot. 61:4339–4349. doi: 10.1093/jxb/erq235.

Hemphill, J.K., Turner, J.C., Mahlberg, P.G. (1980). Cannabinoid content of individual plant organs from different geographical strains of *Cannabis sativa* L. J. Nat. Prod. 43:112–122. doi: 10.1021/np50007a009.

Hideg, É., Jansen, M.A.K., Strid, Å. (2013). UV-B exposure, ROS, and stress: Inseparable companions or loosely linked associates?. Trends Plant Sci. 18:107–115. doi: 10.1016/j.tplants.2012.09.003.

Hikosara, S., Ito, K., Goto, E. (2010). Effects of ultraviolet light on growth, essential oil concentration, and total antioxidant capacity of Japanese mint. Environ. Control Biol. 48:185–190. doi: 10.2525/ecb.48.185.

Hoffmann, A.M., Noga, G., Hunsche, M. (2015). High blue light improves acclimation and photosynthetic recovery of pepper plants exposed to UV stress. Environ. Exp. Bot. 109:254–263. doi: 10.1016/j.envexpbot.2014.06.017.

Höll, J., Lindner, S., Walter, H., Joshi, D., Poschet, G., Pfleger, S., Ziegler, T., Hell, R., Bogs, J., Rausch, T. (2019). Impact of pulsed UV-B stress exposure on plant performance: How recovery periods stimulate secondary metabolism while reducing adaptive growth attenuation. Plant Cell Environ. 42:801–814. doi: 10.1111/pce.13409.

Huarancca Reyes, T., Scartazza, A., Castagna, A., Cosio, E.G., Ranieri, A., Guglielminetti, L. (2018). Physiological effects of short acute UVB treatments in *Chenopodium quinoa* Willd. Sci. Rep. 8:371. doi: 10.1038/s41598-017-18710-2.

Huché-Thélier, L., Crespel, L., Gourrierec, J. Le, Morel, P., Sakr, S., Leduc, N. (2016). Light signaling and plant responses to blue and UV radiations: Perspectives for applications in horticulture. Environ. Exp. Bot. 121:22–38. doi: 10.1016/j.envexpbot.2015.06.009.

Jaeger, K. (2019). Study reveals little-known trick to make marijuana plants grow more bud for less. Marijuana Moment. Retrieved from: https://www.marijuanamoment.net/study-reveals-little-known-trick-to-make-marijuana-plants-grow-more-bud-for-less/.

Jansen, M.A.K. (2002). Ultraviolet-B radiation effects on plants: Induction of morphogenic responses. Physiol. Plant. 116:423–429. doi: 10.1034/j.1399-3054.2002.1160319.x.

Jansen, M.A.K., Klem, K., Robson, T.M., Urban, O. (2017). "UV-B induced morphological changes - an enigma," in UV-B radiation and plant life: molecular biology to ecology, ed. B. Jordan. doi: 10.1079/9781780648590.0000.

Jenkins, G.I. (2017). Photomorphogenic responses to ultraviolet-B light. Plant Cell Environ. 40:2544–2557. doi: 10.1111/pce.12934.

Johnson, C.B., Kirby, J., Naxakis, G., Pearson, S. (1999). Substantial UV-B-mediated induction of essential oils in sweet basil (*Ocimum basilicum* L.). Phytochemistry 51:507–510. doi: 10.1016/S0031-9422(98)00767-5.

Jones-Baumgardt, C., Llewellyn, D., Ying, Q., Zheng, Y. (2019). Intensity of sole-source light-emitting diodes affects growth, yield, and quality of Brassicaceae microgreens. HortScience. 54:1168–1174. doi: 10.21273/HORTSCI13788-18.

Kakani, V.G., Reddy, K.R., Zhao, D., Sailaja, K. (2003). Field crop responses to ultraviolet-B radiation: A review. Agric. For. Meteorol. 120:191–218. doi: 10.1016/j.agrformet.2003.08.015.

Kebbi, Y., Muhammad, A.I., Sant'Ana, A.S., do Prado-Silva, L., Liu, D., Ding, T. (2020). Recent advances on the application of UV-LED technology for microbial inactivation: Progress and mechanism. Compr. Rev. Food Sci. Food Saf. 19:3501–3527. doi: 10.1111/1541-4337.12645.

Kenny, C., Nolin, P.C. (2003). *Cannabis: Report of the senate special committee on illegal drugs.* Toronto, ON: University of Toronto Press.

Kirschbaum, M.U.F. (2011). Does enhanced photosynthesis enhance growth? Lessons learned from CO_2 enrichment studies. Plant Physiol. 155:117–124. doi: 10.1104/pp.110.166819.

Klem, K., Ač, A., Holub, P., Kováč, D., Špunda, V., Robson, T.M., Urban, O. (2012). Interactive effects of PAR and UV radiation on the physiology, morphology and leaf optical properties of two barley varieties. Environ. Exp. Bot. 75:52–64. doi: 10.1016/j.envexpbot.2011.08.008.

Kreyling, J., Schweiger, A.H., Bahn, M., Ineson, P., Migliavacca, M., Morel-Journel, T., Christiansen, J.R., Schtickzelle, N., Larsen, K.S. (2018). To replicate, or not to replicate - that is the question: How to tackle nonlinear responses in ecological experiments. Ecol. Lett. 21:1629–1638. doi: 10.1111/ele.13134.

Krizek, D.T., Mirecki, R.M., Britz, S.J. (1997). Inhibitory effects of ambient levels of solar UV-A and UV-B radiation on growth of cucumber. Physiol. Plant. 100:886–893. doi: 10.1111/j.1399-3054.1997.tb00014.x.

Krizek, D.T. (2004). Influence of PAR and UV-A in determining plant sensitivity and photomorphogenic responses to UV-B radiation. Photochem. Photobiol. 79:315. doi: 10.1562/2004-01-27-ir.1.

Kusuma, P., Pattison, P.M., Bugbee, B. (2020). From physics to fixtures to food: Current and potential LED efficacy. Hortic. Res. 7:56. doi: 10.1038/s41438-020-0283-7.

Larsson, M., Lagerås, P. (2015). New evidence on the introduction, cultivation and processing of hemp (*Cannabis sativa* L.) in southern Sweden. Environ. Archaeol. 20:111–119. doi: 10.1179/1749631414Y.0000000029.

Latta, R.P., Eaton, B.J. (1975). Seasonal fluctuations in cannabinoid content of Kansas marijuana. Econ. Bot. 29:153–163. doi: 10.1007/BF02863315.

Leggett, T. (2006). A review of the world cannabis situation. Bull. Narc. 58:1–155.

Lewis, M.A., Russo, E.B., Smith, K.M. (2018). Pharmacological foundations of cannabis chemovars. Planta Med. 84:225–233. doi: 10.1055/s-0043-122240.

LI-COR Biosciences. (2012). *Using the LI-6400 / LI-6400XT Portable Photosynthesis System Version 6*. Lincoln, NB: LI-COR Inc

Liu, L.X., Xu, S.M., Woo, K.C. (2005). Solar UV-B radiation on growth, photosynthesis and the xanthophyll cycle in tropical acacias and eucalyptus. Environ. Exp. Bot. 54:121–130. doi: 10.1016/j.envexpbot.2004.06.006.

Liu, B., Liu, X. bing, Li, Y.S., Herbert, S.J. (2013). Effects of enhanced UV-B radiation on seed growth characteristics and yield components in soybean. F. Crop. Res. 154:158–163. doi: 10.1016/j.fcr.2013.08.006.

Llewellyn, D., Golem, S., Foley, E., Dinka, S., Maxwell, A., Jones, P., Zheng, Y. (2021). Cannabis yield increased proportionally with light intensity, but additional ultraviolet radiation did not affect yield or cannabinoid content. Preprints. doi: 10.20944/preprints202103.0327.v1.

Lobo, F. A., de Barros, M.P., Dalmagro, H.J., Dalmolin, Â.C., Pereira, W.E., de Souza, É.C., Vourlitis, G.L., Rodríguez Ortíz, C.E. (2013). Fitting net photosynthetic light-response curves with Microsoft Excel - a critical look at the models. Photosynthetica. 51:445–456. doi: 10.1007/s11099-013-0045-y.

Lydon, J., Teramura, A.H., Coffman, C.B. (1987). UV-B radiation effects on photosynthesis, growth and cannabinoid production of two *Cannabis sativa* chemotypes. Photochem. Photobiol. 46:201–206. doi: 10.1111/j.1751-1097.1987.tb04757.x.

Maffei, M., Scannerini, S. (2000). UV-B effect on photomorphogenesis and essential oil composition in peppermint (*Mentha piwperita* L.). J. Essent. Oil Res. 12:523–529. doi: 10.1080/10412905.2000.9712150.

Magagnini, G., Grassi, G., Kotiranta, S. (2018). The effect of light spectrum on the morphology and cannabinoid content of *Cannabis sativa* L. Med. Cannabis Cannabinoids 1:19–27. doi: 10.1159/000489030.

Mah, J.J., Llewellyn, D., Zheng, Y. (2019). Protocol for converting spectrometer radiometric data to photon flux units [Microsoft Excel Spreadsheet]. Guelph, University of Guelph. Available from: http://www.ces.uoguelph.ca/TechNotes.shtml.

Mammoth Lighting. (n.d.). Optimal light intensity. Mammoth Light. Retrieved from: https://mammothlighting.com/pages/photosynthetic-response-of-cannabis-sativa-l.

Manova, V., Gruszka, D. (2015). DNA damage and repair in plants: From models to crops. Front. Plant Sci. 6:885. doi: 10.3389/fpls.2015.00885.

Marcelis, L.F.M., Broekhuijsen, A.G.M., Meinen, E., Nijs, E.M.F.M., Raaphorst, M.G.M. (2006). Quantification of the growth response to light quantity of greenhouse grown crops. Acta Hortic. 711:97–103. doi: 10.17660/actahortic.2006.711.9.

Martínez-Lüscher, J., Morales, F., Delrot, S., Sánchez-Díaz, M., Gomés, E., Aguirreolea, J., Pascual, I. (2013). Short- and long-term physiological responses of grapevine leaves to UV-B radiation. Plant Sci. 213:114–122. doi: 10.1016/j.plantsci.2013.08.010.

Maroon, J., Bost, J. (2018). Review of the neurological benefits of phytocannabinoids. Surg. Neurol. Int. 9:91. doi: 10.4103/sni.sni_45_18.

Marti, G., Schnee, S., Andrey, Y., Simoes-Pires, C., Carrupt, P.A., Wolfender, J.L., Gindro, K. (2014). Study of leaf metabolome modifications induced by UV-C radiations in representative vitis, cissus and cannabis species by LC-MS based metabolomics and antioxidant assays. Molecules 19:14004–14021. doi: 10.3390/molecules190914004.

McElroy, C.T., Fogal, P.F. (2008). Ozone: From discovery to protection. Atmos. Ocean. 46:1–13. doi: 10.3137/ao.460101.

McPartland, J.M., Russo, E.B. (2001). Cannabis and Cannabis extracts: Greater than the sum of their parts?. Cannabis Ther. 1:103–132. doi: 10.1300/J175v01n03_08.

McPartland, J.M. (2018). *Cannabis* systematics at the levels of family, genus, and species. Cannabis Cannabinoid Res. 3:203–212. doi: 10.1089/can.2018.0039.

De Meijer, E.P.M., Bagatta, M., Carboni, A., Crucitti, P., Moliterni, V.M.C., Ranalli, P., Mandolino, G. (2003). The inheritance of chemical phenotype in *Cannabis sativa* L. Genetics. 163:335–346. doi: 10.1093/genetics/163.1.335.

Middleton, E.M., Teramura, A.H. (1993). Potential Errors in the use of cellulose acetate and

Mylar filters in UV-B radiation studies. Photochem. Photobiol. 57:744–751. doi: 10.1111/j.1751-1097.1993.tb02948.x.

Mills, E. (2012). The carbon footprint of indoor Cannabis production. Energy Policy 46:58–67. doi: 10.1016/J.ENPOL.2012.03.023.

Murchie, E., Hubbart, S., Chen, Y., Peng, S., Horton, P. (2002). Acclimation of rice photosynthesis to irradiance under field conditions. Plant Physiol. 130:1999–2010. doi: 10.1104/pp.011098.

Murchie, E., Lawson, T. (2013). Chlorophyll fluorescence analysis: A guide to good practice and understanding some new applications. J. Exp. Bot. 64:3983–3998. doi: 10.1093/jxb/ert208.

Namdar, D., Mazuz, M., Ion, A., Koltai, H. (2018). Variation in the compositions of cannabinoid and terpenoids in *Cannabis sativa* derived from inflorescence position along the stem and extraction methods. Ind. Crops Prod. 113:376–382. doi: 10.1016/j.indcrop.2018.01.060.

Nelson, J.A., Bugbee, B. (2014). Economic analysis of greenhouse lighting: Light emitting diodes vs. high intensity discharge fixtures. PLoS One. 9. doi: 10.1371/journal.pone.0099010.

Neugart, S., Schreiner, M. (2018). UVB and UVA as eustressors in horticultural and agricultural crops. Sci. Hortic. 234:370–381. doi: 10.1016/j.scienta.2018.02.021.

Niinemets, Ü., Keenan, T.F. (2012). Measures of light in studies on light-driven plant plasticity in artificial environments. Front. Plant Sci. 3:156. doi: 10.3389/fpls.2012.00156.

Nuutinen, T. (2018). Medicinal properties of terpenes found in *Cannabis sativa* and *Humulus lupulus*. Eur. J. Med. Chem. 157:198–228. doi: 10.1016/j.ejmech.2018.07.076.

Oh, W., Cheon, H., Kim, K.S., Runkle, E.S. (2009). Photosynthetic daily light integral influences flowering time and crop characteristics of *Cyclamen persicum*. HortScience. 44:341–344. doi: 10.21273/HORTSCI.44.2.341.

Ohyama, K., Manabe, K., Omura, Y., Kozai, T., Kubota, C. (2005). Potential use of a 24-hour photoperiod (continuous light) with alternating air temperature for production of tomato plug transplants in a closed system. HortScience. 40:374–377. doi: 10.21273/HORTSCI.40.2.374.

Pacher, P., Bátkai, S., Kunos, G. (2006). The endocannabinoid system as an emerging target of pharmacotherapy. Pharmacol. Rev. 58:389–462. doi: 10.1124/pr.58.3.2.

Palma, C.F.F., Castro-Alves, V., Morales, L.O., Rosenqvist, E., Ottosen, C.-O., Strid, Å. (2021).

Spectral composition of light affects sensitivity to UV-B and photoinhibition in cucumber. Front. Plant Sci. doi: 10.3389/fpls.2020.610011.

Parry, C., Blonquist, J.M., Bugbee, B. (2014). In situ measurement of leaf chlorophyll concentration: Analysis of the optical/absolute relationship. Plant, Cell Environ. 37:2508–2520. doi: 10.1111/pce.12324.

Pate, D.W. (1983). Possible Role of Ultraviolet Radiation in Evolution of Cannabis Chemotypes. Econ. Bot. 37:396–405.

Peng, S. (2000). Single-leaf and canopy photosynthesis of rice. Studies in Plant Science. 7:213–228. doi.org/10.1016/S0928-3420(00)80017-8

Pertwee, R.G. (1997). Pharmacology of cannabinoid CB_1 and CB_2 receptors. Pharmacol. Ther. 74:129–180. doi: 10.1016/S0163-7258(97)82001-3.

Pertwee, R.G. (2006). Cannabinoid pharmacology: The first 66 years. Br. J. Pharmacol. 147:S163. doi: 10.1038/sj.bjp.0706406.

Pettersen, R., Torre, S., Gislerød, H. (2010). Effects of leaf aging and light duration on photosynthetic characteristics in a cucumber canopy. Sci. Hortic. 125:82–87. doi: 10.1016/J.SCIENTA.2010.02.016.

Poorter, H., Niinemets, Ü., Ntagkas, N., Siebenkäs, A., Mäenpää, M., Matsubara, S., Pons, T. (2019). A meta-analysis of plant responses to light intensity for 70 traits ranging from molecules to whole plant performance. New Phytol. 223:1073–1105. doi: 10.1111/nph.15754.

Posada, J.M., Sievänen, R., Messier, C., Perttunen, J., Nikinmaa, E., Lechowicz, M.J. (2012). Contributions of leaf photosynthetic capacity, leaf angle and self-shading to the maximization of net photosynthesis in *Acer saccharum*: a modelling assessment. Ann. Bot. 110:731–741. doi: 10.1093/aob/mcs106.

Potter, D.J. (2014). A review of the cultivation and processing of cannabis (*Cannabis sativa* L.) for production of prescription medicines in the UK. Drug Test. Anal. 6:31–38. doi: 10.1002/dta.1531.

Potter, D.J., Duncombe, P. (2012). The effect of electrical lighting power and irradiance on indoor-grown cannabis potency and yield. J. Forensic Sci. 57:618–622. doi: 10.1111/j.1556-4029.2011.02024.x.

Potter, D.J., Hammond, K., Tuffnell, S., Walker, C., Di Forti, M. (2018). Potency of Δ^9-tetrahydrocannabinol and other cannabinoids in cannabis in England in 2016: Implications for public health and pharmacology. Drug Test. Anal. 10:628–635. doi: 10.1002/dta.2368.

Punja Z. K., Holmes, J. E. (2020). Hermaphrodism in marijuana (*Cannabis sativa* L.) inflorescences – Impact on floral morphology, seed formation, progeny sex ratios, and genetic variation. Front. Plant Sci. 11:718. doi: 10.3389/fpls.2020.00718

Radetsky, L.C. (2018). *LED and HID Horticultural Luminaire Testing Report Prepared For Lighting Energy Alliance Members and Natural Resources Canada.* Troy, NY: Rensselaer Polytechnic Institute.

Robson, T.M., Aphalo, P.J. (2012). Species-specific effect of UV-B radiation on the temporal pattern of leaf growth. Physiol. Plant. 144:146–160. doi: 10.1111/j.1399-3054.2011.01546.x.

Robson, T.M., Aphalo, P.J., Banaś, A.K., Barnes, P.W., Brelsford, C.C., Jenkins, G.I., Kotilainen, T.K., Łabuz, J., Martínez-Abaigar, J., Morales, L.O., Neugart, S., Pieristè, M., Rai, N., Vandenbussche, F., Jansen, M.A.K. (2019). A perspective on ecologically relevant plant-UV research and its practical application. Photochem. Photobiol. Sci. 18:970–988. doi: 10.1039/c8pp00526e.

Rodriguez-Morrison, V., Llewellyn, D., Zheng, Y. (2021). Cannabis yield, potency, and leaf photosynthesis respond differently to increasing light levels in an indoor environment 2. Preprints. doi: 10.20944/preprints202101.0163.v1.

Rotermann, M. (2020). What has changed since cannabis was legalized?. Stat. Canada 31:11–20. doi: 10.25318/82-003-x202000200002-eng.

Royal Queen Seeds. (2019). The indoor marijuana grower's guide to artificial lights. Royal Queen Seeds. Retrieved from: https://www.royalqueenseeds.com/blog-cannabis-cultivation-tips-how-to-set-up-indoor-grow-lights-n670.

Russo, E.B. (2007). History of cannabis and its preparations in saga, science, and sobriquet. Chem. Biodivers. 4:1614–1648. doi: 10.1002/cbdv.200790144.

Russo, E.B. (2019). The case for the entourage effect and conventional breeding of clinical cannabis: No "strain," no gain. Front. Plant Sci. 9:1969. doi: 10.3389/fpls.2018.01969.

Ruter, J.M. (1992). Influence of source, rate, and method of applicating controlled release fertilizer on nutrient release and growth of "Savannah" holly. Fertil. Res. 32:101–106. doi: 10.1007/BF01054399.

Sadras, V.O., Richards, R.A. (2014). Improvement of crop yield in dry environments: Benchmarks, levels of organisation and the role of nitrogen. J. Exp. Bot. 65:1981–1995. doi: 10.1093/jxb/eru061.

Schreiner, M., Mewis, I., Huyskens-Keil, S., Jansen, M.A.K., Zrenner, R., Winkler, J.B., O'Brien, N., Krumbein, A. (2012). UV-B-induced secondary plant metabolites - Potential benefits for plant and human health. CRC. Crit. Rev. Plant Sci. 31:229–240. doi: 10.1080/07352689.2012.664979.

Schulze, R., and Grafe K. (1969). "Consideration of sky ultraviolet in the measurement of solar ultraviolet radiation," in The Biological Effects of Ultraviolet Radiation, ed. Urbach, F., Pergamon Press, New York.

Searles, P.S., Flint, S.D., Caldwell, M.M. (2001). A meta-analysis of plant field studies simulating stratospheric ozone depletion. Oecologia. 127:1–10. doi: 10.1007/s004420000592.

Sen, A., Wyonch, R. (2018). *Cannabis Countdown: Estimating the Size Of Illegal Markets and Lost Tax Revenue Post-Legalization.* Toronto, ON: C.D. Howe Institute.

Sims, D.A., Pearcy, R.W. (1992). Response of leaf anatomy and photosynthetic capacity in *Alocasia macrorrhiza* (Araceae) to a transfer from low to high light. Am. J. Bot. 79:449-455. doi: 10.2307/2445158.

Singsaas, E.L., Ort, D.R., DeLucia, E.H. (2001). Variation in measured values of photosynthetic quantum yield in ecophysiological studies. Oecologia 128:15–23. doi: 10.1007/s004420000624.

Singsaas, E.L., Ort, D.R., Delucia, E.H. (2004). Elevated CO_2 effects on mesophyll conductance and its consequences for interpreting photosynthetic physiology. Plant, Cell Environ. 27:41–50. doi: 10.1046/j.0016-8025.2003.01123.x.

Slatkin, N.E. (2007). Cannabinoids in the treatment of chemotherapy-induced nausea and vomiting: beyond prevention of acute emesis. J. Support. Oncol. 5:1–9.

Small, E. (2017). Cannabis: A complete guide. CRC Press, Boca Raton, FL.

Small, E., Beckstead, H.D. (1973). Cannabinoid phenotypes in *Cannabis sativa*. Nature. 245:147–148. doi: 10.1038/245147a0.

Small, E., Cronquist, A. (1976). A Practical and Natural Taxonomy for Cannabis. Taxon. 25:405–435.

Stapleton, A.E. (1992). Ultraviolet radiation and plants: Burning questions. Plant Cell. 4:1353–1358. doi: 10.1105/tpc.4.11.1353

Steinmüller, D., Tevini, M. (1985). Action of ultraviolet radiation (UV-B) upon cuticular waxes in some crop plants. Planta. 164:557–564. doi: 10.1007/BF00395975.

Suthaparan, A., Solhaug, K.A., Bjugstad, N., Gislerød, H.R., Gadoury, D.M., Stensvand, A. (2016). Suppression of powdery mildews by UV-B: Application frequency and timing, dose, reflectance, and automation. Plant Dis. 100:1643–1650. doi: 10.1094/PDIS-12-15-1440-RE.

Teramura, A.H., Sullivan, J.H., Lydon, J. (1990). Effects of UV-B radiation on soybean yield and seed quality: a 6-year field study. Physiol. Plant. 80:5–11. doi: 10.1111/j.1399-3054.1990.tb04367.x.

Terashima, I., Hikosaka, K. (1995). Comparative ecophysiology of leaf and canopy photosynthesis. Plant. Cell Environ. 18:1111–1128. doi: 10.1111/j.1365-3040.1995.tb00623.x.

Terfa, M.T., Roro, A.G., Olsen, J.E., Torre, S. (2014). Effects of UV radiation on growth and postharvest characteristics of three pot rose cultivars grown at different altitudes. Sci. Hortic. 178:184–191. doi: 10.1016/j.scienta.2014.08.021.

Thoma, F., Somborn-Schulz, A., Schlehuber, D., Keuter, V., Deerberg, G. (2020). Effects of light on secondary metabolites in selected leafy greens: A review. Front. Plant Sci. 11:497. doi: 10.3389/fpls.2020.00497.

Toonen, M., Ribot, S., Thissen, J. (2006). Yield of illicit indoor cannabis cultivation in the Netherlands. J. Forensic Sci. 51:1050–1054. doi: 10.1111/j.1556-4029.2006.00228.x.

Torre, S., Roro, A.G., Bengtsson, S., Mortensen, L.M., Solhaug, K.A., Gislerød, H.R., Olsen, J.E. (2012). Control of plant morphology by UV-B and UV-B-temperature interactions. Acta Hortic. 956:207–214. doi: 10.17660/ActaHortic.2012.956.22.

Tossi, V.E., Regalado, J.J., Iannicelli, J., Laino, L.E., Burrieza, H.P., Escandón, A.S., Pitta-Álvarez, S.I. (2019). Beyond arabidopsis: Differential UV-B response mediated by UVR8 in diverse species. Front. Plant Sci. 10:780. doi: 10.3389/fpls.2019.00780.

United Nations Office on Drugs and Crime (UNODC). (2009). *World Drug Report 2009.* New York, NY: United Nations.

United Nations Office on Drugs and Crime (UNODC). (2019). *World Drug Report 2019.* New York, NY: United Nations.

Valdez, A., Kaplan, C.D. (2019). Deconstructing US marijuana prohibition policies in the early twentieth century. Aztlan A J. Chicano Stud. 44:111–140.

Valenta, K., Dimac-Stohl, K., Baines, F., Smith, T., Piotrowski, G., Hill, N., Kuppler, J., Nevo, O. (2020). Ultraviolet radiation changes plant color. BMC Plant Biol. 20:253. doi:

10.1186/s12870-020-02471-8.

Vanhove, W., Van Damme, P., Meert, N. (2011). Factors determining yield and quality of illicit indoor cannabis (*Cannabis* spp.) production. Forensic Sci. Int. 212:158–163. doi: 10.1016/J.FORSCIINT.2011.06.006.

Vanhove, W., Surmont, T., Van Damme, P., De Ruyver, B. (2014). Filling in the blanks. An estimation of illicit cannabis growers' profits in Belgium. Int. J. Drug Policy 25:436–443. doi: 10.1016/j.drugpo.2014.01.020.

Viveros, M., Marco, E., File, S. (2005). Endocannabinoid system and stress and anxiety responses. Pharmacol. Biochem. Behav. 81:331–342. doi: 10.1016/j.pbb.2005.01.029.

Vlahos, J.C., Heuvelink, E., Martakis, G.F.P. (1991). A growth analysis study of three *Achimenes* cultivars grown under three light regimes. Sci. Hortic. 46:275–282. doi: 10.1016/0304-4238(91)90050-9.

Walker, D., Jarvis, P., Farquhar, G., Leverenz, J. (1989). Automated measurement of leaf photosynthetic O_2 evolution as a function of photon flux density. Philos. Trans. R. Soc. Lond. B. Biol. Sci. 323:313–326.

Wargent, J.J., Jordan, B.R. (2013). From ozone depletion to agriculture: Understanding the role of UV radiation in sustainable crop production. New Phytol. 197:1058–1076. doi: 10.1111/nph.12132.

Weerasinghe, L.K., Creek, D., Crous, K.Y., Xiang, S., Liddell, M.J., Turnbull, M.H., Atkin, O.K. (2014). Canopy position affects the relationships between leaf respiration and associated traits in a tropical rainforest in Far North Queensland. Tree Physiol. 34:564–584. doi: 10.1093/treephys/tpu016.

Wilson, M.I. (1998). PhotomorphologicaI and Photochernical Effects of UV-B Radiation on *Brassica napus* (L.) and *Arabidopsis thaliana* (L.) Heynh: Morphological, Cellular and Structural Biological Changes. [Thesis]

Yang, Y., Yao, Y., He, H. (2008). Influence of ambient and enhanced ultraviolet-B radiation on the plant growth and physiological properties in two contrasting populations of Hippophae rhamnoides. J. Plant Res. 121:377–385. doi: 10.1007/s10265-008-0163-y.

Yep, B., Gale, N. V., Zheng, Y. (2020). Aquaponic and hydroponic solutions modulate NaCl-induced stress in drug-type *Cannabis sativa* L. Front. Plant Sci. 11:1–14. doi: 10.3389/fpls.2020.01169.

Yin, R., Ulm, R. (2017). How plants cope with UV-B: From perception to response. Curr. Opin. Plant Biol. 37:42–48. doi: 10.1016/j.pbi.2017.03.013.

Younis, B.A., Mahoney, L., Schweigkofler, W., Suslow, K. (2019). Inactivation of plant pathogens in irrigation water runoff using a novel UV disinfection system. Eur. J. Plant Pathol. 153:907–914. doi: 10.1007/s10658-018-01608-8.

Zhang, L., Allen, L.H., Vaughan, M.M., Hauser, B.A., Boote, K.J. (2014). Solar ultraviolet radiation exclusion increases soybean internode lengths and plant height. Agric. For. Meteorol. 184:170–178. doi: 10.1016/j.agrformet.2013.09.011.

Zhang, X., He, D., Niu, G., Yan, Z., Song, J. (2018). Effects of environment lighting on the growth, photosynthesis, and quality of hydroponic lettuce in a plant factory. Int. J. Agric. Biol. Eng. 11:33–40. doi: 10.25165/j.ijabe.20181102.3420.

Zhao, D., Reddy, K.R., Kakani, V.G., Read, J.J., Sullivan, J.H. (2003). Growth and physiological responses of cotton (*Gossypium hirsutum* L.) to elevated carbon dioxide and ultraviolet-B radiation under controlled environmental conditions. Plant, Cell Environ. 26:771–782. doi: 10.1046/j.1365-3040.2003.01019.x.

Zheng, Y. (2020). Soilless production of drug-type Cannabis sativa. Acta Hortic. (In press.).

Zheng, Y., Blom, T., Dixon, M. (2006). Moving lamps increase leaf photosynthetic capacity but not the growth of potted gerbera. Sci. Hortic. 107:380–385. doi: 10.1016/j.scienta.2005.09.004.

Zlatev, Z.S., Lidon, F., Kaimakanova, M. (2012). Plant physiological responses to UV-B radiation. Emirates J. Food Agric. 24:481–501. doi: 10.9755/ejfa.v24i6.481501.

Zou, S., Kumar, U. (2018). Cannabinoid receptors and the endocannabinoid system: Signaling and function in the central nervous system. Int. J. Mol. Sci. 19. doi: 10.3390/ijms19030833.

APPENDIX A

SUPPLEMENTARY INFORMATION: PLANT GROWTH RESPONSE TO INCREASING LI

METHOD

The number of nodes and main stem length (i.e., from the substrate surface to the tip of the tallest shoot, hereafter, height) were measured twice weekly until day 42, when vegetative growth had ceased.

RESULTS

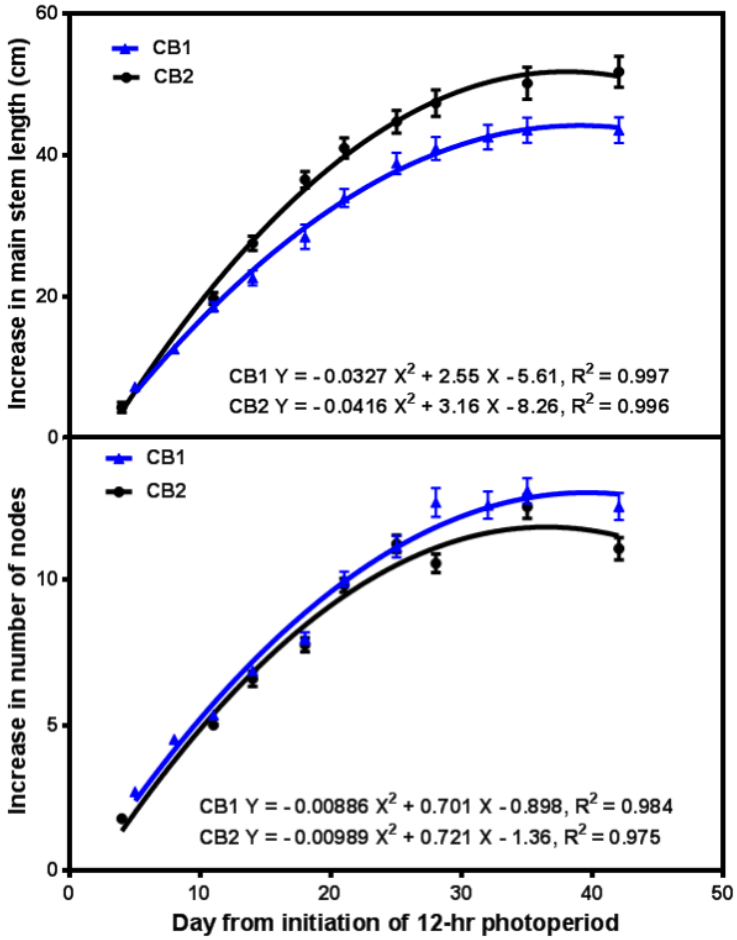

Supplementary Figure 1. The accumulated increase in *Cannabis sativa* L. 'Stillwater' **(A)** main stem length (cm) and **(B)** number of nodes from day 0 (i.e., day from initiation of 12-h flowering photoperiod) over time. Each datum is the mean ± SE increase of main stem length from day 0 of all plants from that particular day (CB1 *n* = 43, CB2 *n* = 48).

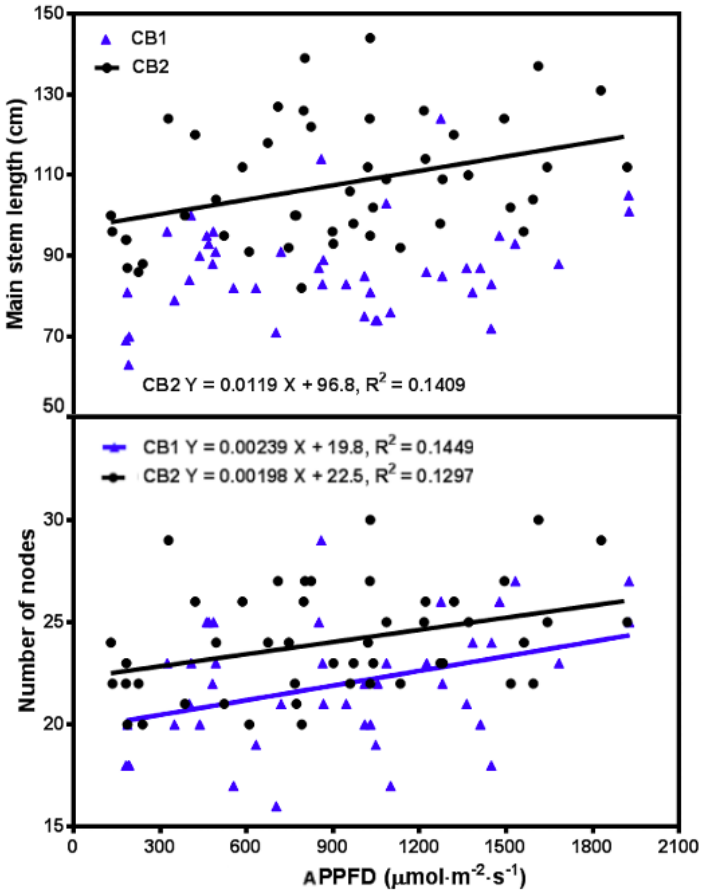

Supplementary Figure 2. *Cannabis sativa* L. 'Stillwater' **(A)** main stem length (cm) and **(B)** number of nodes on day 42 of the flowering stage in response to average photosynthetic photon flux density (PPFD) calculated based on the respective plants' PAR accumulated exposures up to day 42 of the flowering stage. Each datum is a single plant.

Around day 42 after the initiation of the 12-h photoperiod, plant the plants ceased growing vegetatively (**Supplementary Figure 1A, B**). After the cessation of vegetative growth (i.e., on day 42), height increased linearly from 98.2 to 118 cm (i.e., 1.2 times higher) in CB2, but height in CB1 was not affected with mean ± SD of 105 ± 70 (**Supplementary Figure 2A**), as APPFD increased from 130 to 1930 µmol·m^{-2}·s^{-1} (calculated based on the respective plants' accumulated PAR exposures up to day 42 of the flowering stage). Across the same increasing

range of APPFD, number of nodes increased from 20 to 24 (i.e., 1.2 times higher) and 23 to 26 (i.e., 1.1 times higher) in CB1 and CB2, respectively (**Supplementary Figure 2B**). The "topping" technique from plants in the vegetative stage lowered absolute main stem length and number of nodes.

DISCUSSION

After the initiation of the 12-h photoperiod, plants continued to grow their vegetative organs until around day 40. The present study found that "untopped" plants responded to increasing APPFD with increased height. In contrast, topped plants did not demonstrate significant increases in height, likely due to the lack of apical dominance which could evenly distribute the height increases between to the two nodes at the top of the plant and quell the overall height increase (Barbier et al., 2017). Nevertheless, increasing APPFD increased the number of nodes in plants whether they were topped or not. Tall plants can be difficult to manage and harvest, hence growers must consider the potential height increase when increasing their canopy-level LI, which depends on the use of the topping technique.

APPENDIX B

SUPPLEMENTARY INFORMATION: PHOTOBLEACHING AT HIGH LI

METHODS

Photobleaching was recorded based on the visible observation, including a measurement of PPFD directly at the location where the phenomenon occurred.

RESULTS

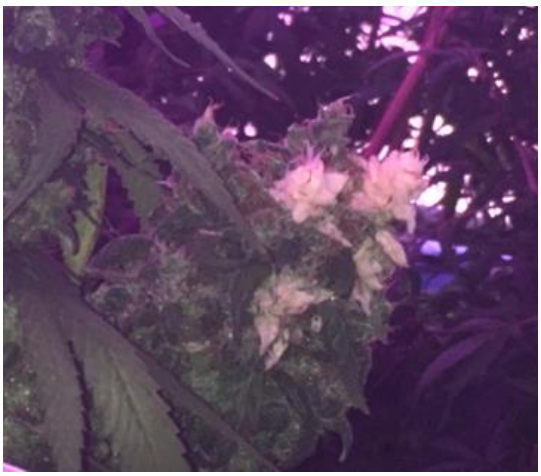

Supplementary Figure 3. Image of inflorescence photobleaching 70 d after the initiation of 12-h photoperiod.

Photobleaching occurred on the apical inflorescences of treatment plants under average PPFDs ranging from 1040 to 1850 $\mu mol \cdot m^{-2} \cdot s^{-1}$ (**Supplementary Figure 3**).

DISCUSSION

When light intensity exceeds a tissue's photoprotective capacity for long-term periods, damage occurs such as photobleaching (i.e., the photodestruction of chlorophyll) (Björkman and Demmig, 1987; Havaux and Niyogi, 1999; Henley et al., 1991; Mooney et al., 1974). However, the photobleaching that occurred in this trial was visible only on the top of apical inflorescences, which are not the primary photosynthetic tissue. Additionally, photobleaching was only observed

on certain plants, not all the plants under high LIs. Further research is required to understand this phenomenon.

APPENDIX C

Supplementary Figure 4. Necrotic patches on ‘Breaking Wave’ (left) and ‘Low Tide’ (right) *Cannabis sativa* L. leaves 9 weeks after the initiation of UV treatments. The black scale bar at the lower right is 2.0 cm.